Elucidating the pro-angiogenic role of GPR81/HCAR-1 in cerebral hypoxic-ischemia

By

Prabhas Chaudhari
Department of Experimental Medicine
McGill University, Montreal

December 2019

A thesis submitted to McGill University in partial fulfillment of the requirements of the degree of Doctorate of Philosophy

Table of Contents

Abstract

Neonatal hypoxic-ischemic encephalopathies (HIE) occurs at an average of 4 in 1000 live births in developed countries and contributes to about 74.72 billion dollars to clinical management of neurological disabilities associated with the same. Although preterm infants are more susceptible to HIE, it has also been documented in infants at term birth. The benchmark effect of HIE insult to the neonatal brain is attributed to reduced blood flow resulting in subsequent decrease in glucose and oxygen supply. The underlying cellular etiology of neonatal HIE is not only a direct result of exicitotoxicity of neurons due to enhanced glutamate secretion, inflammation and oxidative stress, but is also characterized by a metabolic imbalance due to an arrest in oxidative phosphorylation. The accumulation of carbohydrate metabolites such as succinate, alpha ketoglutarate and lactate due to Krebs cycle malfunctioning has been a hallmark marker in several ischemia related pathophysiological conditions.

Lactate has been shown to play an important role in tumor angiogenesis, inflammation, and wound healing. Recently, lactate was demonstrated to be a physiological ligand to a G-protein coupled receptor (GPCR), called GPR81. Lactate acting through its GPR81 receptor has been implicated in the inhibition of lipolysis in fat cells, modulating inflammation by suppressing the secretion of pro-inflammatory cytokines in macrophages, as well as in the angiogenic response in various cancer cell lines. However, how lactate/GPR81 interaction modulates physiological and pathophysiological functions in brain and retina remains elusive. In this study, we Firstly, demonstrate that GPR81 is expressed in the brain, specifically in the neurons. Secondly, it governs postnatal brain developmental angiogenesis and protects the neonatal brain after an HI insult in a Rice-Vannucci mice model. We determined that activation of GPR81 by lactate after a HI insult is utmost essential in reducing brain infarct lesions via production of key pro-angiogenic factors VEGF, ANG-1, ANG-2, PDGF BB and reducing the secretion of angiostatic factor thrombospondin-1 (TSP-1). The repair mechanism was more prominent in the

penumbral region of the brain and near the site of intracerebroventricular injections. In addition, lactate pro-angiogenic effect was confirmed by enhanced endothelial cell sprouting *ex vivo* and *in vivo* experiments of aortic explants and intracerebroventricular lactate injections respectively. On the contrary in GPR81-/- mice, angiogenesis was substantially reduced, making them susceptible to brain injury after an HI insult.

Resume

Les encéphalopathies hypoxiques ischémiques (EHI) du nouveau-né surviennent en moyenne 4 sur 1000 naissances vivantes dans les pays développés et contribuent à environ 74,7 milliards de dollars servant à la gestion clinique des déficiences neurologiques qui y sont associées. Bien que les nouveau-nés prématurés soient plus susceptibles à l'EHI, cette condition a également été documentée chez les enfants nés à terme. L'effet le plus considérable aux dommages des EHI néonataux est attribué à la réduction du débit sanguin entraînant ultérieurement une réduction de l'apport en glucose et en oxygène. L'étiologie cellulaire sous-jacente de l'EHI néonatal est non seulement une conséquence directe de l'excitotoxicité des neurones due à une augmentation de la sécrétion de glutamate, de l'inflammation et du stress oxydatif, mais elle est également caractérisée par un déséquilibre métabolique dû à un arrêt de la phosphorylation oxydative. L'accumulation de métabolites glucidiques tels que le lactate, le succinate et l'alpha-cétoglutarate, en raison d'un dysfonctionnement du cycle de krebs est un marqueur distinctif dans plusieurs conditions physiopathologiques liées à l'ischémie. Le lactate a été démontré comme jouant un rôle important dans l'angiogenèse tumorale, l'inflammation et dans la réparation tissulaire. Récemment, il a été démontré que le lactate agit en tant que ligand physiologique d'un récepteur couplé aux protéines (RCPG), appelé GPR81. Le lactate agissant via son récepteur GPR81 est impliqué dans l'inhibition de la lipolyse dans les cellules adipeuses, en tant que modulateur inflammatoire en supprimant la sécrétion de cytokines pro-inflammatoires dans les macrophages ainsi que dans la réponse angiogénique dans diverses lignées cellulaires cancéreuses. Cependant, la manière dont l'interaction lactate/GPR81 module les fonctions physiologiques et physiopathologiques du cerveau et de la rétine reste difficile à définir. Dans cette étude, nous démontrons tout d'abord que dans le cerveau, GPR81 est spécifiquement localisé dans les neurones qui gouvernent le développement postnatal et protège le cerveau néonatal après une insulte hypoxique ischémique (HI) dans un modèle de souris Rice-Vannucci. Nous avons déterminé que l'activation de GPR81 par le lactate après une agression IH est primordiale pour réduire les lésions d'infarctus cérébraux via la production de facteurs

proangiogéniques clés tels que : VEGF, ANG-1, ANG-2, PDGF BB, et pour réduire le facteur angiostatique thrombospondine-1 (TSP-1). Le mécanisme de réparation était notamment plus important dans la pénombre ischémique du cerveau. En outre, l'effet proangiogénique du lactate a été confirmé par la hausse de croissance cellulaire ex vivo et in vivo dans des expériences utilisant des cellules endothéliales à partir d'explants aortiques et des injections intracérébroventriculaires de lactates, respectivement. Au contraire, chez les souris GPR81-/-, l'angiogenèse était considérablement réduite les rendant susceptibles à des lésions cérébrales après une insulte liée à l'IH.

Acknowledgements

I am forever grateful to Dr. Sylvain Chemtob, for giving me the opportunity to join his dynamic lab. His guidance and mentorship helped me grow both professionally and personally. I will always be indebted to Late Dr. Daya Ram Varma, for his stellar support as an advisor that always provided the impetus and confidence to push forward. His charisma and presence will always be missed. Dr Ankush Madaan has been a mentor, friend and a now a close family member after knowing him for 10 long years. He has been inspirational not only as a colleague but also as a friend to help me get through life hurdles at professional and personal level. Dr Carlos Riveria has been instrumental with his guidance and has been motivational in pursuing my interest in research. I also thank Dr. Christiane Quinou and Dr Xin Hou, who helped in my smooth transition to the lab and for their valuable advice all these years. I am indebted to all my colleagues especially Elizabeth Prairie for her impeccable translation of my thesis abstract in french ☺ and other coauthors for their contributions towards my thesis. I would like to thank all members of my Thesis advisory committee for their time and teachings; in particular, Dr. Thierry Muanza. I am grateful to the Canadian Institutes of Health Research (CIHR); Vision Health Research Network for granting studentship and travel awards during my PhD studies. I want to thank all members of the Thesis evaluation committee for agreeing to examine my PhD work (Dr Pia Wintermark and Dr DiCristo) and for their valuable suggestions. On a personal note, I thank my colleagues for making these years fly by. I am eternally grateful to my parents and elder sister and little sister (Pradnya and Kasturi) for their sacrifices and endless encouragement to pursue my dreams. I would also thank my childhood (Sid, Debesh, Rahul) and lab friends (Elizabeth, Amaryllis, Fanny, Uday, Tapan, Jin, Vincente, Simon, Rasheda, Christina, Mohammed, Sarah Eve, Irene) who have been patient and perseverant during my PhD journey and made it all so ever fun. Last but not the least a special thanks to my extended Canadian and US family (Anouskha, Olivia, Mallika, Vishal, Rayansh, Rushi, Milly, Maeva, Alex, Audrey, Jerry and Konstatine), and close friends (Rahul, Rohan, Apurba, Karim, Emil, Darius, Celestin) for making

the PhD even more rewarding and without them this journey would not have been possible.

Contribution to Original Knowledge

The results presented in the thesis have not been published in previous journals. Hence the research findings are to be distinct and original contribution to knowledge in the following research attributes:

1. This is the first time we determine that GPR81 expression in the brain modulates ***developmental and pathological angiogenesis*** in the rice-vannucci model of cerebral hypoxia using GPR81 KO mice.
2. We also demonstrated that GPR81 via the ERK1/2 signalling pathway could be a potential upstream regulators that can regulate ***developmental angiogenesis***
3. We have also categorically demonstrated for the first time that neurons expressing GPR81 can promote secretion of pro-angiogenic factors that can regulate endothelial cell proliferation.
4. More specifically we were able to elucidate that alternating role of VEGF and TSP-1 are major players in developmental and pathological angiogenesis, which are regulated by neuronal GPR81.

Contribution of Authors

The thesis is traditional based thesis in accordance with the guidelines from the Faculty of Graduate and Post-doctoral Studies and Research of McGill University. The descriptions of the authors' contributions to each chapter have been explicitly stated contribution of the candidate.

Prabhas Chaudhari, Ankush Madaan, Xin Hou, Thierry Muanza, Sylvain Chemtob.

CHAPTER 1 and CHAPTER 2

Prabhas Chaudhari contributed in all aspects pertaining to writing of the thesis.

CHAPTER 3:

Details: Dr Ankush Madaan, Prabhas Chaudhari, Dr Jose Carlos Riviera and Sylvain Chemtob conceptualized and designed the experiments. Prabhas Chaudhari performed 90% the experiments. Xin Hou contributed with intracerebroventricular injections and performed MCAO surgery. Dr Thierry Muanza and Sylvain Chemtob provided scientific advice during troubleshooting. Dr Thierry Muanza and Sylvain Chemtob supervised the study.

CHAPTER 4:

Prabhas Chaudhari did the experimentation and technical part of the result sections. Dr Ankush Madaan provided technical advice. Prabhas Chaudhari wrote the chapters and performed all the experiments. The qPCR data of GPR81 and norrin expression depicted in Figure 4.21 was performed and analyzed by Dr AM

CHAPTER 5, CHAPTER 6 and CHAPTER 7:

Prabhas Chaudhari wrote the aforementioned three chapters, which includes the discussion, conclusion and the references.

List of Figures

CHAPTER 2

CHAPTER 3

CHAPTER 4

List of Abbreviations

Ang angiopoietin

BBB blood-brain barrier

CBF cerebral blood flow

CCL2 chemokine ligand 2

CNS central nervous system

COX cyclooxygenase

EC endothelial cells

GABA gamma amino butyric acid

GPCR: G-protein coupled receptor

GPR81: G-protein coupled receptor 81

HCA1 Hydrocarboxylic acid receptor 1

HI hypoxic ischemia

HIE hypoxic ischemic encephalopathy

HIF-1a hypoxic inducible factor

IGF insulin-like growth factor

IHC immunohistochemistry

IL-1β interleukin-1β

IL-6 interleukin 6

IR ischemic retinopathies

KO knockout

LPS lipopolysaccharide

MC muller cells

NDI nephrogenic diabetes insipidus

NV neovascularization

OIR oxygen-induced retinopathy

PDGFBB platelet derived growth factor BB

RP retinitis pigmentosa

ROP retinopathy of prematurity

TNFa tumour necrosis factor

TSP-1 thrombospondin

SNP single nucleotide polymorphism

VEGF vascular endothelial growth factor

VO vaso-obliteration

CHAPTER 1
INTRODUCTION

1.1 Introduction

Neonatal brain injury or perinatal hypoxic-ischemic encephalopathy (HIE), affects 4 in 1000 of newborns in developed countries, predisposing them to neurological abnormalities, related to mental retardation, cerebral palsy, epilepsy, and visual impairment [1]. The pathogenesis of HIE is a direct result of reduced blood supply to the neonatal brain with subsequent decrease in oxygen and glucose impairment to neurons, astrocytes and endothelium. At the molecular level, the pathology of HIE can be explained by primary insult associated with glutamate toxicity, failure of Na^+/K^+ ATPase pump and increased Ca^{2+} influx due to failure of Ca^{2+}/Na^+ transporters, as a result of arrest in oxidative phosphorylation[2]. The secondary energy failure is a result of inflammation and free radical formation causing mitochondrial dysfunction and necrosis, occurring after 6 to 24 hours after the primary insult. Although a wide variety of therapeutic interventions for HIE have been documented and clinically trialed, hypothermia is the only clinically accepted therapy for neonatal cerebral hypoxia [3,4]. However, hypothermia alone is not sufficient to reduce long term neurological abnormalities leading to cerebral palsy, epilepsy, and mental retardation[5]. There has been substantial evidence that angiogenesis plays a vital role in overcoming the post-Hypoxic ischemic (HI) injuries. The most effective region for therapeutic effectiveness of angiogenesis is the penumbra (a region surrounding the infarct which has high cellular metabolic activity). If angiogenesis is restored in penumbra in a timely manner, there is high probability of salvaging neurons from HI insult[6].

The protective effect of angiogenesis in cerebral hypoxia has been widely studied in diverse HI models. For example, post HI intracereboventricular administration of vascular endothelial growth factor (VEGF) in a transient middle carotid artery occlusion (tMCAO) improved neurological outcomes by increasing angiogenesis and neurogenesis in the striatal penumbral region[7]. In addition, the underlying role of extracellular matrix (ECM) in regulating angiogenesis involving integrin (alpha5betal) and its ligand fibronectin was elucidated [8,9]. A conditional KO of alpha5 integrin in the endothelial cells subjected to cerebral hypoxia resulted in marked

attenuation of angiogenesis. Decreased brain endothelial cell migration and proliferation was a direct result of impaired interaction of fibronectin with alpha5beta1 receptor[10]. Furthermore, clinical data from stroke patients categorically showed a substantial increase in microvessels in the ipsilateral region compared with the control contralateral region. This increase in vessel density was directly proportional to survival times of these patients. Collectively, there is substantial evidence from mice and human stroke pathogenesis, indicative of therapeutic angiogenesis playing a vital role in attenuating size of brain lesions and their subsequent neurological abnormalities [11].

As briefly mentioned earlier, HIE results in arrest in oxidative phosphorylation leading to accumulation of intracellular, succinate, alpha-ketoglutarate and lactate via anaerobic glycolysis. Interestingly, these carbohydrate metabolites serve as physiological ligands for G-protein coupled receptors GPR91, GPR99 and GPR81 respectively [12–14]. The role of GPR91 in retinopathy of prematurity (ROP) and neonatal hypoxic-ischemia (HI) have been recently surfaced, wherein activation of GPR91 by succinate reduces vaso-obliteration (VO) in retina and curtails brain lesions via angiogenesis [15]. Herein, we reveal and discuss a vital and novel regulatory mechanism of GPR81 in unveiling its unprecedented role in neonatal cerebral hypoxia via neuro-angiogenesis.

Hypoxia-ischemic encephalopathy (HIE) is a major cause of neuronal morbidity in premature infants, predisposing them to neuropsychological disorders like epilepsy, mental retardation, cerebral palsy and learning disabilities. It is estimated that 4 in 1000 births are susceptible to HIE. Current health care focuses, on understanding the pathophysiology of HIE to develop effective interventions for newborns with risk of cerebral hypoxic ischemia [1,2,16,17]. Physiologically, it is well characterized that a cerebral (Hypoxic-Ischemic) HI event implicates glutamate toxicity, generation of superoxide radicals, apoptosis, inflammation and cell death in neurons [18]. Perinatal complications have also been associated with hypercapnia, hyperoxia, and hemodynamic alterations resulting in microvascular degeneration and traumatic brain injury [3,4,19,20].

At molecular level, HIE pathophysiology is characterized by glycolysis and oxidative phosphorylation arrest, resulting in accumulation of carbohydrate metabolites (lactate, succinate, ketoglutarate). These physiological and cellular processes are well coordinated by G-protein coupled receptors (GPRs) [3,5,21,22].

Recent research in regenerative biology, have shed insights on brain's innate ability to initiate penumbral repair mechanisms after HIE insult[15,23]. The recovery phase is characterized by neurorestorative changes in neurogenesis, synaptic remodeling and angiogenesis, which possess potential advantages over conventional neuroprotective therapies [7,10,24,25]. Enhanced angiogenesis is a potential outcome in the HIE. Increased angiogenesis, supports tissue regeneration and neuron survival, by restoring oxygen and glucose supply. However, the molecular mechanism of angiogenesis has to be elucidated in order to develop novel therapeutics for HIE in infants[25]. Active neurons utilize glucose and oxygen to remain metabolically and functionally active[26]. Inadequate perfusion, results in hypoxic neuronal distress leading to aberrant vessel formation and vascular degeneration [18,20,27,28]. To better understand the underlying mechanism between neuronal GPCRs and angiogenesis, we previously demonstrated that neuronal sensitivity to hypoxic stress is attributed to interplay between GPR91 and succinate. Furthermore, ensuing GPR91 plays a vital role in regulating angiogenesis via vascular endothelial growth factor (VEGF), angiopoietins and thrombospondin-1 (TSP-1). Hence, elucidating the role of GPR91 as an alternative target for revascularization after hypoxic-ischemia [11,15].

TSP-1 is a molecule that inhibits angiogenesis and promotes vasculature stabilization. While, VEGF is a pro-angiogenic secreted cytokine involved in neovessel formation. The opposing effects of TSP-1 and VEGF in angiogenesis during cerebral hypoxia have been previously discussed. A decrease in expression of TSP-1 and a corresponding increase in VEGF after 24 hours after HI insult were evident, indicating an intricate balance between vessel stabilization effect by TSP-1 and the pro-angiogenic effect of VEGF in vascular and metabolic active region of the ischemic penumbra[36,29].

Lactate injection, immediately after reperfusion has shown to provide neuroprotection in cerebral ischemia by increasing cerebral blood flow[12, 23, 30, 31]. It has also been proposed that lactate participates in metabolic signalling pathways by interacting with receptor GPR81[13, 32]. GPR81, a deorphanized receptor has been found to specifically interact with lactate [14, 22, 33, 34]. It is highly expressed in the adipocytes and is considered to be a therapeutic target for metabolic disorders including diabetes-induced hyperlipidemia[16, 35]. GPR81, being a lactate receptor, we sought to elucidate the mechanism by which GPR81 could reverse injury caused by cerebral hypoxia via angiogenesis in a post-natal hypoxic ischemic mouse model. ***We hypothesized that not only GPR81 via VEGF and TSP-1 play a vital role in regulating normal brain vasculature but also, lactate stimulation of GPR81 through VEGF and TSP-1 reduces infarct size after a hypoxic ischemic insult via a neurorestorative angiogenic mechanism.*** The specific objectives were to

1. Determine expression and sublocalization of GPR81 in brain
2. Evaluate angiogenetic effects of lactate via GPR81 in primary neurons
3. Determine neurorestorative (angiogenesis) role of GPR81 in post-ischemic brain injury in the mice model of Rice-Vannucci.

CHAPTER 2
LITERATURE REVIEW

2.1 G-PROTEIN COUPLED RECEPTORS (GPCRs)

GPCRs are evolutionary conserved family of proteins found in Eukaryotes and Prokaryotes. About 700 GPCRs are found in the human genome, along with 160 in Drosophila [36]. These unique proteins convey signalling information via heterotrimeric G proteins. They are activated via diverse ligands ranging from nucleotides, peptides, amines to cations like calcium. Use of single nucleotide polymorphism (SNPs) has increased our understanding in elucidating the functional properties of GPCRs. SNPs has enabled researchers to discover new ligands for orphan G-proteins coupled receptors. SNPs can also contribute in providing information on structure activity relationships of GPCRs [37].

2.1.1 Classification of GPCRs

GPCRs on their structure and function are classified into:

Class A: GPCRs in class A are characterized by presence of DRY motif responsible for maintaining receptor conformation. Examples include light receptors. As one of the largest class of GPCRs they also include receptors which are activated by small peptides, amines and glycoprotein hormones like luteinizing hormone (LH), follicle stimulating hormone (FSH) and thyroid stimulating hormone (TSH) [37,38].

Class B: These receptors contain a long N-terminal domain of about 100 residues used for ligand binding. Examples of ligands binding to these receptors are large molecular weights molecules like glucagon and calcitonin [39].

Class C: These are the smallest of the three class and consists of a very large N-terminal domain required for ligand binding. In addition, they also contain several conserved Cysteine (Cys) residues in transmembrane domains (TM). Examples are GABA receptors and calcium sensing receptor [21].

Somatic or germline mutations in GPCRs have been attributed to various disorders. This is attributed to alter functioning of GPCRs, which is evident in diseases like X-linked nephrogenic

diabetes insipidus (NPI) and retinitis pigmentosa (RP). Most of the studies use site-directed mutagenesis to elucidate specific functions of each domains of GPCRs which are discussed in further brief [40,41].

2.1.2 Domains of G-protein coupled receptors

The N-terminal Domain: The extra-cellular N-terminal domain of GPCRs are of varied lengths, and functionally, involved in post translational modification like glycosylation controlling intracellular trafficking. In addition, they also contains docking sites for ligand binding and residues for receptor activation and down regulation [42].

***Receptor Down-regulation*:** Polymorphism in the N-terminal domain of Beta-adrenergic receptors (B2-ARs) Arg16Gly and Gln27Glu results in degradation and subsequent downregulation of the receptor. These SNPs were quite evident in children suffering from nocturnal asthma. The homozygous variant of Gly16 was found to be more resistant to albuterol bronchodilation compared to its Arg16 counterpart. Another naturally occurring downregulation of N terminal mutation Gly22Ser of 5-hydroxytryptamine receptor (HT) increases sensitivity to antipsychiatric drugs [42].

Ligand binding: Cys23Ser polymorphism in 5HT receptor, resulted in altered ligand binding to schizophrenic drug clozapine. It was evident that this mutation was responsible for reduced response to the drug [43].

Receptor Trafficking: Post translation modification involving N-glycosylation are required for cellular trafficking of the receptor to the plasma membrane. Henceforth SNPs mutations affecting asparagine are associated with certain diseases. For examples, an Asn40Asp mutation in opioid receptors confers higher binding affinity to endogenous endorphins. Similarly, a point mutation in the rhodopsin receptor results in retinitis pigmentosa, in which the receptor losses its ability to travel to the plasma membrane [44].

Transmembrane Domains (TM): The GPCRs in the plasma membranes are made up of seven alpha helices in a ring like structure. Altogether the TMs consist of amino acids residues necessary for protein folding, ligand binding and G-protein coupling sites. Hence mutations in the TMs structure can be defective to protein structure and lead to deleterious consequences [45].

Receptor Expression: Mutations in proline residues in the TMs can result in lower expression and misfolding of vasopressin receptor leading to NDI. Another naturally occurring mutation in the endothelin B receptor in the TM1 domain causes a congenital disease called the Hirschsprung's disease. This is characterized by decrease ganglion cells in the intestinal tract owing to improper processing, folding and expression of the receptor on the plasma membrane [46].

Ligand Binding: On the other hand, mutations in the TMII and TMIII of the melanocortin I receptor causes malformation of hydrophobic ligand pockets resulting in decreased agonist binding of melanocyte stimulating hormone. A similar mutation in the TMIV (Val194Gly) in the dopamine D4 receptor in the brain results in reducing binding of dopamine. These individuals hence, have less sensitivity to D4 agonists like clozapine and olanzapine [47].

Signalling transduction: In addition, certain mutations in the TMVI (Phe591Ser) domains adversely affect G-coupled signalling pathways, an example is that of Follicle stimulating hormone and Luteinizing hormone, wherein the ligand binding affinity is not affected, however the receptors has lost their ability to inhibit and activate adenylyl cyclase via Gs respectively [48].

Dimerization: Certain TMs in the GPCRs contain amino acid sequences for dimerization, which is required for their proper functioning. Lost of TMV in Calcium sensing receptor (CaR) via a frameshift mutation, as evident in hypercalcemia causes misdimerization leading to a reduced expression of functional truncated CaR [49].

Intracellular Loop Domains (IL): The amino acids sequences in IL region bind to regulatory and signalling proteins. B arrestins and G protein receptor kinase (GRK), interact with IL domains leading to receptor phosphorylation. In addition, they also bind to NcK and Grb2 proteins which play a vital role in receptor internalization [44,50].

Signal Transduction: In D2 dopaminergic receptors variations in IL amino residues resulted in marked difference in inhibition of adenylyl cyclase activity. However, there was a marginal change in the ligand binding affinity of dopamine to D2 receptor. These variations were more commonly seen in individuals with high substance abuse and schizophrenia [51]. Mutations in the highly conserved DRY motif in the GPCRs of asparagine, degenerates the conformation of certain receptors, wherein ILs cannot activate GRK2 kinases. In addition, the arginine in the DRY motif is essential in providing correct conformation required for binding with the G protein.

Extracellular Loops (ELs): As compared to other GPCRs domains the ELs, disulfide cysteine bridges functions in building a ligand and specificity binding site and protein receptor folding. Nonetheless, the binding affinities of certain agonists are modulated by ELs [53].

The C-terminal Domain: The C terminal domain of GPCRs provides sites for GRK activation and signalling. They also contain cysteine residues, which undergoes palmitoylation. Mutations in these cysteine amino acids confer a delayed change in second messenger, which in turn diminish the pharmacological effect of activated receptor [54].

2.1.3 GPCRs and signalling pathways

GPCRs activation is attributed to various stimuli, ranging from light, odorants, hormones and neurotransmittors [55]. The heptahelical GPCRs forms a cavity on the cytoplasmic side serving as a docking site for G-proteins [56]. Upon sufficient activation of the receptor the Guanine nucleotide exchange from guanine diphosphate (GPD) to guanine triphosphate (GTP) commences the signalling transduction [57]. The dissociation of GTP α-subunit and $\beta\gamma$-subunits activates ion channels, enzymes or other G proteins to elevate signal amplification [58,59]. Since, GPCR activation costs a lot of energy, inactivation of the signal is utmost important to conserve the energy of the cell. This is brought about by a two-step mechanism, involving the phosphorylation of G-protein receptor kinases and β-arrestin [60].

G-protein coupled receptor dependent pathway

The G protein dependent signalling pathways comprises of activating G proteins (Gαs, Gαi/o, Gαq/11 and Gα12/13) and Gβγ subunits [61]. Upon ligand binding, a conformational change in the receptor results in active binding of GTP to Gα and subsequent dissociation of Gα and Gβγ subunits. The Gα in turn stimulates adenylyl cyclase to produce cAMP and proteinkinase A to initiate a cellular response. cAMP in turn also activates exchange protein activated by cAMP (EPAC). EPAC unlike, cAMP, sequentially activates phospholipase C, proteinkinase C and calmodulin-dependent protein kinase II (CAMKII) [62]. Gβγ, on the other hand acts as a scaffold protein intiating a response via increased phosphoinositide-3-kinase (PI3K) activity [63]. Gαq/11 controls Ca levels via phospholipase C β (PLCβ). PLCβ converts inositol phospholipids to inositol triphosphate (IP3) and diacylglycerol (DAG) [64].

G-protein receptor kinases

G-protein receptor Kinases (GRKs): GRKs are soluble proteins, capable of phosphorylating GPCRs [65]. The GRK mediated signalling transduction was pioneered in early 1970s, on rhodopsin and Beta-adrenergic receptors [66]. GRKs were found to bind and phosphorylate the G-proteins to minimize their activation. The GRKs have a characteristic pleckstrin homology (PH) domain, which binds to the GBg subunit of G protein to inhibit cell signalling. In addition, they also undergo prenylation at their C terminal domain, which localizes them to the plasma membrane [67]. Some GRKs, which lack PH domain, undergo palmitoylation of at their C terminal end [68]. GRKs through their phosphorylation of rhodopsin and beta-adrenergic receptors reduce G protein coupled signalling, they do not completely stop it.

Arrestins and arrestin mediated signalling

Arrestins are 40kD proteins, which are classified into visual arrestins and B arrestins. For about 700 know GPCRs there are 4 arrestin proteins, two visual and two

non-visual. Visual arrestins functions by preventing the interaction of phosphorylated rhodopsin to transducin [69]. Similarly, GRK2 and β-arrestins perform complete inhibition of Gs signalling [70]. Visual arrestins compete with G proteins to bind to the GPCRs at their inter-helical cavity and phosphorylated parts of the receptor [71]. The non-visual arrestins are also called as β-arrestins, binds to clathrin and AP-2 complex via their C terminus. This additional binding of β-arrestins enables receptor internalization leading to more efficient signal reduction [72].

As mentioned earlier, the GRKs are able to diminish the G protein signalling. However, to bring the signalling to a complete halt, another set of proteins called arrestins play a crucial role [73]. Together the GRKs and arrestins inhibit rhodopsin and β-adrenergic receptor signalling via physical blockade of guanosine nucleotide exchange factor (responsible for converting GDP to GTP) [74]. In addition to their suppressing effects on G protein signalling, β arrestin was found to promote cellular signalling via ERK1/2, p38 and c-Jun N kinases by acting as scaffold protein. β-arrestins unique ability to form endocytotic vesicles via interactions with clathrin was recently studies in GPCR signalling. These activated endosomes were evident in Angiotensin 1A receptor (AT1aR) mediated ERK phosphorylation. In this study angiotensin was able to promote ERK phosphorylation at 2 min and 30 mins respectively. It was found that the latter signalling effect was attributed to a delayed response required for receptor internalization and in subsequent β-arrestin GPCR complex formation in the endosomes [75].

2.1.4 G-Protein coupled receptor 81 or Hydroxyl carboxylic acid-1 (GPR81/HCA1)

GPR81 or HCA1 is activated by an endogenous carbohydrate metabolite called lactate. The physiological effective concentration (EC50) of activation was found to be 5 mM. However, the concentration of lactate varies between 5mM to 20mM in pathophysiological conditions like cerebral hypoxia, cancer and metabolic disorders like diabetes, dyslipidemia, indicating that GPR81 could be an attractive target in the aforementioned diseases. In addition to the elevated

levels, lactate, has a low affinity and a fast turnover rate, hence derivatives of lactate with higher affinity would be more suitable to further elucidate functional properties of GPR81. Moreover, lactate can be converted into glucose by process of gluconeogenesis [76].

Through mutational analysis it was determined that GPR81, although similar to their GPR109a (activated by niacin) and GPR109b (3-OH-Octanoic acid) counterparts, is only activated by lactate [77]. This selective activation of GPR81 is due to unique position and interaction of alpha hydroxyl group of lactate. Furthermore, the presence of a highly conserved sequence Cys-Glu-Ser-Phe motif in the extracellular loop 2 (EL2) of GPR81 was essential for activity. Mutations in the above-mentioned residues resulted in completed abrogation of receptor activity. Glu interacts with hydroxyl group of lactate, while Phe is responsible maintaining a stable docking site, thereby indirectly controlling GPR81 and lactate interaction. Furthermore, six conserved cysteine residues in the extracellular domains may interact to form homodimers and receptor surface expression. The six-cysteine residues also form disulphide bonds forming a Cys knot. The Cys knot enhances interaction with lactate by bringing the extracellular domains and N terminus is close proximity to each other, thereby, forming a rigid binding pocket [14].

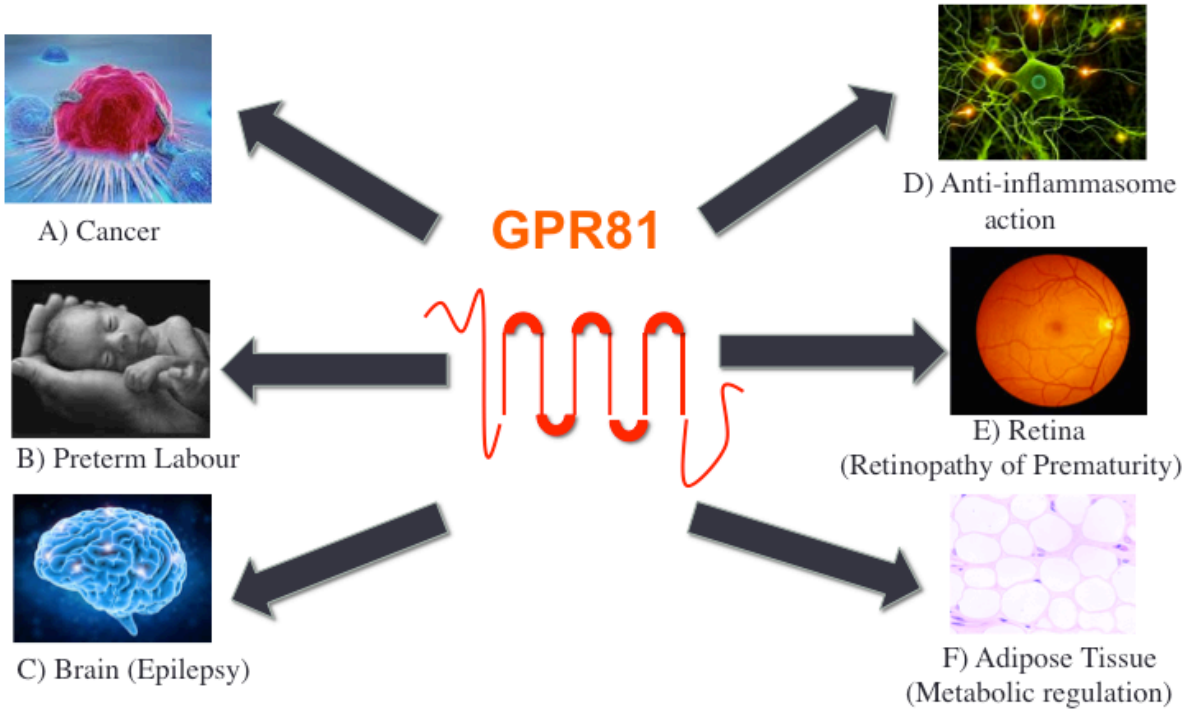

Figure 2.1 GPR81 actions in different pathological conditions. A) Increased expression of GPR81 was evident wide varieties of cancer cell lines (lung, breast, pancreas, cervical) resulting in increased survival. B) In pre-term labour GPR81 reduced inflammation by modulation the secretion of IL-1B. C) In brain, GPR81 reduced neuronal firing thereby protecting the brain in the model of epilepsy. D) GPR81 acts as an anti-inflammatory receptor by inhibiting the action of NLRP3 inflammasome. E) In retina, GPR81 modulates inner retinal vasculature via norrin and promotes therapeutic angiogenesis in mice model of retinopathy of prematurity (ROP). F) GPR81 reduces lipolysis in adipocytes in a synergistic manner along with insulin.

GPR81 and lipolysis

The first and initial studies of GPR81 were focused on adipocytes. The expression analysis shows that GPR81 is highly expressed in the white adipose, which is consistent among different species. With the help of mutational analysis and binding assays, the scientists were able to validate L-lactate as a physiological ligand for GPR81 and put forth the mechanism that

Lactate/GPR81 interaction inhibits adenylyl cyclase and lipolysis in adipocytes. In addition, it was also predicted there is a direct binding of lactate to GPR81, resulting in receptor internalization. There have been contradicting evidence of GPR81 during intense exercise, the plasma concentration of lactate increases to about 10 to 20mM, which in turn inhibits lipolysis in adipocytes. This physiological effect is due to body's inherent ability to use fatty acid as a source of ATP production when glycolysis and mitochondrial respiration are arrested. On the other hand, aerobic glycolysis and abundant glucose supply results in inhibition of lipolysis (Changlu et al). In contrast, it is also documented that lactate levels of 3mM and 10mM were unable to inhibit lipolysis in adipocytes (Fain et al and Ahmed et al). However, GPR81/lactate interaction along with insulin/insulin receptors in adipocytes synergistically, downregulates cAMP and thereby, decreases lipolysis in an autocrine or paracrine manner. This elucidated the hormone like role of lactate [78,79].

GPR81 and Cancer

The hallmarks of all cancers are characterized by increased lactate accumulation in the tumor microenvironment. The expression of GPR81 was found to be elevated in various cancer cells lines ranging from colon, breast, lung, cervical and pancreas. Recently, it was shown that GPR81 expressing cancer cells in the presence of lactate were more prone to survival. In order to determine the underlying mechanism, the GPR81 was silenced in CapanII cells via shRNA and were compared with sham control. The activation of GPR81 by lactate resulted in increased gene expression of monocarboxylate transporter-1 (MCT-1), co-activator of peroxisome proliferator activated receptor (PPAR) PGC-1alpha, CD-147 and MCT-4. MCT-1 and MCT-4 are highly expressed in oxygen and hypoxic rich area of the tumor regulating lactate influx and efflux respectively. CD-147 is an important caperone protein, which is critical in regulating the expression of MCT-1 and MCT-4 on the plasma membrane. Increase expression of all the above genes increased the survival of cancer cells. In addition, the silenced GPR81 cells, reduced lactate

uptake and mitochondrial activity [80]. Furthermore, GPR81 is implicated in conferring resistance to doxorubicin by increasing the expression of ATP binding cassette ABCB1 in cervical cancer cells. Although the effect of GPR81 would be cell specific, its effects of other ATP binding cassette proteins (ABBC1, ABCG2) have to be elucidated in other cell lines[81]. Since, uncontrolled cancer cells require precise DNA damage repair mechanism to promote replication and in turn cellular proliferation. The two DNA repair enzymes controlling DNA repair activity are histone acetyltransferases (HAT) and histone deacetylase (HDAC). Hyperacetylation is favoured by HAT, facilitates easy of transcription, whereas HDACs hypoacetylation hinders transcription. Lactate along with GPR81 were able to control the expression of certain DNA damage repair genes (NBS1, LIG4 and APTX) along with decrease in HDAC activity leading to increase in DNA protein kinases (DNA PKs) involved in Non-homologous end joining (NHEJ). Together, these contribute to increased double stranded break (DSB) repair in cell cycle favouring cancer cell growth [82]. In breast cancer cell lines, an increased expression of GPR81 and GPR109A caused an increased fatty acid production. The proliferation of breast cancer cells was in turn inhibited by use of etomoxir and perhexiline (inhibitors of fatty acid metabolism), in addition silencing GPR81 and GPR109A mediated cancer cell death via caspase activation[83]. In breast cancer cell line MCF-7, heruglin interaction with HER2/HER3 receptor complex leads to reduced GPR81 expression and increased extracellular lactate via MAP3K and G-protein interacting protein (GIT). Silencing either GIT or MAP3K diminished GPR81 expression. This also confirmed, MAP3K and GIT interaction is utmost important for GPR81 expression [84]. Similarly, in MCF-7 breast cancer cell line, GPR81 expression was related to increase angiogenesis by increasing phosphoinositide 3-OH kinase (PI3K)/Akt-cAMP response element binding protein (CREB) mediated effect of amphiregulin (AREG). Silencing GPR81 by shRNA resulted in abrogation of amphiregulin [85]. In non-cell small lung cancer (NCSLC), GPR81/lactate promotes increased expression of programme cell death protein (PD-1) via increased TAZ/TEAD transcriptional regulation by reducing the expression of second messenger cAMP and proteinkinase A.

Unphosphorylated TAZ is restricted to the cytoplasm of the cancer cells, however upon lactate activation of GPR81 phosphorylated TAZ enters the nucleus and binds to TEAD inducing PD-1 expression [86].

GPR81 and inflammation

Lactate and GPR81 role in liver and pancreas is related to reduction in macrophages and monocytes are well elucidated. LPS induction of IL-1B in macrophages and monocytes was substantially reduced by lactate via GPR81 by reducing caspase-1 activity, thereby reducing IL-1B production. In addition, there was a significant decrease in NRLP3 inflammasome activity [87]. However, it should be noted that this effect is mainly due to GPR81 expressed on macrophages and monocytes. A similar effect in the acinar cells of pancreas in case of acute pancreatitis is highly unlikely, since reduction in intracellular pH by lactate will induce premature secretion of proteases in acinar cells through activation of trypsinogen and cathepsin K. Hence lactate via GPR81 in acute pancreatitis confers anti-inflammatory effect in a cell and dose dependent manner [88]. Inflammation of LPS stimulation via TLR-4 and zymogen mediated TLR-2 resulted in prominent decrease GPR81 mRNA levels in adipocytes. On the contrary to the findings of hoque et al, lactate was shown to inhibit proinflammatory response to LPS in GPR81 independent manner in the bone derived marcophages [88]. However, there was a decrease in Lipin1 3T3-L1 cells treated with cytokines. A plausible reason for this discrepancy could be the presence of other pro-inflammatory factors that are responsible of inhibition of GPR81 in adipocytes. GPR81 mRNA expression was also reduced in the diabetic ob/ob mice associated with mild inflammation [89]. Colitis is a pathophysiological condition characterized by upregulation of pro-inflammatory cytokines IL-1β, Interferon gamma, TNFa and IL-6. These effects of pro-inflammatory cytokines signalling are tightly regulated by antigen presenting cells like, dendritic cells and macrophages. GPR81 diminishes the aforementioned response by precise regulation of immuno regulatory factors. GPR81 expressed in colonic dendritic and macrophages mediated reduction of Th1/Th17 cell differentiation and a corresponding increased expression of IL-10, RA

and IDO immunoregulatory factors. Thereby regulating intestinal homeostasis by reducing inflammation. PPARy mediated signalling regulation of GPR81 in APCs may contribute to its anti-inflammatory effect [90].

GPR81 and retina

GPR81 expression in retina is mainly restricted to retinal ganglion cells, retinal pigmental cells and muller glia. Recently the protective role of GPR81 via Wnt/Norrin signalling was well elucidated in the pathophysiological condition of retinopathy of prematurity (ROP) [91]. The absence of GPR81 caused a significant time and age dependent decrease in inner retinal vasculature, with a corresponding decrease in norrin, wnt ligands and its cognate receptors frizzled (FDZ), low density lipoprotein receptor (LRP-1). Furthermore, in pathophysiological condition like ROP, there was a significant increase in vaso-obliteration and neovascularization in the GPR81 deficient mice. This classical ROP phenotype was rescued by subretinal LV injections of Norrin in the GPR81 deficient mice, indicating GPR81 regulated norrin expression was sufficient to promote pro-angiogenesis, thereby preventing vaso-obliteration and subsequent neovascularization. The scientists further were able to elucidate that GPR81 mediated norrin regulation was dependent on ERK1/2 pathway [91]. Furthermore, activation of GPR81 by lactate resulted in increased survival of Muller glia. The dual role of lactate as a metabolite and signalling molecule contributes to the aforementioned survival of Muller cells. Metabolic effect is directly related to increase mitochondrial metabolism. As a signalling molecule via interaction with GPR81 it increases the expression of MCTs, therein, increasing the intracellular concentration of lactate, which is used as a primary energy substrate [92].

GPR81 and Brain

Although GPR81 is lower expressed in the brain as compared to the adipocytes, its role in neuronal signalling has been well elucidated. Lactate shuttling into neurons from astrocytes is a

prime source of energy for neurons to promote neuronal excitability. With the use of KO mice of GPR81 it was evident that GPR81/ lactate interaction decreases neuronal excitability as compared to the KO mice. GPR81 mediated this effect via Gi protein signalling reduction of adenylyl cyclase, cAMP and protein kinase A activity. In addition, interaction of GPR81 with adenosine receptor, GABAa and a2 adrenergic receptors contributed to the fine-tuning of the neuronal firing [93]. Indeed to support the aforementioned result, Bozzo et la, were able to deduce GPR81 specifically reduced neuronal firing in the cortical neurons. This was evident with a decrease in calcium spiking frequency upon lactate and 3,5 DHBA treatment[94]. Indeed, to determine the GPR81 effect is mediated to Gi coupled proteins; primary neuronal cells were incubated in the presence of pertussis toxin (PTX), (potent inhibitor of Gi activation). The results showed there was a significant reduction in neuronal firing frequency in the GABAnergic and principal glutaminergic neurons solely with lactate treatment, on the contrary the effect was completely nullified with pre-incubation of PTX. Bacterial meningitis, a pathophysiological condition associated with inflammation associated with increased infiltration of leukocytes, production of pro-inflammatory cytokines and eventually neuronal cell death. LPS injections in mice have found to disturb the integrity of the blood brain barrier (BBB) by reducing the microvasculature integrity of endothelial cells. This is attributed to increased secretion of pro-inflammatory cytokines (IL-1β, IL-6 TNF-α and chemokines)[94]. Apparently, LPS also increases lactate production and via GPR81 stimulates mitochondrial biogenesis. Boitsova et al elucidated that LPS induced a decrease in GPR81 and MCT-1 expression leading to loss of BBB integrity, indicating that GPR81 plays a vital role in maintaining tight JAM junctions of BBB and thereby preventing subsequent leakage[95].

2.2 LACTATE: A ligand for GPR81

Lactate was first discovered in 1780 and isolated by Carl Wilhelm Scheele from milk. The *old paradigm* was based on the fact lactate produced from glycolysis lacks function in the

organism other than contributing to pathological muscle acidosis during high intensity exercise [96]. Berzelius, a Swedish chemist in 1808, proposed lactic acid as an energy donor in muscle contraction [97]. It was considered to be a metabolically inert product with no physiological role at the molecular level. However, in late 1940s, Embden and Meyerhof elucidated the glycolysis pathway and determined that there are high levels of lactate accumulation in hypoxia. In last 4 decades of research it has become more evident that lactate plays a crucial role in as a signalling molecule and is contributed in several pathophysiological conditions[98]. Daily normal lactate circulation in the human body is about 1500 mM, the main contributors are skin, skeletal muscles, brain, RBC and intestine. The excess lactate is cleared from the blood by the liver via a process of gluconeogenesis (conversion to glucose) and ATP production (oxidative phosphorylation, kreb cycle) [99]. Lactate transported is facilitated across the cell membrane by several monocarboxylated transporters (MCTs). Out of the 14 MCTs discovered, MCT-1 to MCT-4 are well studied. These primarily transport monocarboxylates, like lactate, pyruvates, acetoacetates and B-hydroxybutyrate. MCT-1 are more prominently expressed in major organs like brain, kidney, liver and skeletal muscles. As mentioned in detail before, lactate activates GPR81 with an effective concentration of 1mM to 5 mM. In, addition higher concentration of lactate from 10mM to 30mM in pathophysiological conditions of cerebral hypoxia and cancer have also found to activate GPR81 [100].

The *new lactate paradigm* on the contrary challenged the old believe that lactate is merely an excretion product. Rodergs et al proposed that all carbohydrate metabolites including lactate of glycolysis have low pK at the body pH levels and exists in their basic forms[101]. The signalling effect of lactate was evident with studies in muscle fibers. Muscles fibers are further classified into:

1. Glycolytic fibers

During high intensity exercise, the glycolytic fibers promote glycolysis leading to catabolism of glucose to increase production of pyruvate. However, increased consumption of pyruvate by glycolytic fiber leads to production of lactate with aid of the enzyme lactate dehydrogenase A (LDH A). The lactate is then transported out of the cell fibers by MCT-4. The lactate in the intercellular space is later taken in by oxidative fibers with help of MCT-1[102].

2. Oxidative fibers

Lactate in the oxidative fibers is converted into pyruvate by the enzyme lactate dehydrogenase (LDH B), which further enters into aerobic oxidative phosphorylation. Hence export of lactate out of the glycolytic fibers, protects them intracellular acidosis and at the same time acts an energy source by oxidative phosphorylation. This lead to the generation of lactate shuttle (Astrocyte-Neuron lactate shuttle hypothesis) theory, wherein lactate can act as a signalling molecule and has the ability to be produced in cells and tissues away from their site of action [102,103]. The molecular mechanism of ANLSH is based on the ability of neurons to produce glutamate after neuronal firing. The glutamate is taken up by astrocytes via Na transporters. Increase production of glutamate results in increase uptake of glucose and increase activation of Na-K Atpase pump and glutamine synthetase. This causes an increase in lactate export out of astrocytes into extracellular space, which is taken up by neurons as an energy source. Although this proposed mechanism is perfectly sound for glutaminergic neurons, its role in non-glutaminergic neurons has to be well elucidated[104].

2.2.1 Role of Lactate as signalling molecule

Lactate and HIF: Hypoxia inducible factor (HIF) 1a and 1b production is directly dependent on lactate. Under normal oxygenated conditions, HIF1a is hydroxylated by prolyl hydroxylases. The hydroxylated HIF1a is recognized by Van hippel lindau ubiquitin ligase (VHL) for ubiquitination-mediated degradation. However, during hypoxic condition the inhibition of prolyl

hydroxylase, which decreases HIF-1a degradation and promotes increased HIF mediated gene expression. HIF-1a promotes increased expression of glycolytic, and pro-angiogenic genes [105].

Lactate and inflammation: Immune dendritic cells, when treated with lactate increased anti-inflammatory productions of interleukin-10 (IL-10) and decreases pro-inflammatory cytokine productions of IL-12 mediated via Toll-like receptor stimulation of LPS. A similar effect of lactate on natural killer cells resulted in decreased cytotoxic activity of NK cells via downregulation of NKP-46 (NK activating receptor). Indeed, NMDA receptors in neurons also play a major role in anti-inflammation. However, it would be interesting to elucidate if NMDA and GPR81 synergistically are responsible for controlling secretion of anti-inflammatory cytokines [106].

Lactate and memory formation and neuroprotection: Lactate plays a crucial role in synapse formation and synaptic plasticity. By activation of Arc, cFOS, Zif268 genes lactate modulated the expression of NMDA receptor (receptor critical in long term memory and learning). The expression of NMDA receptor at the molecular level was associated with increased cellular NADH, intracellular calcium activation and ERK1/2 activation. Impaired cognitive function associated with acute and chronic stress is related to increased cAMP levels. Similarly, aging is concerned with increased expression of glutamate receptor and over activation of glutamate signalling. Lactate via GPR81 activation can reduce cAMP and glutamate mediated signalling and would be a potential target to prevent memory decline and senile dementia [107].

Lactate and synaptic plasticity: Synaptic plasticity is a unique feature of the central nervous system wherein; the strength of synapse formation between two or more neurons confers the neural basis of memory formation and storage. Memory can in layman term, be divided into short term and long-term memory. Synaptic plasticity can be further divided into functional

(related to efficiency of neuronal signalling transmission) and structural (related to information storage) memory. With the aid of electrophysiological recordings, changes in function synaptic plasticity can be elucidated on the basis of long-term depression (LTD) and long-term potentiation (LTP). Generally, LTP is associated with formation of stronger and larger synapsis and dendrite spines. On the contrary, LTD is associated with weaker and smaller synapsis. Experiments with lactate have shown that at physiological concentration, lactate can induce expression of key synaptic plasticity genes (BDNF, Arc and Zif268). Indeed, lactate was able to abrogate the blocking effect of 1,4-dideoxy-1,4-imino-D-arabinitol (DAB) on LTP when injected into the hippocampus (DAB specifically inhibits glycogen transport rather than glucose metabolism). Peripheral administration of lactate was also able to produce anti-depressant effects associated with dysfunctional synaptic plasticity. Microglia has been shown to play a major role in modulating synaptic plasticity via secretion of TNFα in the model of fear memory. Indeed, lactate can also affect synaptic plasticity by maintaining pH homeostasis [108].

Lactate and angiogenesis: Lactate in the presence of oxygen was found to initiate formation of mature blood vessels. This was evident when lactate polymer was implanted to improve wound healing. There was a substantial increase in collagen deposits, along with increase expression of angiogenic factors like VEGF, TGFB, and lowering of IGF-1. Indeed, the concentration of lactate was found to increase from 6mM to 9mM. These results were indicative of the fact the lactate participates in wound healing process via production of angiogenesis, and also participates in redox control mechanism. Lactate mediates the redox system by tricking the cell to believe that it's in a hypoxic state leading to formation of HIF1a. Furthermore, lactate also reduces ADPRibosylation pathway resulting in increased angiogenesis and collagen deposition. Collagen deposits are essential for vessel maturation and without it, results in vessels which are weak and leaky as seen in diseases such as scurvy [109]. The question how lactate modulates certain signalling transduction pathways to promote angiogenesis was also elucidated in endothelial

cells. It was determined that lactate via tyrosine kinases activation of Axl, Tie-2 and VEGFR2 enhances phosphatidylinositol-3-kinase (PI3K)/Akt pathway. Increased activation of the aforementioned receptors were essential in proper lumen formation and vessel sprouting. Indeed, lactate also increased production of proangiogenic ligands Gas6, angiopoietin and VEGF [110].

2.2.2 Warburg Effect

Otto Warburg discovered the Warburg effect in 1920s. The effect was mainly studied in cancer cells where Warburg and his colleagues found that tumors cells had high rate of glycolysis as compared to normal cells and interestingly, glucose was converted to lactate by cancer cells even in the presence of oxygen, which he termed as aerobic glycolysis. This ground-breaking work was further confirmed by Herbert Crabtree, who further discovered that tumors are heterogeneous and have different rate of aerobic glycolysis[111].

Although it is widely accepted that oxidative phosphorylation is more energy efficient in producing ATP from a single molecule of glucose, the rate of glucose metabolism by glycolysis is 100 times faster than mitochondrial oxidative phosphorylation. Hence for a given time the ATP production by glycolysis will be similar to oxidative phosphorylation[112]. With the advent of genomics and pharmacological studies it was unequivocally proved that Warburg effect is necessary for the survival of cancer cells. Besides, uncontrolled cell proliferation is a hallmark of cancer progression and hence to support increased proliferation high rate of glycolysis can contribute to de novo lipid synthesis via the pentose phosphate pathway. High glycolysis rate is also associated with increased production of NAD+ from the conversion of pyruvate to lactate. At the cell signalling level the Warburg effect also modulates the production of reactive oxygen species (ROS) [113]. The sufficient levels of ROS are maintained by redox potential in the cells via NADH. Glycolysis is able to maintain the NADH balance via malate-aspartate shuttling through the mitochondria [114]. Indeed, increased pentose phosphate pathway and denovo serine metabolism is responsible for the production of NADPH and glutathione which also regulate ROS levels[115].

Moreover, there is increase DNA repair and gene transcription in the cancer cells due to increased histone acetylation and increased activity of enzyme called ATP citrase (aids in conversion of citrate to acetyl COA). These studies have suggested that there is a direct link in between DNA chromatin structure and glycolysis [116].

The Warburg effect hence also is applied to other pathophysiological conditions that are attributed to metabolic dysfunction like cerebral hypoxia to further elucidate the underlying functioning and cellular mechanis

2.3 The Brain

The brain, a master regulator of the body is a highly complex and an extraordinary organ in the central nervous system. The brain is capable of performing diverse functions, ranging from simple proprioception, to complex ones of decision-making, thought processing and critical thinking. Structurally, the brain is divided into three major parts: **cerebrum, cerebellum,** and **brain stem.**

2.3.1 Cerebrum

The cerebrum is the largest part of the brain, which is divided into two hemispheres. The cerebral hemispheres are further divided into four lobes each specialized in performing specific functions. **The frontal lobes** are located in the anterior parts of the cerebral cortex. It is responsible for co-ordinating body movements, speech (Broca's area) and complex cognitive tasks. The latter function is performed in conjunction with sensory and motor cerebral association cortices of parietal lobe. Injury to the frontal lobe impairs creative thinking, speech, contributes to personality changes and affects language learning in an individual. Furthermore, there is significant reduction in executive functions associated with reduced decision-making ability, attention span and future planning. Less common side effects seen in frontal cortex damage are attributed to confabulation, reduplicative paramnesia and capgras delusion. Indeed,

pathophysiological brain conditions such as, schizophrenia, depression and obsessive-compulsive disorder have been associated with abnormal frontal cortex functioning [117,118].

The parietal lobes are situated posterior to the frontal lobes and superior to the occipital lobes. Their major function is to receive and process sensory information by the somatosensory cortex located in the parietal lobes. In order words, the parietal lobe is responsible for object recognition (2D, 3D discrimination, graphesthesia, localization) via sense of touch. In association with other lobes of the brain, the parietal lobe carries out specialized function of spatial recognition, precise navigation, performing complex mathematical calculations and processing writing and reading information. Damage to the specific parts of parietal lobe can causes number of difficulties. For example, lesion in the dominant hemisphere of parietal lobe contributes to dyslexia, apraxia, agnosia, and problems associated with performing mathematical calculations [119]. On the contrary, damage to the non-dominant hemisphere results in spatial disorientation and anosognosia [120].

The temporal lobes are located anterior of occipital lobe and inferior to frontal and parietal lobes. Their main functions are associated with hearing and contain the primary auditory cortex, which is responsible for converting the sensory inputs into precise speech and words. The auditory inputs from the cochlea are also processed in the primary auditory cortex, relating the information to cerebral cortex [121]. In, addition the temporal lobes perform complex visual functions, spanning from face to object recognition [122]. In conjunction, with the Broca's area of frontal lobes the temporal lobes Wernicke's area performs the complex speech comprehension function. The temporal lobes also contain the hippocampi, which are essential for memory storage[123]. Damage to the temporal lobes are associated with difficulty in speech, visual agnosia, anterograde amnesia and complex hallucinations [124].

The fourth lobes are called the *occipital lobes*, which are located in the posterior part of the brain contains the primary visual cortex. The visual cortex is further divided into ventral and dorsal streams each containing visual areas. The V2 and V5 visual cortical areas in the ventral

stream are responsible for storing vital sensory information in memory. The dorsal stream (V3 and V5 visual cortical areas), in turn processes this information to respond to external stimuli [125]. Lesions to the occipital lobes results hemianopsia vision loss, visual hallucinations, agraphia and idiopathic epilepsy [126].

2.3.2 Cerebellum

The cerebellum is located under the two cerebral hemispheres and makes up a large portion of the hindbrain. Cerebellum is functionally connected to the cerebrum via tentorium cerebelli, and via pons with other parts of the brain. The pons and cerebellum together are called metencephalon, like the cerebrum the cerebellum is divided into 3 lobes, the anterior, posterior and flocculonodular lobes[127].

The anterior lobes are responsible for maintaining unconscious kinaesthesia, also referred to the sixth sense of the body.

The posterior lobes, are connected to the cerebral cortex and brain stem and receives sensory inputs from the same. The main function of the posterior lobe is to inhibit involuntary movements via GABA inhibitory neurotransmission. Indeed, it also functions in regulating fine motor co-ordination [128].

The flocculonodular lobes, consists of a floccule and a nodule and receives sensory inputs from the vestibular and visual neural networks from the cerebrum. This information is translated in the flocculonodular lobes to regulate body posture, balance and eye movements [129].

2.3.3 The Brain Stem

The brain stem, the lower part of the brain located below the cerebrum, consists of three major parts: (a) Midbrain, (b) Pons and (c) Medulla oblongata[130].

Midbrain: (upper part of the brain stem). The main function of midbrain is associated with receive inputs from sensory organs such as eyes and ear, owing to which it controls

involuntary eye movements along with visual and auditory sensory reflexes. Indeed, it also relates information concerning wakefulness to hypothalamus, thalamus and forebrain thereby playing a crucial role in maintaining sleep and wake cycles[131].

Pons: This middle part of the brain stem, which is connected to cerebellum, it forms integrated circuitry with the inner ear thereby maintaining balance function. Furthermore, it also modulates pain sensation radiating from facial nerve endings.

Medulla oblongata: The lower part of the brain stem is concerned with controlling vital body functions ranging from sneezing, coughing and vomiting to modulating heart rate and breathing [132].

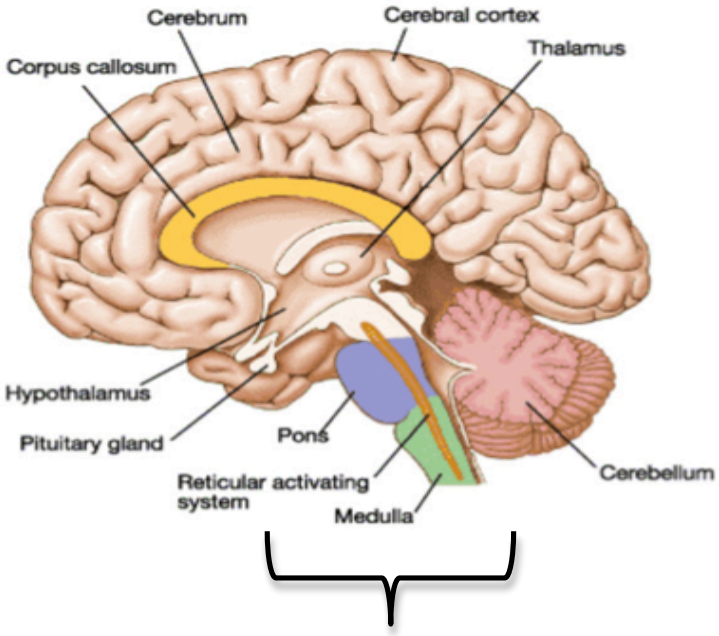

Figure 2.2 Brain Anatomy

Brain consists of three major parts namely the cerebrum, cerebellum and brain stem. These subdivision works in unison to co-ordinate voluntary and involuntary actions necessary for organism survival

2.4 Cerebral hypoxia or stroke

Cerebral hypoxia is the fourth leading cause of death in North America. In 2017, about 283,000 people were killed by stroke and there were 700,000 new stroke cases reported. It is reported to be one of the most debilitating diseases associated with long term complications like cerebral palsy and mental retardation[133].

Cerebral hypoxia is divided mainly into 3 categories:

1. Diffuse Cerebral Hypoxia
2. Focal Cerebral Hypoxia
3. Global Cerebral Hypoxia[134].

Out of the aforementioned categories ischemic stroke leading to reduction in cerebral blood flow (CBF) is more common contributing to 61% of the total stroke cases. There are multiple causes of the same, reduction of CBF due to cardiac arrest, occlusion of cerebral arteries and systemic hypotension. During a primary insult prolonged deprivation of cerebral blood flow to the brain results in substantial decrease in glucose and oxygen supply to the neurons and accumulation of toxic substances. At the molecular level neurons are deprived of energy due to reduction in ATP, and subsequent energy failure. Ischemic insults can further be divided into focal/global and permanent/transient [135].

Neurons show a predominant susceptibility due to restricted blood supply to the brain. CBF reduction of 25ml/100g/minute in rodent was found to be enough to cause cell death. The severity of ischemia and duration play a vital role in cellular vulnerability. Short burst of ischemia causes specific neuronal death while long exposure leads to ischemic infarction involving endothelial, astrocytes and microglial cell death. In clinical aspects the penumbra is the most important region after an ischemic insult. Penumbra can be defined as the region

surrounding the ischemic insult which is highly metabolic active and contains an unique mixture of ischemic neurons and healthy neurons which can be rescued if angiogenesis is restored [136].

2.5 Animal models to study stroke:

It is utmost important to choose an appropriate model to study focal or global cerebral ischemia, to understand the in-depth mechanism and provide a neuroprotective strategy. Although many therapeutic pharmacological agents have been tested in clinical trials, unfortunately, many of them have failed due to complexity involving drug administration, low therapeutic window, length and duration of ischemia, age, gender differences etc[137]. Indeed, improper clinical trial designs have confounded the underlying problem. In order to design an appropriate model, we need to clearly differentiate between global, focal and multifocal ischemia[138].

Global Ischemia: In global ischemia there is a substantial reduction in the cerebral blood flow throughout the entire brain. The main cause can be associated to cardiac arrest, hypotension and significant blood loss due to accidents[139]

Focal Ischemia: Is characterized by reduction in blood supply to a specific part of the brain. This can be due to formation of blood clots or blockage of carotid artery[140].

Multifocal Ischemia: In multifocal ischemia there is intermittent reduction of cerebral blood flow. The main aim of a cerebral hypoxic model is based upon reducing oxygen and glucose supply to the brain[141].

2.5.1 Model of Focal cerebral ischemia*:*

This model is focused on occlusion of middle cerebral artery (MCAO) in small animals like mice and rodents. This occlusion can either be permanent or temporary depending upon the type of injury that is out to be studied. Permanent MCAO model resulted in a decrease of CBF of 25ml/100g/min causing substantial histological aberration in the region with reduced blood flow. In case of model of reperfusion injury, the common carotid artery is temporarily occluded with a

help of a stent, which is removed at further time to allow blood flow. However, the infarct size was not consistent in the cerebral cortex [142].

Indeed to the combination of models mentioned above, researchers have also tried a photochemical MCAO model. This model uses an argon-based laser beams which irradiates various branches of cerebral arteries. Although this model provides a much consistent infarction, the potential disadvantage is associated with destruction of microvasculature due to photo bleaching.

Another non-invasive method consists of an insertion of a nylon suture into the carotid artery and pushing the thread forward upto 20mm up towards the cranium to block the middle cerebral artery. The nylon suture can be coated with poly-L-lysine to ameliorate the adhesion of the suture to the endothelium, which in turn also improved the consistency of infarction. The advantage of the model is that it is well suited to perform a reperfusion injury simply by removing the thread [143,144]

2.5.2 Models for global ischemia:

Neonatal hypoxic ischemia (HI) or hypoxic ischemia encephalopathy (HIE) in clinical terms refers to asphyxia of the umbilical cord in the humans leading to restricted blood flow to the foetus. This leads to traumatic brain injury or stroke in the neonates which is termed as HIE.

During the 1980s, neck cuff technique was introduced which involved venous congestion and vagal nerve compression resulting in variable ischemic insult. However, the neck cuff occlusion of vertebral arteries was necessary to promote an ischemic insult. Another modification of cuff technique involved reduction of arterial blood pressure before cuffing the animal. However, the ischemia produced by this method had the disadvantage that vertebral and spinal arteries are not occluded leading to incomplete ischemia [145].

By far the most efficient and reproducible model for global ischemia is ventricular fibrillation. The model is based upon induction of cardiac arrest, followed by pulmonary

resuscitation CPR and a dose of epinephrine after 10 min of cardiac arrest. This process results in reduced cerebral blood flow to the brain as compared to the control. The technique is reproducible but requires intensive care monitoring of animals (dogs and pigs) after inducing cardiac arrest. Using ventricular fibrillation can also cause ischemia to other organs. In other to specifically induce ischemia in brain, ventricular fibrillation is combined with occlusion of cephalic arteries (neck and thorax). This modification completely abolishes ischemia to other organs (kidneys and liver) [146].

In 1979, a reversible cerebral ischemic model was developed called four-vessel occlusion model (4-VO). This required a two-stage surgery; initial stage included loose attachment of common carotid artery followed by the second state involving the occlusion of the vertebral arteries. The disadvantage was there was variable ischemic injury owing to difference in rat strains. The advantage on the other hand was reduced cerebral blood flow to 3 % and specific injury to various part of the brain depending upon the extent of ischemia. For example, a 30 min ischemia resulted in striatal neuronal injury while an exposure to 3 to 6 hours resulted in injury to the hippocampus after reperfusion [147].

An alternative to 4-VO model was a 2-VO model, characterized by simultaneous induction of ischemia and reperfusion. Unlike the 4-VO model, the 2-VO model involves bilateral carotid artery occlusion coupled with bleeding (to induce hypotension) resulting in reversible forebrain ischemia. In this model there was a reduction of CBF of 5% in the cerebral cortex after 15 min of ischemia. The injury obtained during this model was localized to neurons of hippocampus, caudoputamen and neocortex. A potential advantage of 2-VO method over the 4-VO model is attributed to a relative simple surgery with an added possibility to induce reperfusion and it is more suitable to study chronic effects of cerebral ischemia. The disadvantage on the other hand is that it may require the use of hypotensive drugs that may obscure data interpretation [148].

2.5.3 Neonatal Hypoxic-Ischemic model:

Although, the above-mentioned models have shed tremendous light on understanding the cellular functions of cerebral hypoxia, these models are not suitable to study neonatal cerebral hypoxia, owing to difference in brain maturation and more susceptibility to an HI insult. Hence an alternative HI model was developed by Rice and Vannucci to determine the underlying causes of HI insult in neonates. The model was adopted from Levine HI model in adults. It was been proposed that P7 mice brains are equivalent to a preterm human infant. Briefly, Rice-Vannucci model is based on unilateral ligation of common carotid artery in P7 mice under general anaesthesia, followed by a recovery period of 2 hours[149]. The pups are then exposed to hypoxia of 8% oxygen in a chamber where the body temperature is maintained at 37C for a period of 2 hours. It is utmost necessary to expose the pups to hypoxia after unilateral carotid ligation since ligation alone does not contribute to ischemia due to compensatory blood flow of circle of Willis between cerebral hemispheres. The HI injuries to the brain are time sensitive to the hypoxic exposure. Researchers have elucidated that exposure of 45 mins causes selective damage to the hippocampus while an exposure of 60 min resulted in infarction to the hippocampus, striatum and the cortex [150]. In our experiments we injected lactate intracerebroventricularly at P4 in order to assess the prophylactic and pre-conditioning neuroprotection effect of lactate via GPR81 signalling. The main cause of infarction is attributed to glutamate excitotoxicity and oxidative stress. Although Rice- Vannucci model is considered to be gold standard for neonatal HI insult, the injury does not precisely mimic the white matter injury in humans. This is important to take into consideration for studying pathophysiological conditions of cerebral palsy (CP). CP is characterized by prominent damage to the white matter with earlier maturation of oligodendrocytes. Rice-Vannucci model have shown to have injury-associated infarction in both white and gray matter [151].

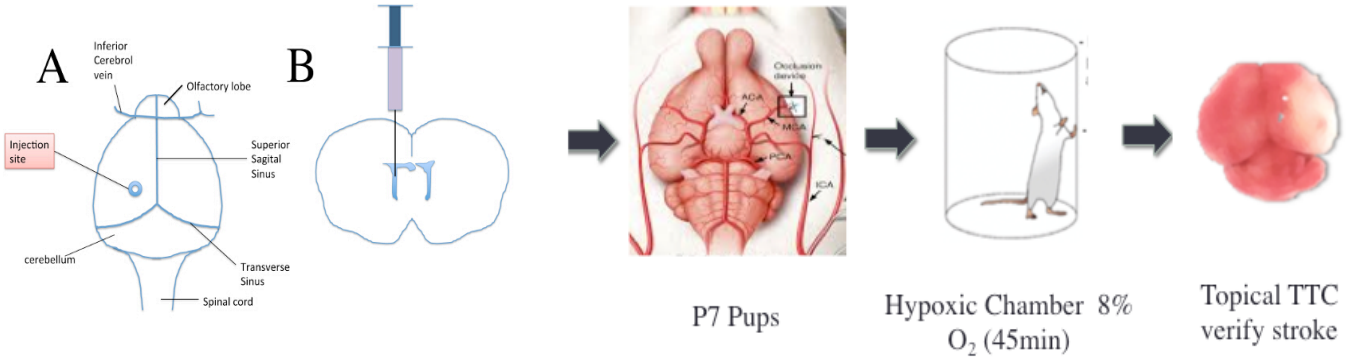

Figure 2.3 The Rice-Vannucci model.

In our experiments, A and B intracerebroventricular lactate injections were performed at on P4 pups, followed by permanent artery occlusion and hypoxic insult at 8% oxygen and 45 mins. The brain infarction was determined by topical tetrazolium chloride (TTC) staining.

2.6 Causes and therapeutic current interventions for neonatal cerebral hypoxia

Clinicians normally use neonatal encephalopathy (NE) to differentiate from HIE in the fact that it HIE has a known etiology whereas NE does not have a known cause. In order to improve the therapeutic interventions in HIE it is utmost necessary determine the underlying causes of HIE. The most common causes are mentioned below:

1. Congential disorders of cardiovascular system.

2. First line pathological conditions such as cardiac arrest leading to HIE.

3. Genetic disorders such as epilepsy, seizures and neurometabolic disorders.

4. Antepartum risk factors include maternal hypotension, emergency caesarean surgery, and obesity (BMI > 40 kg/m^2).

5. Other known causes are uterine rupture, (pregnant mothers who have undergone previous caesarian surgery are more susceptible), breech presentation, placenta previa and abrupto placenta [152].

The diagnosis is based on certain clinical parameters; these include 5 min apgar scores, delivery tube intubation, umbilical cord arterial pH, lack of sucking and hypotonicity of the

muscles. Indeed, electroencephalography (EEG) and magnetic resonance imaging (MRI) have contributed immensely to the clinicians in determining the neurodevelopmental outcomes of a neonate after a HIE[153].

Neuroprotective strategies to manage HIE

The majority of the drugs or therapies have focused to ameliorate HIE conditions by targeting the secondary energy phase failure. The main goals are associated with reduction of glutamate-induced excitotoxicity (inhibit glutamate release, blocking glutamate receptor or increasing the uptake of glutamate by astrocytes), decrease inflammation and oxidative stress via reduction in production of pro-inflammatory cytokines and free radicals[154].

Moderate Hypothermia: Hypothermia is considered to be the most effective therapy in treatment of mild to moderate HIE. This is achieved by either by whole body cooling where the body temperature or selective head cooling wherein the temperature is dropped and maintained between 33.5C to 36C for a period of 72 hours, followed by a slow and steady rewarming to normal temperature, this is done to prevent pulmonary hypertension and seizures[155]. At the molecular levels moderate hypothermia works by reducing the free radical formation thereby reducing mitochondrial dysfunction leading to decrease apoptosis. Furthermore, the release of glutamate from neurons is drastically reduced resulting in decreased exictotoxicity. Indeed, overall oxygen demand of the brain is reduced sparring the cells from using more ATP. Moderate hypothermia results in reduced injuries to the CA1 region of hippocampus, putamen, basal ganglia, thalamus and the parasagittal cortex[156].

Randomized trials of 1440 infants subjected to hypothermia showed encouraging results in reducing mortality, cerebral palsy, cognitive delay functioning and blindness. On the contrary hypothermia was not effective in reducing deafness. Indeed, infants at 18 months age did have a significant neurodevelopmental disability. Moreover, the effect was very much restricted to infants who suffered moderate HIE. In cases, of infants suffering with severe HIE, moderate hypothermia was not effective. Hence to improve neurological disability and survival rate of

infants' alternative methods have to be developed or tested in a synergistic approach along with hypothermia[157].

Erythropoietin (EPO): Historically erythropoietin was discovered as a glycoprotein, which is produced by kidneys. The primary role of EPO is stimulation of angiogenesis. With the advent of research, it was determined that EPO is also expressed by neurons, astrocytes and oligodendrocytes, more specifically near the site of injury of an HI insult. It's been reported that there is an increased expression of EPO receptors along with EPO after 24 hours of insult. The neuroprotective mechanism of EPO is attributed to reducing inflammation and thereby edema by inhibiting the activity of aquaporin 4 channel (AQP4). Indeed, there is decreased apoptosis of astrocytes and neurons in the hippocampus thereby promoting neuronal survival via promoting axon regeneration[158].

Clinical trials of EPO have been carried out in a dose dependent manner. Lower dose of 500U/kg within 48 hours of injury with a continuous dose foe two weeks therein significantly reduced infant mortality till 18 months of age[159]. However, administration of higher dose of EPO 2500U/kg within 4 to 6 hours of the injury produced a far better and longer survival up to 6 months. Although promising results were seen at the clinical trials, mortality rate in infants suffering from severe HI was the same as the hypothermia. Furthermore, administration of higher dose EPO predisposes the infants to liver and kidney damage, hypertension, allergic reaction and thrombosis. There could a high possibility of have a synergistic effect of using EPO and hypothermia together, however this additive effect needed to be evaluated more precisely in the clinical trials[160].

Stem Cell therapy: The use of cord cells from the umbilical cord has been used in the ongoing clinical trials in infants who have suffered moderate to severe HI insult. The cord cells are sought to act by reducing inflammation via decreasing the activation of microglia, inhibiting

neuronal death resulting in reduced infarct size in hippocampus and cerebral cortex[161]. The potential limitation is associated with the large volume of cord cells required to produce the desired protective effect[162]. Further technological advances in reducing the volume size in conjunction with a large clinical trial will be needed to address the potential shortcomings.

Antiepileptic drugs: The use of antiepileptic drugs was proposed due to seizures and hyperactivity of neurons associated with increased release of glutamate by neurons, reduced uptake by astrocytes and hypersensitivity of the glutamate receptors[163]. Clinical trials of an antiepileptic drug topiramate were found effective in moderate HI insult in a dose dependent manner. The dose of topiramate 20mg/kg/day was more efficacious compared to 10mg/kg/day when administered within 1 hr of the ischemic insult[164]. The effect of another drug phenobarbital when used alone did not significantly reduced neurological outcome. However, when used along with hypothermia the effect was more pronounced in reducing the infarct size. The additive effect of topiramate and hypothermia however was not assessed.

Xenon: The effectiveness of this anaesthetic gas at 50% concentration was found to drastically reduce the infarct size in the neonatal mice, when administered immediately after the induction of HI insult. The mechanism of action of xenon was directly based upon decreased activation of NMDA, AMPA and kainite receptors by glutamate[165]. Xenon acts as a direct antagonist of glutamate by inhibiting the interaction of glutamate with NDMA receptors. Although xenon was efficacious in neonatal mice model, sole use of xenon in infants was not found to be effective[166]. However, when it was combined with hypothermia together for a period of 3 hr there was selectively injury to the thalamus, hippocampus and basal ganglia was significantly reduced. The probable hindrance to use xenon as a potential neuroprotective agent is attributed to its uneasiness of route of administration and cost[167]. However, the potential advantage

is that xenon does not affect heart rate or blood pressure thereby reducing the potential side effects.

Docosahexaenoic acid (DHA): DHA is a long chain fatty acid, which is found in fish and fish oils. Research on neonatal HI animals has found to have a protective effect by reducing inflammation, oxidative stress and apoptosis[168]. Unlike the curative effects of all the already mentioned neuroprotective agents, DHA was administered 4hr before HI insult. This indicated that it could be used as a preventive molecule in preventing HI insult. Indeed, there was reduction in injury to hippocampus and a corresponding increase in brain volume[169]. These interesting preventing effect of DHA are yet to be monitored in human infants.

Cannabinoid Agonists: Agonist of cannabinoids activates cannabinoid receptor 1 and 2 (CB1 and CB2) present on the neurons. Activation of CB1 and CB2 receptors by an agonist WIN-55212 have proven to be neuroprotective in HI by reducing glutamate release from neurons[170]. The MRI images showed that viability of neurons drastically improved and the atrophy in the cerebral cortex was marginal when compared to the control.

Melatonin: Physiologically melatonin functions in controlling the circadian rhythm, however when used at a higher pharmacological doses melatonin possesses anti-oxidant and anti-apoptotic effect. Preclinical trials of melatonin on rodents resulted in 43% reduction in infarct size while in pig's melatonin along with hypothermia provided increased protection compared to cooling only [152].

Allopurinol: Allopurinol is marketed as a drug for gout, kidney stones due to its unique ability in reducing uric acid concentration in the body. Recently its role has also been tested in preclinical and clinical trials. In HI model of pig's allopurinol was found to reduce infarct size,

which was evident from MRI scan. In terms of clinical trials ALBINO trial in europe has started in 2017 to determine the synergistic effect of allopurinol and hypothermia with cooling alone. Allopurinol protective mechanism is based on scavenging free radicals and acting as a free iron chelator[171].

2.7 Molecular mechanism of neonatal brain injury

As mentioned earlier neonatal hypoxic ischemia is considered to be the main cause of neurological disability in children. The underlying cause of HI insult is complex and is attributed to the combination of different factors, including infection, inflammation and neuronal excitotoxicity. The brain injury hence can be divided into three different phases

1. Primary phase, 2 Secondary phase and 3. Tertiary phase.

The primary phase is characterized by increase in CBF in the first few hours of an HI insult, followed by a sudden decrease, due to vasoconstriction and reduced cardiac output. This results in increase cellular death via apoptosis and subsequent necrosis. Primary energy failure at the molecular level results in reduction in ATP production and increased lactate accumulation. Since CBF is restricted resulting in decrease glucose and oxygen supply to the neurons oxidative phosphorylation is arrested causing less ATP production and subsequent failure of Na/K pumps resulting in increased influx of Na ions into the cells. The changes Na and K ion concentrations results in direct depolarization neurons stimulating release of excitatory neurotransmitter glutamate with a parallel influx of calcium ions into the cell via the activation of Ca transporters [172].

The secondary phase normally occurs within days of the primary injury which includes an inflammatory response. The time period of 6 to 48 hours after initial injury is termed as secondary energy failure. During this phase there is aberrant production of inflammatory cytokines and free radical formation causing mitochondrial dysfunction and permeabilization.

Indeed, immature brains are high in lipid content, making them susceptible to lipid peroxidation. Since the neonatal brain have low antioxidants they cannot cope with these oxidative stress signal ultimately resulting in necrosis[16].

Finally, **tertiary phase** is associated with failure of repair mechanism due to inflammatory response and occurs after weeks to months of an HI insult. Each of these phases have different molecular mechanisms which have been studied in great details to better understand the underlying cause of HI [173].

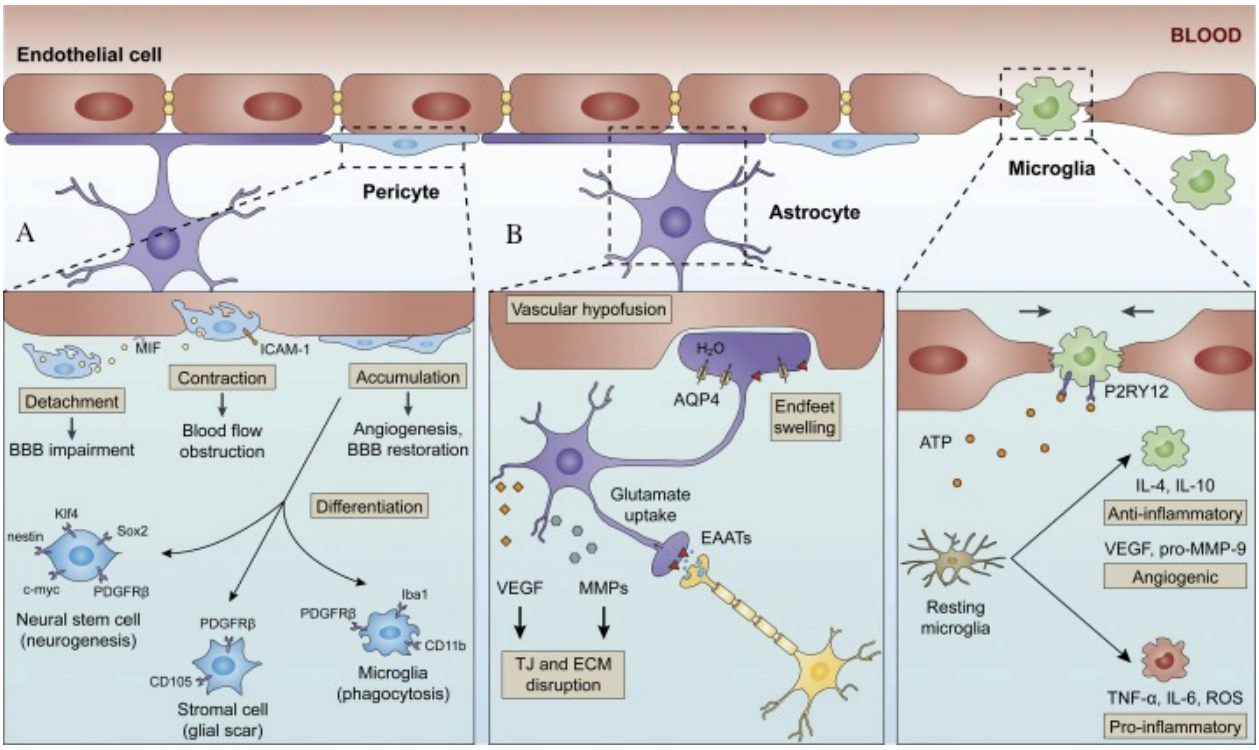

Figure 2.4 Blood Brain Barrier

A) An intact neurovascular unit showing a synchronized functioning between astrocytes, neurons and endothelial cells. B) Pathophysiological condition such as cerebral edema or hypoxia can contribute degeneration of neurovascular unit and promote endothelial cells remodelling in conjunction with other cells[274].

2.7.1 CNS excitotoxicity:

The primary injury to brain cells to neurons is due to post-synaptic toxicity. Increase in glutamate and adenosine neurotransmitters causes substantial neuronal depolarization due to reduced uptake of glutamate by astrocytes, resulting in increased concentration in the synaptic cleft and overstimulation of glutamate receptors. Indeed, since the expression of glutamate receptors, peaks during neonatal developmental phase contributing to excitatory synapse formation, any unwanted event causing an imbalance in the secretion of these excitatory neurotransmitters can lead to necrosis of neurons [174].

2.7.2 Free Radical formation and oxidative stress:

Increase damage to the brain via oxidative stress is due to formation of reactive oxygen and reactive nitrative species. Since HI insult results in mitochondrial dysfunction there is a significant increase in the generation of ROS. Nitric oxide (NO) is a free radical capable of performing diverse physiological roles from controlling the brain flow, to generation of mitochondrial ROS. NO is synthesized by nitric oxide synthetase in neurons (nNOS), endothelial cells (eNOS), astrocytes,microglia (iNOS). Following an HI insult there is increased in expression of eNOS and nNOS in endothelial cells and neurons leading to increased production of NO. Conditional KO of neuronal Nitric oxide synthase (nNOS) enzyme in the neurons has shown to be resistant to HI insult. On the contrary KO of eNOS mice were more susceptible to HI insult, mainly owing to its loss of protective effect on neuronal outgrowth and angiogenesis. Indeed, owing to the high lipid make of the brain, the brain is more vulnerable to lipid peroxidation. The formation of peroxynitrite (OONO), via interaction of NO and superoxide is detrimental to immature oligodendrocytes which contributes to selective white matter damage in neonates [175].

2.7.3 Mitochondrial Dysfunction:

During an HI insult the primary injury, which is characterized by decrease in ATP production that is followed with a brief recovery period before the start of the second injury. There is subsequent increase in free radical formation that affects the respiratory chain leading to cell death. Hence mitochondrial biogenesis and function is utmost important to consider in and apoptotic process of HI insult during the early primary phase of injury. At the molecular, an HI insult was sufficient to increase the production of AMP-activated protein kinase (AMPK) which ought to act as an energy sensor detecting subtle changes in AMP/ATP ratio. Activation of AMPK aims in increasing mitochondrial biogenesis via PGC1a and conserve energy by inhibiting fatty acid pathway and promoting glycolysis[273]. The mitochondria also have a unique ability to divide and fuse termed as mitochondrial fission and fusion respectively. The fusion proteins like cytochrome c decreases apoptosis while fission proteins DRP-1 on the contrary induces apoptosis via Bax leading to mitochondrial leakage and outer membrane permeabilisation [176].

2.7.4 Mitochondrial permeability (MP):

MP is mainly associated with the secondary phase of brain injury. MP induction in cell results in cell death due to leakage in the outer membrane and subsequent inner membrane of mitochondria. The translocation of Bax from the cytosol to the mitochondria and its interaction with Bak promotes the leakage of proteins into the cytosol leading to necrotic cell death. MP directly results in the release of apoptopic factors like apoptosis inducing factor (AIF), endonuclease G, cytochrome c and Smac/diablo. These proteins either promote apoptosis via caspase induction or independently, via translocation to the nucleus causing DNA damage. Smac/diablo on the contrary inhibits the action of inhibitors of apoptosis (IAP), which in turn promotes caspase mediated cell apoptosis[177]

2.7.5 Inflammatory cells:

During HI secondary phase injury, inflammatory cells like the microglia and mast cells produce pro-inflammatory factors (IL-1β, TNFα, IL-18, TWEAK, TRAIL, FasL). These ligands interact with their corresponding receptors (TNFR1, IL-1R, Fas, DR4, DR5) to activate the so-called extrinsic pathway of apoptosis. The formation of death inducing signalling (DISC) complex promotes the cleavage of pro-caspase 8 to active caspase 8, which in turn via caspase 3 converts Bcl2 activating domain to truncated Bid. tBid translocate itself into the mitochondria leading to necrosis via activation of intrinsic pathway. Indeed, to contributing to intrinsic and extrinsic injury via mitochondria, microglia are also responsible to exacerbate neuronal excitotoxicity by enhance the release of glutamate and nitric oxide (NO). Since HI insult results in a leaky BBB, microglia gain easy entry into the circulation producing pro-inflammatory cytokines, which synergistically contributes to increase excitotoxicity[178].

2.8 Brain angiogenesis

The earliest outline of a circulatory system by Leonardo da Vinci via analogy for vasculature was laid in from of a tree, where seed was the heart of the vasculatory system, the live capillary networks as the roots and the aorta and arteries depicting the branches of the tree. In scientific terms sprouting of blood vessels from pre-existing ones is termed as angiogenesis. However, it is well established that the primitive vascular system is laid down even before the heart is beating.

Vasculogenesis: The primitive vascular system is formed form the mesoderm by differentiating angioblasts. The precursor mesodermal cells differentiate into a bipotential precursor cell termed as haemangioblast. These cells lacks VEGF-R2 receptor and have a unique ability to differentiate into either the hematopoietic stem cells or angioblasts (expressing VEGF-R2) which continue to differentiate to form the primitive vascular plexus. The role of VEGF-R2 is sought to be essential during the earlier periods of angioblast differentiations while that of

VEGF-R1 play a vital role during the later phases[179]. The studies on VEGF-R1 KO mice revealed that there was no alteration in the production of angioblasts however; these mice did lack substantial functional blood vessels. VEGF ligand on the other hand acts in a paracrine manner, released from the endoderm and acting on receptors, which are produced from mesoderm. The questions related to what types of mesodermal signals are required to express VEGF receptors and VEGF, along with the how the bipotential haemangioblast commits itself to a specific lineage is yet to be answered [25,180].

Angiogenesis: The generation of new blood vessels or capillaries from pre-existing ones is termed as angiogenesis. There are two types of angiogenesis that are defined, first is sprouting angiogenesis and second, non-sprouting angiogenesis.

Sprouting angiogenesis: The first process of sprouting angiogenesis was studied in tumour angiogenesis in 1977. Ausprunk et al systematically devised four steps to explain sprouting angiogenesis in tumour cells. First step involves degradation of basement membrane near dilated venules. Secondly, there is a significant interweakning of connections between endothelial cells. Thirdly, in presence of certain chemotactic stimulation there is migration and proliferation of the endothelial cells and lastly, this is followed by lumen formation and solid maturation of the endothelium[181].

Pruning: The primitive vascular plexus once formed undergoes remodelling to for mature large and small blood vessels; this process is called as pruning. The endothelial cells have unique ability to migrate from their site of origin to different locations to differentiate into larger blood vessels such as dorsal aorta. These results confirm that endothelial cells possess plasticity during earlier embryonic and post-natal stages, which enables them to take part in the process of angiogenesis and vasculogenesis. The destination of endothelial cells is dependent upon angiogenic factors and antiangiogenic factors such as VEGFR2, VEGFR1, TIE1 and TIE2, along with their respective ligands[180,182].

Maturation and Remodelling: Blood vessel maturation is dependent various factors including shear stress associated with circulation. Shear stress strongly modulates endothelial cell junctions via upregulation of PDGF-BB. At the same time there is enormous remodelling of the basement membrane that is facilitated by pericytes and smooth muscle cells. In postnatal and adulthood, the endothelial cell maturation is regulated by other factors namely, transforming growth factor B (TFGb), fibronectin and integrins receptors. Indeed to the pro-angiogenic modulators the role of anti-angiogenic cytokines such as angiostatin and plasminogen also contribute to vascular remodelling [183,184].

Molecular Mechanism of sprouting angiogenesis:

Two main cells are sought to partake in the process of initiation of sprouting angiogenesis, these are the tip cells and stalk cells. The tip cells are characterized by presence of a polar charge and reduced proliferation, in contrast the stalk cells have high proliferation rate which are responsible for stable lumen formation and maturation. The activation and functioning depend upon critical and precise balance between angiogeneic and anti-angiogenic factors. These include VEGF, jagged 1 (JAG-1), delta like ligand (DLL-4) and notch activity. Tips cells highly express pro angiogenic receptors such as VEGFR2, DLL4, VEGF3, PDGF-B, Unc homolog b (UNC5b) and low levels of notch. The tips cells have unique ability to produce filopodia in mouse retina, which are directed towards an angiogenic stimulus such as VEGF. On the contrary stalk cells have maximum proliferation and functions in developing tubes, branches and well-developed lumen. Indeed, they form strong junctions with neighbouring cells and promote basement membrane formation [182].

VEGF and VEGFRs:

Tips cells filopodia has high expression of VEGFR-2 which upon stimulation of VEGF results in extensive outward migration of filopodia. The formation of filopodia is also stimulated by VEGF

by interacting with another receptor called cdc 42. VEGF also stimulated the production of DDL-4 from the tip cells which aid in generation of new blood vessels. On the contrary the expression of VEGFR-1 in conjunction with Notch-1 on the stalk cells diminishes the activity of VEGF on VEGFR-2 thereby reducing the migration of filopodia [185].

Notch and Notch ligands:

The effects of Notch receptors and its three known ligands DLL-4, JAG-1 and DLL-1 have been extensively studied on mechanism of vessel regression. The KO of Notch-1 signalling pathways results in pronounced vascular defects and embryonic lethality. Notch-1 is highly expressed on the stalk cells and its activation by its ligands results in reduced sprouting, which is a direct result of lower expression of VEGFR2 and VEGFR3 receptors on the tip cells. Tip cells have low Notch signalling with high expression of VEGFR2 and DLL-4 receptor leading to increase ability of becoming a tip cell compared to its neighbouring cells. Endothelial cells, which express high levels of VEGF, also have high expression of DLL-4, which induces the selection of this cell as the tip cell for migration. On the contrary stalk cells has high levels of Notch signalling activity along with high expression of JAG-1. JAG-1 expression directly antagonizes the activity of DLL-4 resulting in increased sensitization to VEGF of the neighbouring tip cells. Collectively, the fine-tuning angiogenic response of VEGF/VEGFR and Notch signalling contributes to precise and well-co-ordinated growth by sprouting angiogenesis[186]

Semaphorin 3E and Netrin-UNC5B signalling:

Semaphorins (SEMA) and netrins functions as guidance cues, which contribute to the negative feedback mechanism of vessel formation. SEMA4E is predominantly expressed by endothelial cells inhibits integrin functions to regress vessel growth. On the contrary SEMA4D have shown contributes to endothelial cell migration and vessel formation. SEMA4E interacts with plexin-D1 receptors on the tip cells thereby controlling the blood vessel formation by monitoring VEGF

activity. Netrins like SEMA4E functions in reducing the blood vessel growth via interaction with UNC5B receptor mediated signalling (Kim, J. 2011).

2.9 Brain Vasculature and Cerebral hypoxia

Cerebral vasculature degeneration during focal cerebral ischemia causes increased risk of edema and haemorrhage ultimately leading to irreversible brain damage. Since traditional approaches of treating vascular diseases such as hypertension and myocardial infarctions uses drugs (ACE inhibitors, angiotensin receptor blockers) to modulate vascular dysfunction. It is intriguing to determine if similar vascular rescue could occur in stroke[187,188].

Current therapeutic drug that is available for adult cerebral hypoxia is tissue plasminogen activator (tPA), however the therapeutic window for tPA is extremely low of 2 hours. Furthermore tPA results in reperfusion injury leading to haemorrhage[189,190]. Vascular deterioration is evident during the three phases of cerebral ischemia. During the acute phase, there is substantial BBB leakage and change is vascular tone leading to changes in blood perfusion and vasoconstriction. The vascular smooth muscle cells along with vasoactive factors such as vascular endothelial growth factor (VEGF), endothelin-1 and Nitric oxide (NO) contribute to the initial remodelling of the endothelial cells[191,192]. Endothelin-1 is a potent vasoconstrictor, which modulate and promotes BBB leakage via regulating the smooth muscle function thereby, increasing influx of albumin and other high molecular weight proteins leading to cerebral edema[193]. VEGF on the other hand improves endothelial cell integrity via NO production. However, during the acute phase of cerebral ischemia NO strongly reacts with superoxide to form a highly reactive species called peroxynitrite[194,195]. Angiopoietin-1 expression on the other hand decreases in the acute and thereby could have a protective effect on BBB integrity. Hence in acute phase of cerebral hypoxic insult the protective effect could be achieved by reducing the BBB permeability and free radical formation[196].

The subacute phase of cerebral hypoxia involves intense modulation at gene transcriptional level, mainly inflammation. There is a substantial increase in expression of endothelial cell proteins such as intracellular adhesion protein-1 (ICAM-1), E-selectins, P-selectins and tight junction proteins V-cadherins[197,198]. Inflammatory cells mainly leukocytes interact with these adhesion proteins promoting an inflammatory response around 24 hours after the initial insult. This increase in tight junction and gap proteins along with MMP-2 and MMP-9 degrade the vascular endothelium basement membrane[199,200]. As a result it suffers trauma via haemorrhage and further leakage of BBB. During subacute phase there is also a significant increase in VEGF, ANG-2 and FGF2, which can contribute extensively to modulate endothelial cells via a protective feedback mechanism aiding in reducing BBB permeability. Hence, in a subacute phase augmenting angiogenic factors and reducing inflammatory response mediated by infiltrating leukocytes, neutrophils and macrophages[201,202].

In the chronic phase cellular apoptosis of endothelial cells is carried out due to induction of apoptotic factors namely, B cell lymphoma-leukemia 2 (Bcl2)-associated X protein (Bax) and reduction of anti-apoptotic factors such as Bcl2 and inhibitor of apoptosis (Iap)[203,204]. Collectively, indicating the augmentation of antiapoptotic factors in the chronic phase of cerebral hypoxia as a potential therapeutic intervention.

Although the molecular mechanisms of the above-mentioned phases are well documented, clinically therapies for stroke in general have not been very successful. In order develop successful therapies its utmost necessary to understand the pathogenesis of stroke. The destruction of neurovascular unit and the blood barrier is main characteristics of stroke and should be taken into consideration, with an emphasis on understanding the cross talk between cells that make the neurovascular unit (astrocyte, neurons, macrophages and oligodendrocytes).

2.11 Retinal Vasculature

The major arterial blood supply to the retina is the ophthalmic artery, which branches out of the internal carotid artery. The ophthalmic artery further divides into posterior and anterior capillaries that provide blood supply to the posterior (vitreous humour, retina, choroid and optic nerve) and the anterior (cornea, iris, ciliary body and aqueous humour) parts of the eye. The vascularization retina is maintained by two blood vessels, retinal artery that branches out from the ophthalmic artery and the posterior choriocapillary arteries. The retinal artery further bifurcates into three layers forming the superficial, intermediate and the deep inner vasculature as shown in **Figure 2.5**. The retinal blood vessel provide the major supply to 3/4th of the retina, whereas the remaining 1/4th part involving the photoreceptors depend on choriocapillaries, wherein the oxygen diffuses across the blood to the photoreceptors [205].

The choroid receives blood supply from the choriocapillaries, which emerge out from ciliary arteries. The choroidal vasculature is divided into three layers that are served by choriocapillaries. The Bruch's membrane, the Sattler's layer and the Haller layers that make up the internal, middle and external parts of the choroidal vasculature. Since the choriodal capillary are sinusoidal and fenestrated their site is one of the highest site of blood flow in the retina contributing to 85% of the total blood flow in the eye [206].

Retinal vasculature in humans is completed just before birth, in contrast in rodents the retinal vasculature continues in the postnatal development and is completed matured after three weeks. Hence it's more feasible to use rodent namely, rats or mice to study the normal developmental and pathological vasculature as models for OIR [207].

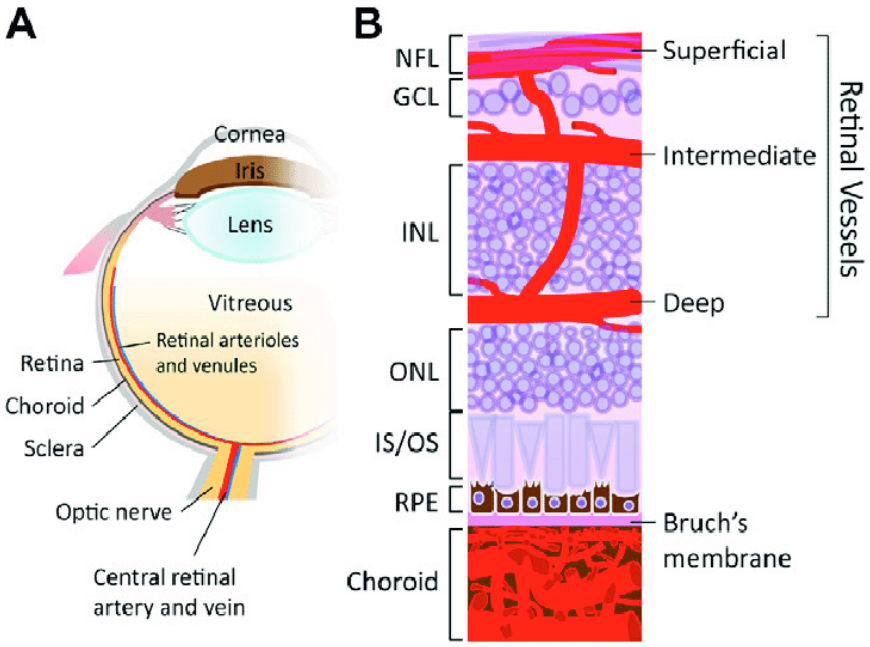

Figure 2.5 Vasculature of retina

A. The cross section of the eye showing different parts from the retina internally to cornea externally. B, cross section of the retina showing different layers from the choroid to nerve fibre layer (NFL) directing outwards to parts of the retina. GCL (ganglion cell layer), INL (inner nuclear layer), ONL (outer nuclear layer), RPE (retinal pigmented cells)[208].

2.12 Factors that regulate retinal vasculature

***Oxygen*:** As mentioned earlier oxygen plays a substantial and a vital role in regulation of normal as well as pathological retinal vasculature. During physiological hypoxia there is induction and increased expression of hypoxic inducible factor (HIF1a), which in turn promotes increased vascularization of the retina via VEGF production. This is mainly due to increased metabolic demand of the retinal glial and neuronal cells, which are actively proliferating and contributing to maturation of the retina. Physiological hypoxia is essential in these circumstances since it promotes angiogenesis and inturn improves oxygen and nutrition (glucose) supply to the developing cells. In contrast, in a pathophysiological condition such as retinopathy of

prematurity (ROP), diabetic retinopathy (DR) and age related macular degeneration (AMD) hypoxia plays a vital role in undermining the molecular mechanisms associated with the same.

Retinopathy of prematurity or ROP is a biphasic disease characterized by vaso-obliteration (VO) and neovascularization (NV). Since the *inutero* environment in the mother's womb is hypoxic compared to the *exutero* environment, there is a significant vessel regression leading to avascular area in the retina due to external hyperoxic enviornment. This effect is largely attributed to the suppression of pro-angiogenic factors of VEGF and erythropoietin. Moreover, as the retina matures it has a high metabolic activity leading to induction of hypoxic inducible factor (HIF) [209]. HIF in turn increases the production of angiogenic factors such as VEGF contributing to the second phase of ROP characterized by vessel destruction and tufts formation.

Diabetic retinopathy (DR) is one of the leading causes of blindness in young adults from age 24 to 50 years. Blindness associated with DR is most commonly associated with young adults, who suffer from diabetes mellitus I compared to diabetes mellitus II. DR is a pathological condition that is characterized by metabolic dysregulation and hyperglycemia (increase blood and urine glucose levels). At the vascular level there is increased microaneurysms, haemorrhages and microangiopathy leading to hypoxic induced angiogenesis resulting in increased production of VEGF resulting in pathological angiogenesis also termed as neovascularization. DR is further divided into non-proliferative or proliferative DR depending upon presence of neovascularization [210]. Non-proliferative DR is associated with microaneurysm causing extensive pericytes loss and subsequent haemorrhage. In contrast proliferative DR is characterized by neovascularization and vitreous humour haemorrhage leading to retinal detachment.

Age related macular degeneration involves choroidal neovascularization (CNV) wherein pathogenic angiogenesis contributed to invasion of choriocapillaris blood vessels into the Bruch's membrane. The disruption of Bruch's membrane by CNV is the first step in AMD. This is

followed by entry of the blood vessels into subretinal space eventually leading to retinal detachment and blindness [211].

Vascular growth endothelial factor (VEGF)

VEGF expression is regulated by HIF1a and is subdivided into different isoforms such as $VEGF_{121}$, $VEGF_{165}$, $VEGF_{189}$ and $VEGF_{209}$. The action of VEGF on its receptor modulates its angiogenic or anti-angiogneic effect. For example, the activation of VEGF-R2 receptor promotes angiogenesis, while the activation of VEGF-R1 promotes an anti-angiogenic regression of blood retinal vasculature [212]. The reduction in oxygen levels leads to a direct increase in HIF1a which contributes to an increase in VEGF levels, resulting in pathological angiogenesis. Increase VEGF production is a direct result of reduced oxygen levels or tension in the retina. Moreover, VEGF, promotes increased expression of placental derived growth factor (PIGF). PIGF has shown to reduced the neovascularization in OIR model of mice thereby indicating a potential retinoprotective role of PIGF in ROP [213].

Erythropoietin (EO):

EO is a potent stimulator of angiogenesis and along with VEGF it promotes neovascularization in ischemic retina. The reduction of neovascularization by inhibiting EO and VEGF in ROP and diabetes retinopathy (DR) has been suggested therapies in the aforementioned pathologies. Moreover, EO and VEGF act via independent pathways and the fact that EO has neuroprotective effects, inhibition of EO should taken into cautious consideration before targeting EO as a therapeutic target [214].

Wnt and Norrin:

Wnt-Norrin signalling via frizzled4 promotes and regulates normal inner retinal vasculature in the developing retina. Norrin like Wnt ligands binds to frizzled4 (FDZ4) along with its co-receptor Lrp-5 and chaperone protein tetraspanin12 (TSPAN12) (Ye et al 2010). Norrin is predominantly secreted by muller glia and activates the Wnt canonical pathway. The canonical

Wnt pathway plays a vital role in CNS vasculature in maintaining the blood brain barrier (BBB) and blood retinal barrier (BRB). The canonical Wnt signalling pathways ligands Wnt7a, Wnt7b and B-catenin play important role in CNS vascular development. Mutations in Wnt ligands gens results in reduced endothelial cell migration in the CNS. Moreover, Norrin is a specific and high affinity ligand for FDZ-4 out of the ten frizzled receptors that have been discovered. The loss of decrease in FDZ4 expression results increased permeability in the BBB and BRB, as a direct result of decreased claudin-5 protein levels [215].

CHAPTER 3

MATERIALS AND METHODS

3.1 Cell Culture

RGC-5 cell line was kindly gifted from Neeraj Agarwal. RGC-5 cells were thawed and grown in normal (Dulbecco's modified Eagle medium; containing 5 mM glucose), supplemented with 2 mM L-glutamine, 100 U/mL penicillin/streptomycin, and 10% (vol/vol) bovine growth serum (BGS) in a humidified incubator with 5% CO_2 at 37°C. The doubling time of cells was determined to be 24 hours and the cells were passaged in 1:10 ratio. Cells were plated on poly-L-lysine coated cover slips in a 12 well plate for immunocytochemistry. For western blot and qPCR analysis, cells were plated in 6 well plates and subsequently treated with phosphate buffered saline (PBS; 137 mM NaCl, 5.4 mM KCl, 1.28 mM NaH_2PO_4, 7 mM Na_2HPO_4; pH 7.4) or 10mM lactate for 6 hours and 24 hours respectively. The cells were then collected in ribozol for qPCR and lysis buffer for protein analysis.

3.2 Cell treatment and differentiation of RGC-5

RGC-5 cells were passaged and plated accordingly in 12 well or 6 plates for ICC or qPCR or western blot purposes. Cells were not used for experiments after 12 passages. After adhering, cells were allowed to grow and differentiate for minimum of 20 hours. Before treatment with staurosporine (STSN), the cells were washed with sterile PBS thrice. The cells were then embedded in serum free media for 24h. After 24hrs cells were treated with 316nM STSN for another 24 hours and the differentiation of the cells was monitored under phase contrast microscope. Cells underwent substantial neurite formation after 24 hours, however similar neurite formation was also observed with 1mM STSN treatment for 6 hrs. The differentiated RGC-5 cells were treated with either PBS or lactate for another 6h to 24 h duration. After which cells were collected for performing qPCR, and conditioned media was used for invitro matrigel and aortic explants experiments.

3.3 Immunocytochemical analysis of RGC-5 protein expression

Cells that were subjected to immunocytochemical analysis, as mentioned above were plated on coated cover slips for a period of 24 hours until 80 percent confluent. The media was aspirated and the cells were washed with PBS twice at 5 mins intervals. Cells were treated and fixed with 4% paraformaldehyde (PFA) solution for 20 mins at room temperature. After fixation and subsequent washing with PBS for 10 mins, cover slips were permeabilized in 0.1% triton in PBS for another 15 mins, followed by 15min PBS washes. The cells were blocked in blocking solution of 1% bovine serum albumin (BSA), 1% normal goat serum (NGS) in 0.1% trition in PBS for 1 hour. The coverslips were further incubated in primary antibody solutions of Anti-GPR81 (Sigma aldrich) in 1:500 and anti-NeuN in 1:200 (EMD Millipore), prepared in blocking solution (1% BSA in 0.1% triton in PBS) for a minimum of 18h or overnight at 4C in a humidified chamber. Subsequently the cells were washed in washing solution (0.1% triton in PBS) for 10 mins each followed by incubation for 2 hr by secondary streptavidin conjugated Alexa-fluor antibody (Alexa-488, Alexa 594) 1:1000 in dark. Cells were further counterstained with the fluorescent nuclear binding label 4′,6-diamidino-2-phenylindole (DAPI; 500 ng/mL) for 5 mins and PBS washed with PBS for 15 mins. The stained cells along with cover slips were then transferred on to the microscopy slides with the help of mounting medium for immunofluorescence imaging. Images were captured using 20x and 40x objective with Eclipse E800 (Nikon) fluorescence microscope.

3.4 Electrophoresis and immunoblot analysis of RGC-5 protein

The stimulated RGCs were treated with lactate, U0126, anisomycin, epidermal growth factor (EGF), SB230359 to elucidate the role of lactate in ERK1/2 and P38 signalling transduction pathways. For ERK1/2 mechanism differentiated RGC-5 were pretreated with U0126 for 1h followed by lactate or EGF treatment for 15 mins. The cells were washed with ice cold PBS and scrapped by use of lysis buffer (20 mM Tris/HCl buffer (pH 7.4) containing 2 mM EDTA, 0.5

mM EGTA, 1 mM dithiothreitol (DTT), and the protease inhibitors phenylmethylsulfonyl fluoride (0.1 mM), leupeptin (50 μg/mL), aprotinin (50 μg/mL), and pepstatin A (50 μg/mL) as well as a phosphatase inhibitor cocktail). Subsequently, the cells collected in lysis buffer, were subjected to rotational shaking for 1hr followed with centrifugation at 30,000 rpm for mins. The supernatent so collected was used to perform western blot analysis. Protein concentration was measured using bradford assay and 50ug of protein was loaded on the gels. The samples were prior mixed with laemmli buffer (62.5 mM Tris/HCl, pH 7.4, containing 4% sodium dodecyl sulfate, 10% glycerol, 10% β-mercaptoethanol, and 0.002% bromophenol blue) and the samples were boiled for 5 min at 95C. Electrophoresis was carried out on 12% gels containing 0.1% sodiumdodecyl sulphate (SDS) at 120V for 2h. The proteins were then transferred to onto polyvinylidene difluoride (PVDF) membranes at 90V for 120mins. Membranes were blocked with 5% BSA in 0.1 % tween 20 in PBS for 1hr and were further incubated overnight with primary antibodies anti-phospoERK1/2 1:1000 (cell signalling), anti-total ERK1/2 1:1000 (cell signalling), anti-phosphoP38 1:1000 (cell signalling) and anti-totalP38 1:1000 (cell signalling). After 18 to 24h of incubation the membrane was washed six times for 5 mins each with 0.1% tween 20 in PBS (TBST) solution and incubated with their respective secondary HRP conjugated antibodies in 1:5000. After another six washes 5 mins each of TBST, the bands were revealed by using an enhanced chemiluminescence (ECL) solution on GE western blot analyser.

3.5. RT-PCR mRNA expression of RGC-5 cells

Differentiated RGC-5 cells were harvested after 6 hrs of lactate or PBS treatment. Prior to collecting the cells were scrapped in ribozol solution and stored in -80C. Briefly, the cells were homogenized by sonification in the ribozol solution. The extraction was carried out by using adding chloroform in 1:5 ratio. This was followed by centrifugation at 13,000 rpm for 30mins. The aqueous phase so formed was collected and solution of isopropanol was added in 1:2 ratio. The solution was incubated at -20C for 45 mins and centrifuged at 13,000 rpm for 30mins. The pellet was collected and washed twice with 70% ethanol and once with 100% ethanol for 5 mins

each, followed by a brief centrifugation at 10,000 rpm. The pellet was allowed to dry under a fume hood for approximately 30 mins and further dissolved in DEPC water. The RNA concentration and integrity were measured with a NanoDrop 1000 spectrophotometer. Reverse transcription was carried out using MMLV kit protocol from life technologies or cDNA synthesized using iScript cDNA SuperMix (Biorad laboratories). Primers were obtained from alpha DNA. ANG1-F: ACAGGGGATGGTGGTTTGATGCT, ANG1-R: TCACCTGGCAGC TTCTCCGGA. ANG2-F: ACAGGAGGCTGGTGGTTTGATGC ANG2 R: TGCGCAGCCGTGACTTTCAGT IL1B-F: AGATGAAGGGCTGCTTCCAAA IL1B-R: GGAAGGTCCACGGGAAAGAC IL6-F: GCAAGAGACTTCCAGCCAGT IL6-R: TTGCCATTGCACAACTCTTTTCT. PDGF BB-F: TCCGTAGATGAAGATGGGGC, PDGF BB-R: GAGCTTTCCAACTCGACTCC VEGF-F: CAATGATGAAGCCCTGGAGT VEGF-R: AATGCTTTCTCCGCTCTGAA.

3.6 Animals

C57BL/6 mice were obtained from Charles River Inc. (Montreal, CA) with pups at P2 and were allowed to acclimatize for 2 days prior to experiments. Animals were used according to a protocol of the Animal Care Committee of Hôpital Sainte-Justine along the principles of the Guide for the Care and Use of Experimental Animals of the Canadian Council on Animal Care. The animals were maintained on standard laboratory chow under a 12:12 light:dark cycle and allowed free access to chow and water. GPR81-/- mice were obtained from Lexicon Pharmaceuticals (Texas, USA). The GPR81-/- was backcrossed with adult C57BL/6 mice to obtain a pure C57/BL. The transmembrane domain 2 of mice GPR81 coding region (100 base pairs) is replaced by a 4-kb IRES-lacZ-neo cassette.

3.7 Immunohistochemistry:

GPR81 expression analysis was performed on 12um coronal or sagittal sections of brain tissue. Age matched mice from WT and GPR81 KO mice from P5 to P19 were weighed and given steady flow of isoflurane anesthesia. The mouse was placed on a collection pad and surgical cut was made over the xiphoid process to expose the abdominal wall. With careful use of forceps and pair of scissors lateral cuts were made through the diaphragm and utmost care was taken not to damage other organs. Next the ribs were cut open with a parallel cut to the lungs and the heart was exposed. The exposed heart was held with a forceps at its apex and using a scissor with the other hand an incision was made in the left ventricle, which was followed by an insertion of a 25-gauge needle containing PBS. The PBS was injected slowly at approximate rate of 5 ml per minute. This was followed by transcardially perfusion of ice-cold 4% paraformaldehyde at the rate of 3ml per minute. After the 4% PFA perfusion, the mice were decapitated and the brain was placed and immersed fixed in 4% PFA for additional 24 hours at 4C. The brains were then transferred to 30% sucrose solution for cryopreservation for a period of 48h at 4C. After cryopreservation the brains were immersed in OCT solution and freezed over dry ice and stored at -80C until cryosectioning. 12 micron sections were cut on cryostat prechilled at -20C and was transferred on charged slides, which were stored at -20C for later staining. Sections were thawed at room temperature for 15 min and blocked with 5% bovine serum albumin and 0.1% TritonX-100 (T-8787; Sigma) in PBS for a period of 1 h, and were subsequently incubated overnight with rabbit anti-GPR81 (Sigma; 1/500), mouse anti-NeuN (Millipore; 1/100) or mouse anti-GFAP (IF03L-100ug (Millipore), 1/100). Secondary antibodies conjugated with Alexa Fluor (Molecular Probes) directed against mouse and rabbit (Alexa Fluor 488, (#A11070) (1/1000) and Alexa Fluor 594, (#A11012) (1/1000) respectively) were incubated for 2 hours at ambient temperature. Nuclei were stained with Dapi (Invitrogen; 1/1000). Images were captured using 20x and 40x objective with Eclipse E800 (Nikon) fluorescence microscope.

3.8 Lectin Staining:

Brain tissue samples were collected after perfusion fixation with 4% paraformaldehyde. Whole brain was further immersed fixed for 24 hrs at 4C. Tissue was then transferred to 30% sucrose solution overnight for another 24hrs or until the brains were settled at the bottom of the falcon tube. Adequate dehydrated and cryopreserved brain samples very cut on the cryostat at 12-micron sections. The sections were transferred on charged slides (VWR international) and stored at -20C until later use. Prior to staining the sections were thawed for 15 mins and liquid blocker was applied on the sides of the slides to prevent liquid spillage. The sections were washed with washing solution (0.1% triton in PBS) for a total of 15 mins with an interval of 5 mins. The sections were then blocked in 10% fetal bovine serum (FBS) in 0.1% trition in PBS for 1hr. Lectin *(Griffonia simplicifolia)* 2mg/ml stock solution in 1:100 dilutions was used at a working concentration of 20ug/ml. The sections were further incubated overnight lectin solution prepared in blocking solution (10% FBS in 0.1% triton in PBS). Density of the cortical capillary network was assayed by quantification of *Griffonia simplicifolia* (1:100, Sigma). The vessel density was quantified by image J software (NIH software).

3.9 Primary neuronal cell culture:

2 days prior to the neuronal cell culture 35mm petri dish were embedded with slides coated with polylysine solution and incubated overnight. The polylysine slides were washed twice with deionized water prior to use and stored at 4C in fridge until further use. Mice pups (P0-P3) were cryoanaesthetized, their brains were rapidly removed and transferred into ice-cold dissociation solution ($NaS0_4$ 90 mM; $K_2SO_4$30 mM; $MgCl_2$ 5,8 mM; $CaCl_2$;HEPES 10 mM; glucose 20 mM; pH 7,4). Briefly the mice pups were decapitated and by using a fine pair of scissors the brain was detached from the base. The brain was then cut into two halves by at the mid hemisphere. The meninges were carefully removed and the cerebellum was discarded. Under the dissecting microscope the midbrain and thalamus were carefully removed until the horseshoe structure of hippocampus was seen. By using a pair of forceps the meninges surrounding the

hippocampus was removed and discarded. The isolated hippocampi were transferred to dissociation medium and washed twice each with 10ml volume. Hippocampi isolated from the brain was minced and rinsed in HBS solution under sterile condition. Minced tissues were treated with trypsin and were incubated for 20mins at 37C. Cells were then separated by trituration using polished pipettes. The dispersed cells were then plated on the polylysine-coated slides in petri dishes. After plating, cells were incubated at 37°C in 5% CO2 and incubated for 2 to 5 days. After which the cells were subjected to western and immunohistochemistry analysis or western blotting.

3.10 Real time PCR:

Brain tissues from aged matched mice WT and GPR81 KO from P5 to P19 were snapped freeze in solid $CO_2$and mRNA was extracted from the cerebrum by ribozol reagent (Amerisco) as per the manufactures protocol. Briefly, the brain was homogenized by sonification in the ribozol solution. The rest of the protocol was the same as described in the RT-PCR mRNA expression of RGC-5 cells. The extraction was carried out by using adding chloroform in 1:5 ratio. This was followed by centrifugation at 13,000 rpm for 30mins. The aqueous phase so formed was collected and solution of isopropanol was added in 1:2 ratio. The solution was incubated at -20C for 45 mins and centrifuged at 13,000 rpm for 30mins. The pellet was collected and washed twice with 70% ethanol and once with 100% ethanol for 5 mins each, followed by a brief centrifugation at 10,000 rpm. The pellet was allowed to dry under a fume hood for approximately 30 mins and further dissolved in DEPC water. The RNA concentration and integrity were measured with a NanoDrop 1000 spectrophotometer. Reverse transcription was carried out using MMLV kit protocol from life technologies or cDNA synthesized using iScript cDNA SuperMix (Biorad laboratories). Primers were obtained from alpha DNA, ANG1-F: ACAGG GGATGGTGGTTTGATGCT, ANG1-R: TCACCTGGCAGC TTCTCCGGA. ANG2-F: ACAGGAGGCTGGTGGTTTGATGC ANG2 R: TGCGCAGCCGTGACTTTCAGT CCL2-F:

GCTCAGCCAGATGCAGTTA, CCL2-R: TGTCTGGACCCATTCCTTCT. COX2-F: ACCTCTCCACCAATGACCTGA, COX2-R: CTGACCCCCAAGGCTCAAAT. IL6-F: GCAAGAGACTTCCAGCCAGT IL6-R: TTGCCATTGCACAACTCTTTTCT. PDGF BB-F: TCCGTAGATGAAGATGGGGC, PDGF BB-R: GAGCTTTCCAACTCGACTCC. TSP1-F: GCTGCCAATCATAACCAGCG, TSP1-R TTCGTTAAAGGCCGAGTGCT, VEGF-F: CAATGATGAAGCCCTGGAGT VEGF-R: AATGCTTTCTCCGCTCTGAA.
IL1B-F: AGATGAAGGGCTGCTTCCAAA IL1B-R: GGAAGGTCCACGGGAAAGAC TNFA-F: GCCTCTTCTCATTCCTGCTTG TNFA-R: CTGATGAGAGGGAGGCCATT. Quantitative gene expression analysis was performed on Stratagene MXPro3000 (Stratagene) and Roche diagnostic PCR with SYBR Green Master Mix (BioRad). Expression was normalized to 18S universal primer (Ambion) and calculation made using the Ct method. The PCR reaction was carried out at 95C-5mins, 95C-30sec, 58C-30sec, and 72C-30sec. Dissociation curves were also acquired to test primer specificity.

3.11 Western blotting

Proteins from aged match brain tissue samples (P7, P9 and P11) were homogenized by sonification and lysed in RIPA buffer (150mM NaCl, 1% NP-40, 0.5% sodium deoxycholate, 0.1% Sodium dodecyl sulphate, 50Mm Tris-HCl, pH 8.0, cocktail of proteases inhibitors, 1mM PMSF). The lysates were diluted in 1:1000 and were subsequently quantified using Bradford's method (Bio-Rad). 50 ug of protein sample were loaded onto 6% and 12% SDS-PAGE gel depending upon the molecular weight of the proteins. Lower percentage of 6% was used for thrombospondin and the loading control vinculin, whereas 12% gels were used for vascular endothelial growth factor (VEGF) and GPR81 separation. The gel was electrophoresed at 120 V for 2h and electrotransferred onto PVDF membranes for another 2h. Neurons from WT and GPR81-null mice were plated up to 400,000 cells per well in 12 well plate, and incubated overnight in Neurobasal media with B27 (Gibco) supplement and the cells were allowed to

acclimatized and grow for a further 4 days. Cells were then treated with PBS or lactate (10 mM) for 24h, and the ligand binding reaction was inhibited by addition of 2 ml ice-cold PBS. 300 ul of ice-cold RIPA buffer was added to lyse the cells. The cells were scraped off and agitated on a rocking platform for 1h at 4C. The lysate was further centrifuged for 30mins at 13000xg at 4C. The supernatant was electrophoresed on 6%, 12% and 15% polyacrylamide gel for 2 h, after which it was transferred to a PVDF membrane for another 2h. The membranes were immunoblotted using anti-GPR81 (SAB1300790, Sigma-Aldrich) antibody (1:250), anti-TSP-1 (Abcam, 1:200), anti VEGFA (Santa cruz 1:200) and were detected with their respective secondary antibodies conjugated to HRP substrate. Enhanced chemiluminescence (GE Healthcare) was used for detection using the ImageQuant LAS- 500 (GE Healthcare, Little Chalfont, United Kingdom).

3.12 Invitro matrigel assay

In vitro matrigel gel principle is based on formation of tubules, wherein endothelial cells interact with each other to form a lumen. The endothelial cells needs to be embedded in fibrin, collagen or a matrigel where it provides a 3D environment for the cells to form tube like structure. The tube formation or cell differentiation assay is performed as follows. Rat brain endothelial cells (RBEC) are cultured in a specialized media called endothelial growth media in T75 flask prior coated with attachment factor solution. The cells were allowed to grow upto 80% confluence before carrying out the further experiments. 12 well plates were initially coated with 50ul matrigel (the matrigel was thawed and maintained on ice for the entire experiment and the tips used to aspirate the matrigel were prechilled at -20C to prevent premature solidifcation) and allowed to solidify by incubating at 37C. Cells were trypinized, counted and about 200,000 cells were embedded on the solidified matrigel. Another 50ul of matrigel was added and the wells were allowed transferred to the incubator for 30 mins to form a 3D structure matrix with entrapped endothelial cells. The cells were further treated with endothelial growth media for

period of 24 hours. After 24 to 36 hours the matrigel cells were treated with the conditioned media obtained from WT or KO neurons treated with or without lactate. The tube formation was observed and the images were obtained by phase contrast microscopy (Eclipse 300 Nikon TE300; Nikon), over a period of 72 hours.

3.13 Aortic Explants:

Aortas from the adult C57 mice were extracted and cut into 1mm rings and were placed in growth factor reduced Matrigel (BD Biosciences) in 24-well tissue culture plates. The explants were cultured for 2 days in EGM-2 media followed by treatment with conditioned media of primary neurons from WT and GPR81-/- mice treated with lactate and PBS. The neutralizing agents used were neutralizing antibody to rat VEGF (AF564; 1 mg/ml) and recombinant Tie-2–Fc (3874-T2; 1 mg/ml) from R&D Systems. 4 weeks mice were used to perform the aortic explants. In brief the mice were killed by cervical dislocation. Using sterile pair of scissors and forceps the thoracic cavity was cut and the lungs and heart were carefully excised and removed. The exposed aorta is visible as a fat covered blood vessel running down the spine. The anterior end of the aorta is held using the forceps and a fine scissor was used to cut off the aorta and detach it from the spine. The excised aorta was transferred to a petridish containing glutamax media and was subsequent fatty tissue along the aorta was cleaned. The aorta was further cut into rings of 1mm length and embedded into reduced matrigel. The explants were then cultured in the EGM2 media for a period of 24-48h to initiate sprouting. After 48h the medium was treated with conditioned media treated with or without lactate from the wild type and KO neurons. The change in sprouting angiogenesis was observed for the next 72 hours and photos were taken after 24hr. The photomicrographs of individual explants and quantified microvascular sprouting by measuring the area covered by outgrowth of the aortic ring with ImagePro Plus 4.5 (Media Cybernetics).

3.14 Animal experimentation and Rice-Vannucci model:

Animal Care Committee of Hôpital Sainte-Justine approved animal experimentations along the principles of the Guide for the Care and Use of Experimental Animals of the Canadian Council on Animal Care. Cerebral hypoxia-ischemia was generated using the Rice-Vannucci model of permanent unilateral ligation in 7 days old (P7) mice, followed by exposure to 8% O2 for 45 minutes with ambient temperature maintained at 37°C. C57Bl/6 wild-type mice (The Jackson Laboratory) and GPR81-/- mice were utilized. The mice were fully anesthetized with isoflurane with a flow rate sufficient enough to carry out the surgery. A small incision was made at the neck using a fine scissor to expose the common carotid artery (CCA). The CCA was ligated using a 5-0 silk suture and then the cut in the neck was sealed using cyanoacrylate adhesive. The body temperature of the pups were maintained at 37C on a warming pad and then returned to their dams to recuperate for 2 hrs. The pups were then placed on the heat-warming pad in the hypoxic chamber maintained at 8% oxygen/92% nitrogen gas flow attached to an automated biospherix oxycycler machine. A continuous flow of the gas mixture and the body temperature of the pups were maintained at 37C throughout 45 min of exposure. At the end of 45 min to maximum 1hr the pups were returned to their dams. The pups were further sacrificed after 48h and 72h for immunohistochemistry, TTC staining and qPCR analysis.

3.15 Lactate quantification assay:

Age-matched mice from the intracerebroventricular lactate injections and control (room air) at P4 were sacrificed and the brains were snap frozen in liquid nitrogen and stored at 80C until further use. A fragment of 100 mg of each brain was homogenized by sonification and used to quantify tissue lactate concentration using a colorimetric assay, following manufacturer's protocol (Eton Bioscience, San Diego, CA). The frozen brain tissues were thawed till -20C and were cut into pieces, which were subsequently weighed. The samples were processed by

immersing in 80% ethanol and homogenized by shear stress inducing sonificator. In addition the samples were gently rotated on an oribital shaker for 30 min at 4C. The supernatent was collected after centrifugation at 10000rpm at 4C for 20 mins. The extracted supernatent was further diluted in milli Q water in 1:100. The lactate assay buffer and lactate acid reagent were thawed on ice from -80C and mixed is equimolar concentration. At the same time standards were prepared in increasing order of their concentration from 0uM to 3000uM with a standard reagent provided along with the kit. The diluted brain samples and the prepared standards were treated with and thoroughly mixed the lactate assay solution in a microplate and further incubated at 37C in a CO_2 free incubator for another 30 mins. The plate was agitated intermittently during the incubation period and the change in colour was noticed after 15 mins of incubation in the standards as well as in the samples. The readings were made on a microplate reader (EnVision Multilabel reader; PerkinElmer) adjusted for 490 nm. Results were then converted into a concentration unit (mmol/L) using a standard curve.

3.16 Infarct size and TTC staining

Infarct and penumbra volumes were measured using 2,3,5-Triphenyltetrazolium chloride (TTC) staining; The principle is based on mitochondrial damage, lesser insult results in faint pink staining called the penumbra, and an normal cells show bright reddish-pink staining indicating normal active metabolic tissue. This is a semi-quantitative method used for determining the infarct size. Thickness of sections was measured with a digital caliper and regions corresponding to infarct and penumbra were quantified using Image J (NIH software). After 96h of hypoxic-ischemic exposure of the pups the brains were rapidly removed and freezed in solution of isopentane. The cryofreezed fresh tissue was stored at -20C until further use. Brain slices of 1mm were cut using a prechilled blade on an ice-cold plate or the whole brain was immersed in the solution for topical TTC staining to determine global infarct area. The slices and or whole brain

were then quickly transferred to a 0.1% TTC solution prepared in PBS buffered at pH 7. The brain slices/ whole brains were then incubated at 37C for 30 mins away from light. The area of infarcted region on the ipsilateral side and the undamaged region on the contralateral side were measured using ImageJ.

3.17 Preterm double hit model for Neuroinflammation:

Animal Care Committee of Hôpital Sainte-Justine approved animal experimentations along the principles of the Guide for the Care and Use of Experimental Animals of the Canadian Council on Animal Care. In the preterm double hit model inflammation followed by hypoxic-ischemic insult was developed to determine the dual role of bacterial infections and HI in preterm. In brief as described in the following figure, mice pups were injected with lipopolysaccharide (LPS) for a period of 6 days from postnatal 1 to postnatal 6. At P7 the WT and GPR81 KO mice were subjected global isoflurane anesthesia prior and during the surgery. As mentioned in material and methods in 3.8, the pups were subjected to carotid artery ligation followed by exposure to 8% hypoxia for 45 mins. The pups were then either sacrificed 24 hours later to determine pro-inflammatory cytokines by qPCR or for immunohistochemical analysis of microglial activation by Iba-1.

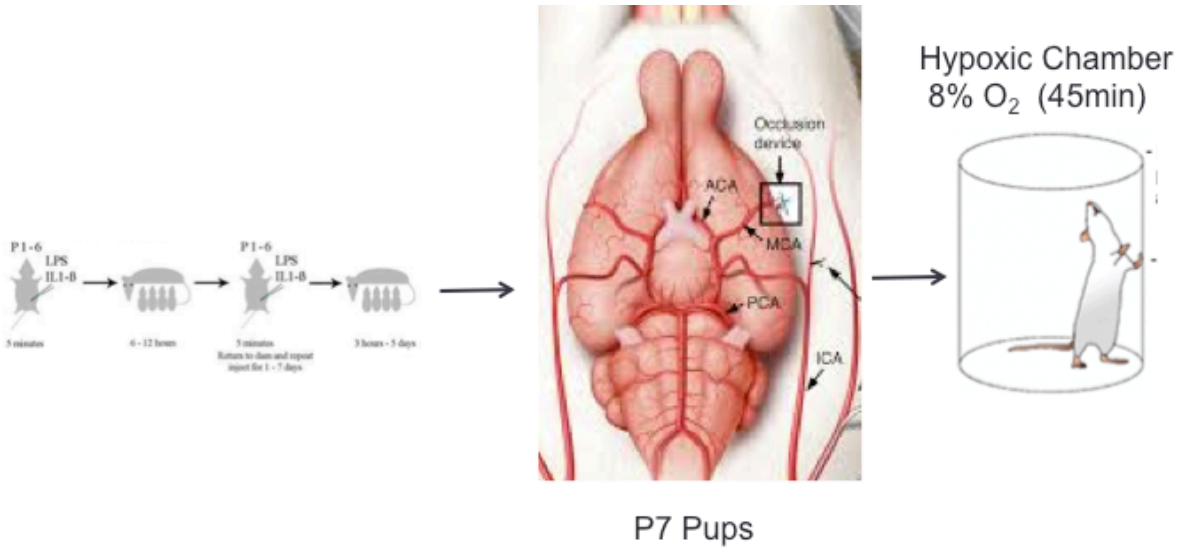

Figure 3.1 Double hit model for preterm inflammation

Post-natal mice from P1 to P6 were injected with Lipopolysaccaride (LPS) using a hamilton syringe intracerebroventricularly. This was followed followed by HI insult wherein unilateral permanent artery occlusion of the carotid artery was performed. Before subjecting the pups to hypoxia they were allowed to recover from the surgery for a period of 1 hr. The pups were then transferred into an hypoxic chamber maintained at 8% oxygen for 45 mins.

3.18 Primary Muller cell culture and treatment:

Primary muller cells (pMC) were cultured from retinas of aged matched P8 pups from WT and GPR81 KO mice. The pups were anesthetized with isoflurane and decapitated; the eyes were carefully enucleated with the help of sharp forceps and scissors sterilized with 70% ethanol, keeping the optic nerve intact. The eyes were transferred to sterile PBS solution containing 1% penicillin/streptomycin solution followed by immersion in DMEM (Dulbecco's modified Eagle medium; containing 5 mM glucose), supplemented with 2 mM L-glutamine, 100 U/mL penicillin/streptomycin, and 10% (vol/vol) bovine growth serum (BGS). In the sterile PBS solution under a dissecting microscope the intraocular muscles along with the fascia and conjuctiva tissue were carefully removed. The cleaned eyeball was then transferred to the sterile

DMEM media and the cornea, eye lens and iris were dissected and removed. Finally the retina was detached from the retinal-pigmented epithelium (RPE). The retinas were carefully collected and transferred to 15ml falcon tube containing DMEM media with bovine trypsin, collagenase and DNAse solution. The tube with the retinas was incubated at 37C for 60min with intermittent flickering of the tube at 10 min intervals. After 60mins the solution was triturated gently with 5ml pipette to allow the dissociation of retinal tissue into cells. The solution was centrifuged at 300g for 5mins. The supernatant was discarded and the pellet was resuspended in a new solution of sterile DMEM containing reconstituted albumin-ovomucoid inhibitor solution and DNAas solution. The cells were centrifuged at 100g for 6mins and the pelleted, the supernatant was discarded and the pellet was treated with 5ml of albumin inhibitor solution and re-centrifuged at 100g for 6 mins. After this centrifugation step the pellet is resuspended in the DMEM plating media and the dissociated cells were plated in T75 flask prior coated with 0.1% gelatin solution. The dissociated cells at this stage consist of mixture of photoreceptors, muller cells and retinal neuronal cells. The flask is incubated at 37C for 7 days and the media was replaced after 5 days. After 2 to 3 passages 80 to 85% of cells were identified to be pure culture of Muller cells.

The Muller cells were further used to perform experiments to elucidate the mechanism of norrin regulation by GPR81. pMC were plated in 6 well plates and the incubated until they reached the confluence of 80%. Subsequently, the cells were treated with either PBS or lactate at different time points. For phospho-ERK1/2 and total ERK1/2 experiments the pMC were treated for 5 mins and the cells lysed in RIPA buffer (150mM NaCl, 1% NP-40, 0.5% sodium deoxycholate, 0.1% Sodium dodecyl sulphate, 50Mm Tris-HCl, pH 8.0, cocktail of proteases inhibitors, 1mM PMSF).

3.19. Quantitative Polymerase Chain Reaction (RT-PCR) for Primary Muller cells and retina

Primary muller cells were harvested after 6 hrs of lactate or PBS treatment. mRNA extraction

was also carried out age matched retinas from WT and GPR81 KO mice at P8, P9 and P14. Prior to collected the cells or tissues were scrapped in ribozol solution and stored in -80C. Briefly, the cells were homogenized by sonification in the ribozol solution. The extraction was carried out by using adding chloroform in 1:5 ratio. This was followed by centrifugation at 13,000 rpm for 30mins. The aqueous phase so formed was collected and solution of isopropanol was added in 1:2 ratio. The solution was incubated at -20C for 45 mins and centrifuged at 13,000 rpm for 30mins. The pellet was collected and washed twice with 70% ethanol and once with 100% ethanol for 5 mins each, followed by a brief centrifugation at 10,000 rpm. The pellet was allowed to dry under a fume hood for approximately 30 mins and further dissolved in DEPC water. The RNA concentration and integrity were measured with a NanoDrop 1000 spectrophotometer. Reverse transcription was carried out using MMLV kit protocol from life technologies or cDNA synthesized using iScript cDNA SuperMix (Biorad laboratories). Primers were obtained from alpha DNA. Primers were designed using the National Center for Biotechnology Information's Primer Blast: Plasma lemma vesicle-associated protein (PLVAP), 5 CGTCAAGGCCAAGTCGCT-3 (forward) and 5 -CATCCACAGGTGGGCGATT-3 (reverse); and Claudin-5, 5- GCAAGGTGTATGAATCTGTGCT-3 (forward) and 5 GTCAAGGTAACAAAGAGTGCCA-3 (reverse). Quantitative gene expression analysis was performed on the Stratagene MXPro3000 (Stratagene, San Diego, CA) with SYBR Green Master Mix (Bio-Rad). Gene expression levels were normalized to 18S universal primer (Ambion Life Technology, Burlington, ON, Canada). Dissociation curves were also acquired to test primer specificity.

3.20 Western Blotting of Primary Muller cells and retina

Proteins from aged match retinal tissue samples (P9 and P14) or primary muller cells treated with or without PBS or lactate for 24 hrs were homogenized by sonification and lysed in

RIPA buffer (150mM NaCl, 1% NP-40, 0.5% sodium deoxycholate, 0.1% Sodium dodecyl sulphate, 50Mm Tris-HCl, pH 8.0, cocktail of proteases inhibitors, 1mM PMSF). The lysates were diluted in 1:1000 and were subsequently quantified using Bradford's method (Bio-Rad). 50 ug of protein sample were loaded onto 12% SDS-PAGE gel depending upon the molecular weight of the proteins. 12% gels were used for claudin-5, GPR81, B-actin, pERK and Total ERK separation. The gel was electrophoresed at 120 V for 2h and electrotransferred onto PVDF membranes for another 2h. Neurons from WT and GPR81-null mice were plated up to 400,000 cells per well in 12 well plate, and incubated overnight in Neurobasal media with B27 (Gibco) supplement and the cells were allowed to acclimatized and grow for a further 4 days. Cells were then treated with PBS or lactate (10 mM) for 24h, and the ligand binding reaction was inhibited by addition of 2 ml ice-cold PBS. 300 ul of ice-cold RIPA buffer was added to lyse the cells. The cells were scraped off and agitated on a rocking platform for 1h at 4C. The lysate was further centrifuged for 30mins at 13000xg at 4C. The supernatant was electrophoresed on 15% polyacrylamide gel for 2 h, after which it was transferred to a PVDF membrane for another 2h. The membranes were immunoblotted using anti-GPR81 (SAB1300790, Sigma-Aldrich) antibody (1:250), anti-claudin-5 (Santa Cruz, 1:200), anti-pERK (Cell Signalling 1:1000) and anti-total ERK (Cell Signalling 1:1000) and were detected with their respective secondary antibodies conjugated to HRP substrate. Enhanced chemiluminescence (GE Healthcare) was used for detection using the ImageQuant LAS- 500 (GE Healthcare, Little Chalfont, United Kingdom).

3.21 Retinopathy of Prematurity model in mice

We used mice model of ROP to assess the role of GPR81 in developmental and pathophysiological condition. In this model, neonatal mice pups at P7 were exposed to hyperoxic environment in an oxycycler maintained at 75% oxygen for 5 days till P12 mimicking the first

vaso-obliteration phase of ROP. During this stage of hyperoxia the C57 pups were kept with surrogate CD-1 lactating mums to avoid possible cannibalism by C57 mums. After hyperoxic exposure for 5 days the litters were transferred to normal air in this case a hypoxic environment to the pups, which would mimic the second neovascularization phase of ROP. The pups were sacrificed and their retinas were collected at specific time points at VO (P12) and NV (P17) phases, and also in between the VO and NV phases such as P14 and after NV at P21. Retinas were collected from aged matched WT normoxia mice and WT mice exposed to OIR. GPR81 protein levels and mRNA expression levels of GPR81 was determined by western blotting.

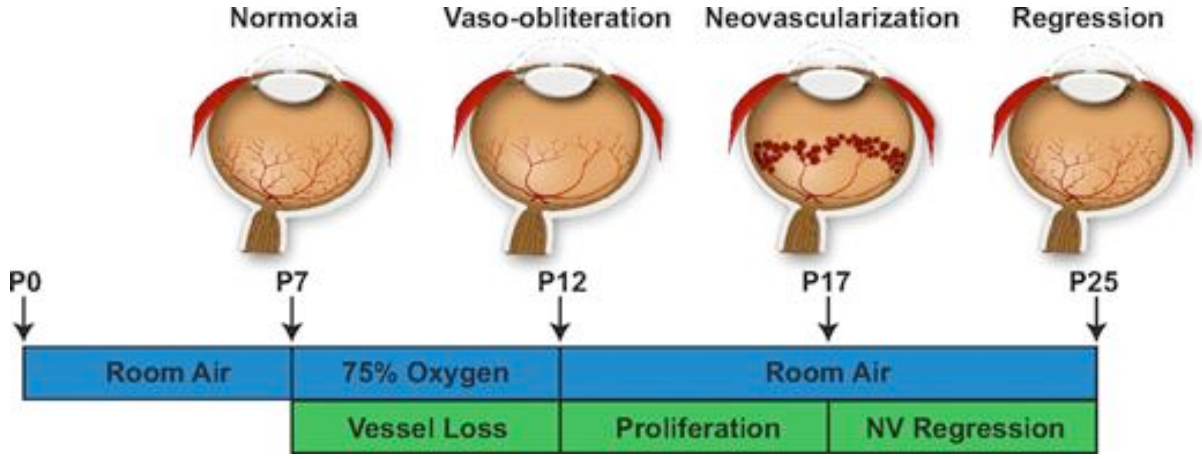

Figure 3.2 Schematic diagram showing the retinopathy of prematurity (ROP) model in mice. [206]

The ROP mice model is characterized by two phases vaso-obliteration and neovascularization at P12 and P17 respectively. The first phase of VO is associated with vessel loss due to reduction in pro-angiogenic factors, and the second phase of NV is characterized by abnormal vessel proliferation leading to microvasculature destruction and subsequent tufts formation.

CHAPTER 4:

Neuronal GPR81 regulates developmental brain angiogenesis and promotes brain recovery after a hypoxic ischemia insult

4.1 GPR81 localization in retinal ganglion cell line (RGC-5)

As mentioned earlier, GPR81, like GPR91 could have the potential to act as metabolic sensing receptor. Unlike GPR91, which is activated solely by carbohydrate metabolite ligand called succinate, GPR81 is activated by lactate. Since the expression of GPR91 was well documented in Retinal ganglion cells, neurons and astrocytes, we sought to determine if GRP81 has similar expression pattern in the above-mentioned cells. However, due to absence of neuronal cell line in vitro, we decided to perform preliminary *invitro* experiments on RGC-5 cells. Another reason due to which RGC-5 cells were used is because of their unique property to differentiate morphologically into neurons of the CNS with extended neurite outgrowth upon staurosporin treatment. The RGC-5 cells were treated with 316nM staurosporin for a period of 24hrs. **Figure 4.1** Immunocytochemistry analysis of RGC-5 showed a strong co-localization of GPR81 with Neuronal N (NeuN) suggesting GPR81 presence in differentiated retinal ganglion cells also called as stimulated retinal ganglion cells (sRGCs). Further experiments were performed to determine the pro -angiogenic role of lactate on sRGCs. Also since RGCs were difficult transfect to knockdown GPR81, all rest of the major experiments determining the exact role of GPR81 and lactate were performed *invivo* in GPR81 KO mice.

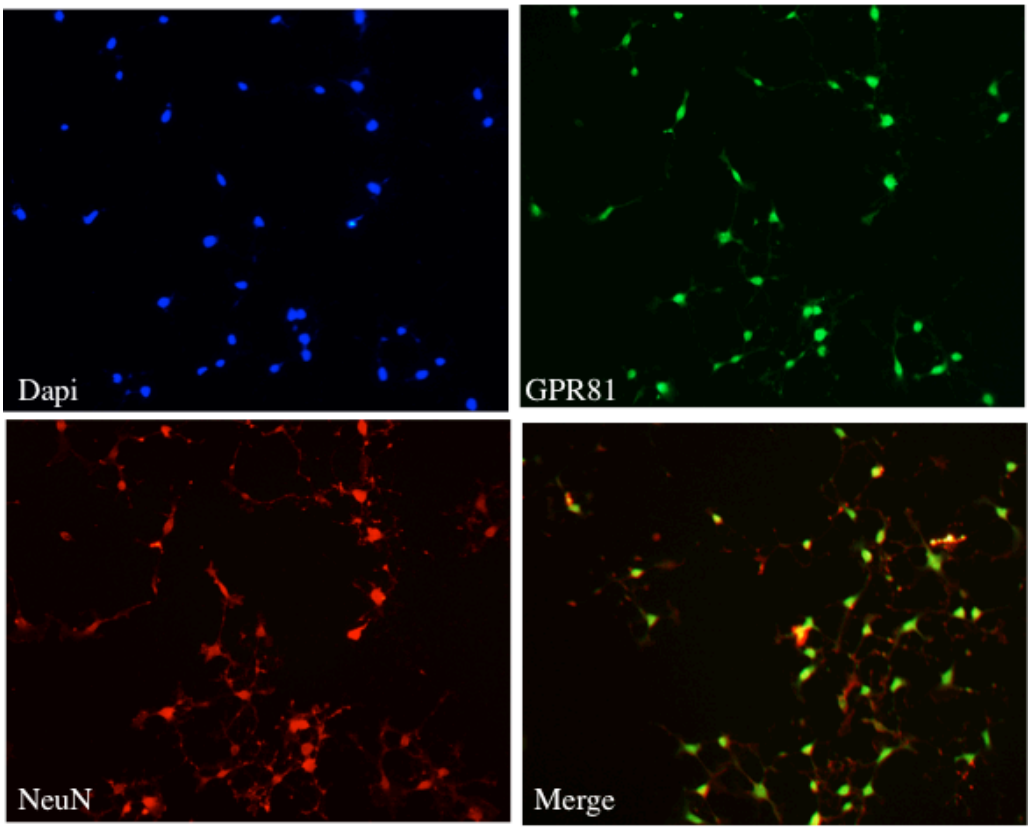

Figure 4.1 GPR81 expression in retinal ganglion cell line 5 (RGC-5).

Colocalization of GPR81 with Neuronal N (NeuN), a neuronal marker. RGC-5 were treated with staurosporin 316 nM for 24 hours to differentiate them into neuronal cells characterized by extended neurite growth.

4.2 Lactate stimulated conditioned media enhances angiogenic sprouting and tube formation in endothelial cells.

To determine the pro-angiogenic role of lactate and GPR81 *invitro* and *exvivo* the stimulated RGCs (sRGC) were treated with either lactate or PBS. The cells were treated for 24 hours and conditioned media (CM) was collected and concentrated by ultracentrifugation. Figure 4.2 shows increased tube formation and angiogenic sprouting by lactate conditioned media as compared to sole lactate treatment in the *invitro* matrigel and *exvivo* aortic explant assay. This indicates that although lactate has angiogenic properties as mentioned elsewhere, lactate also promotes secretion of other angiogenic factors, which facilitates an angiogenic response. The possible explanation for increased angiogenic sprouting and invitro tube formation in the endothelial cells in lactate treated conditioned media (CM) could be attributed to a receptor-mediated action of GPR81. Wherein exogenous addition of lactate may stimulate GPR81 on sRGCs that promotes the secretion of angiogenic factors into the CM.

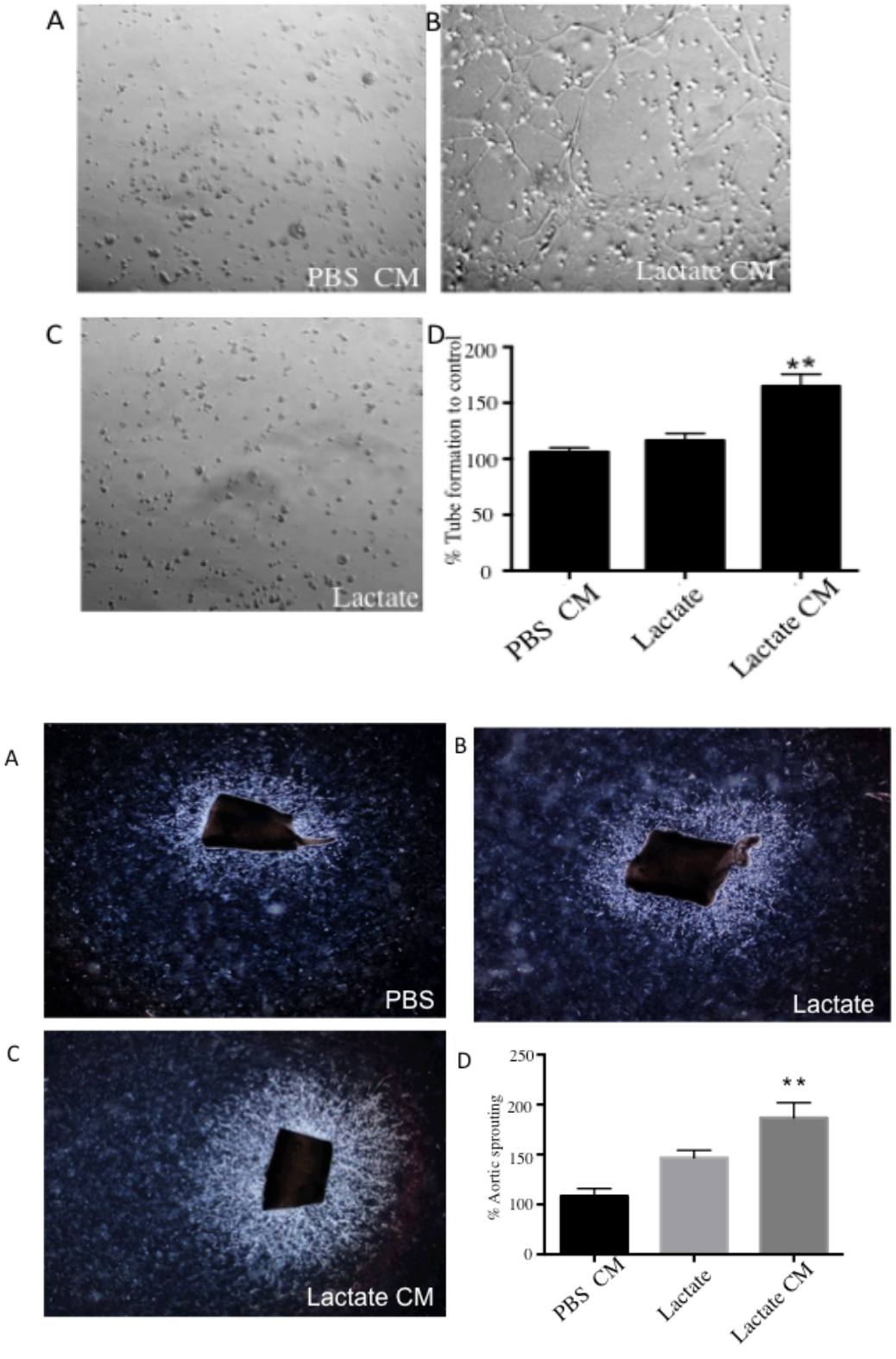

Figure 4.2 Pro-angiogenic role of lactate.

(i), Invitro tube formation assay lactate treatment, (ii) Exvivo angiogenesis sprouting effect of lactate and lactate conditioned media on aortic explants. A) PBS or control conditioned media (CM) from RGC-5 cells collected after 24hrs. B) Lactate treatment of RGC-5 cells for 24hrs. C) Lactate treated conditioned media (CM) collected from RGC-5 cells after 24 hrs of treatment. Increased tube formation and angiogenesis sprouting is seen in endothelial cells and aortic rings treated with Lactate containing conditioned media compared to lactate treatment. Values are presented, as mean ± S.E.M. Data are representative of 3 experiments per group; **, $p<0.01$ as determined by Tukey's multiple comparison test

4.3 Lactate promotes secretion of angiogenic and neurotropic factors in sRGCs.

Differentiated RGCs were treated with lactate for 6 hrs and mRNA expression of pro-angiogenic, neurotrophins and inflammatory factors were assessed by qPCR. As depicted in **Figure 4.3**, lactate promoted an increased in brain derived neurotropic factor (BDNF), ciliary neurotropic factor (CNTF), VEGFA, ANG-1, ANG-2, PDGF BB and IL-6, whereas a decrease in IL-1B secretion. This result indicated that lactate could play a vital role in regulation of angiogensis via stimulation of RGCs or neurons. Furthermore, most of the factors assessed are cytokines they have a higher probability of being secreted into the conditioned media, which might explain why there is a significant increase in angiogenic sprouting and tube formation in endothelial cells. This could also suggest that lactate might regulate the expression of the aforementioned factors via a receptor mediated action, as sole lactate treatment effect on endothelial cells in the invitro matrigel and exvivo aortic explants were significantly lower when compared to lactate conditioned media as shown in **Fig 4.2.**

To further elucidate the potential mechanism by which lactate could promote secretion of pro-angiogenic factors and reduce the expression of pro-inflammatory cytokine such as IL-1B, we focused on ERK1/2 and P38 pathways. The roles of these pathways have been well studied in neurogenesis, cell proliferation, angiogenesis and inflammation. As seen in **Figure 4.4**, lactate was able to increase ERK1/2 phosphorylation and corresponding decrease P38 phosphorylation. Epidermal growth factor with lactate had an additive effect on ERK1/2 phosphorylation compared to phosphor ERK1/2 activation of EGF alone; this effect was significantly reduced with U0126 (a specific ERK1/2 inhibitor). Collectively these results indicated that lactate is a pro-angiogenic carbohydrate metabolite and facilitates its angiogenesis and anti-inflammatory action via modulating ERK1/2 and P38 signalling pathway.

A

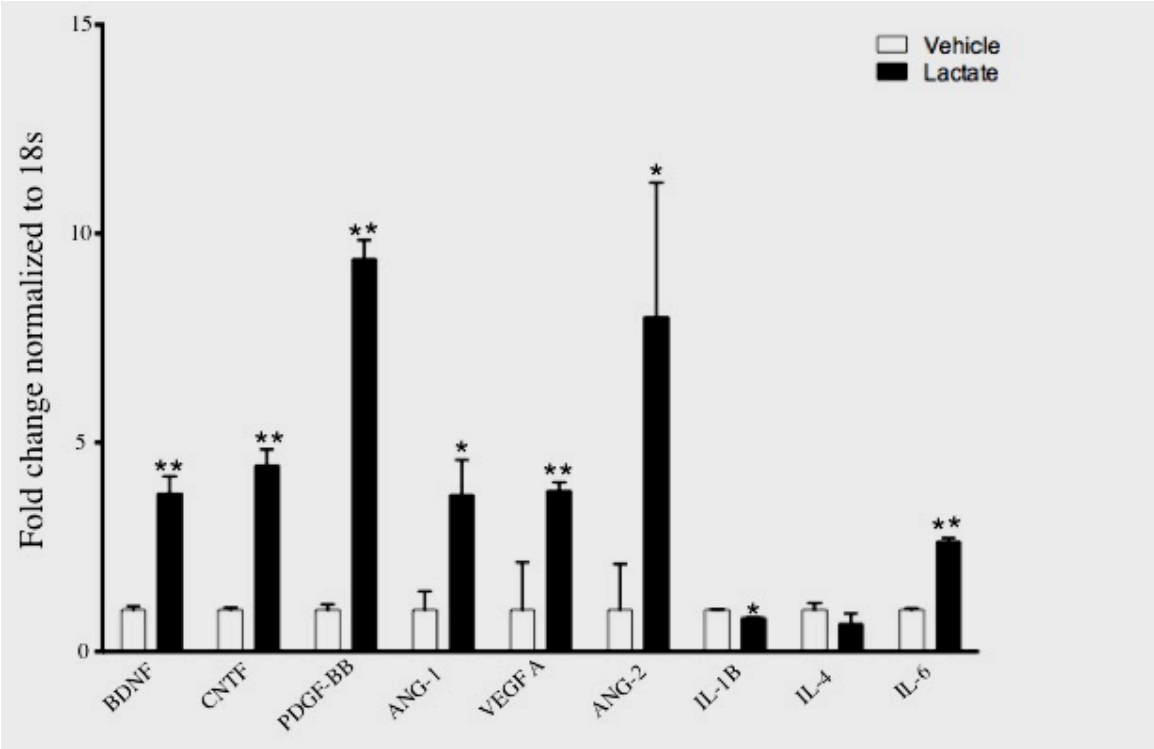

Figure 4.3 Lactate promotes increased secretion of pro-angiogenic, neutrophins and decrease in pro-inflammatory factors

Lactate facilitates increased expression of BDNF, CNTF, ANG-1, ANG-2, PDGFBB, IL-6 and VEGFA. Values are presented, as mean ± S.E.M. Data are representative of 3 experiments per group; **, $p<0.01$ as determined by Tukey's multiple comparison test

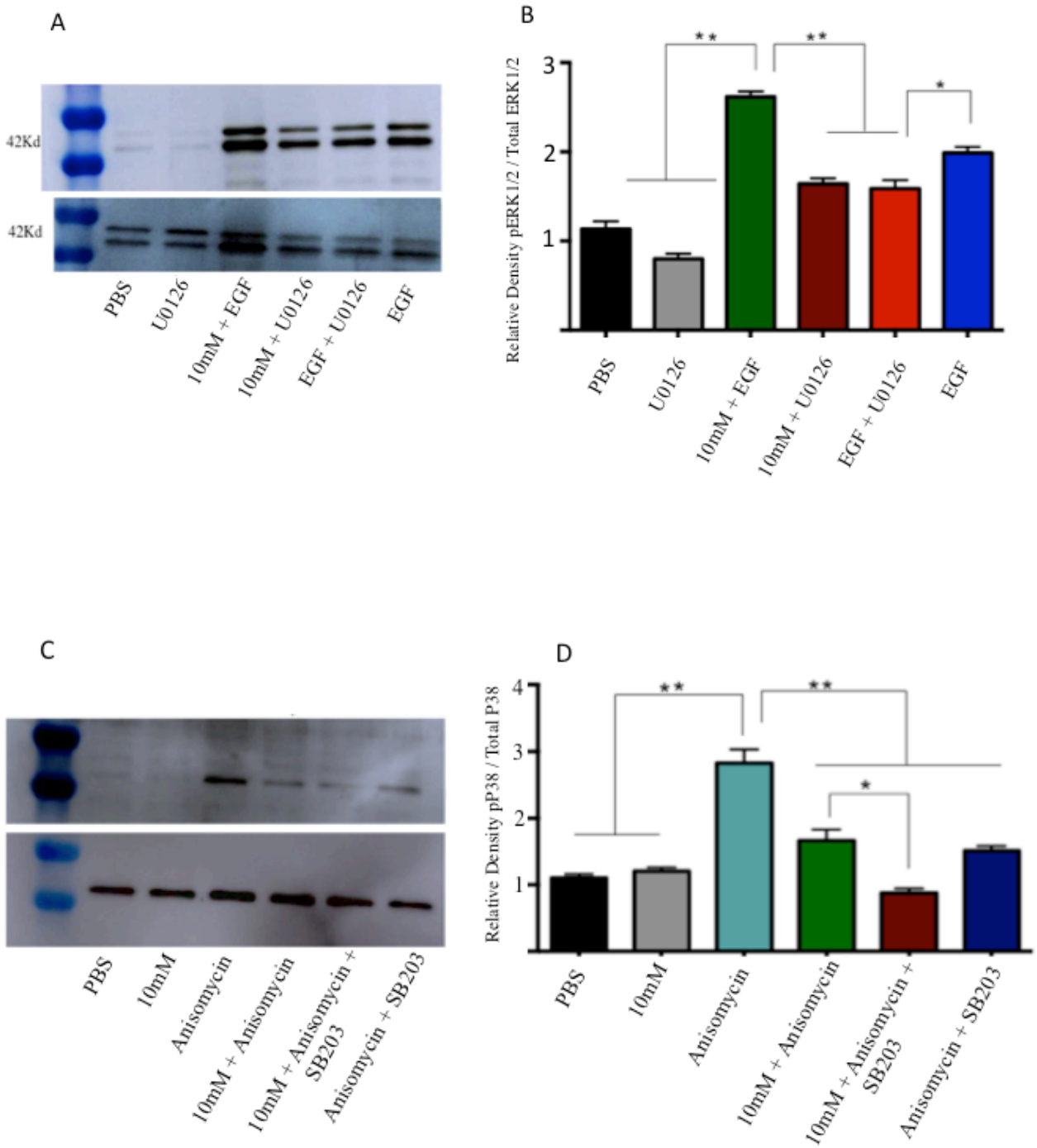
A
42Kd
42Kd
PBS
U0126
10mM + EGF
10mM + U0126
EGF + U0126
EGF
B
Relative Density pERK1/2 / Total ERK1/2
3
2
1
**
**
*
PBS
U0126
10mM + EGF
10mM + U0126
EGF + U0126
EGF
C
PBS
10mM
Anisomycin
10mM + Anisomycin
10mM + Anisomycin + SB203
Anisomycin + SB203
D
Relative Density pP38 / Total P38
4
3
2
1
**
**
*
PBS
10mM
Anisomycin
10mM + Anisomycin
10mM + Anisomycin + SB203
Anisomycin + SB203

Figure 4.4 Lactate increases ERK1/2 phosphorylation and decreases Pp38 protein levels in sRGC.

Lactate decreases phosphorylation of P38 in sRGCs mediated by anisomycin (activator of pP38 pathway) and increases pERK1/2. A) Treatment of sRGC with PBS, U0126, 10mM lactate + EGF, 10mM lactate + U0126, EGF + U0126 and EGF. B) Quantification of western blot analysis of the same. C) Treatment of sRGC with PBS, 10mM lactate, anisomycin, 10mM + Anisomycin, 10mM + Anisomycin +SB203 and Anisomycin + SB203. D) Quantification of western blot analysis of the same. There is an additive increase in ERK phosphorylation upon EGF and 10mM treatment compared to only EGF treatment. The specific pP38 inhibitor SB20359 acts in a similar way as lactate suggesting the specific inhibition of p38 pathway is mediated by lactate. Values are presented, as mean ± S.E.M. Data are representative of 3 experiments per group; **, $p<0.01$ as determined by Tukey's multiple comparison test

4.4 Localization and expression of GPR81 in developing brain

Immunohistochemistry was performed on coronal sections of brain tissue to determine GPR81 localization. At cellular level, to detect the presence of GPR81 on neurons, endothelial and astrocytes, sections were stained with neuronal marker Neuronal N (NeuN), lectin and astrocyte marker (GFAP) respectively. GPR81 colocalization with neuronal marker (NeuN) was specifically detected, in the cerebral cortex and hippocampal pyramidal neurons **(Fig 4.5a and 4.5b)**. In addition, as seen in **Figure 4.6**, increased GPR81 expression was evident during P9 and P11 postnatal stages. During postnatal mice brain developmental angiogenesis between P7 to P14, there is massive proliferation and extensive migration of bed capillary network via sprouting angiogenesis. We found that GPR81 expression significantly increases during this period suggesting that it could play a major role in remodeling of arterioles-venous capillary bed migration and proliferation.

Since we also observed no change in vessel area after at P15 to P19 in the later postnatal stages, we sought that there could be other metabolic receptors (GPR91, GPR99 and GPR109) that could collectively articulate and compensate for the loss of GPR81 function in post-natal angiogenesis. Furthermore, no GPR81 colocalization was detected with GFAP and lectin as depicted in Figure 4.7, indicating that the expression of GPR81 is either very weak in these cells or completely absent. To further validate our data, we cultured primary pyramidal neuronal cells from the hippocampus from WT GPR81 mice and confirmed the presence of GPR81 in neurons (Fig 4.5c). Co-localization of DAPI with GPR81 indicated that receptor has a nuclear or peri-nuclear location in the cell.

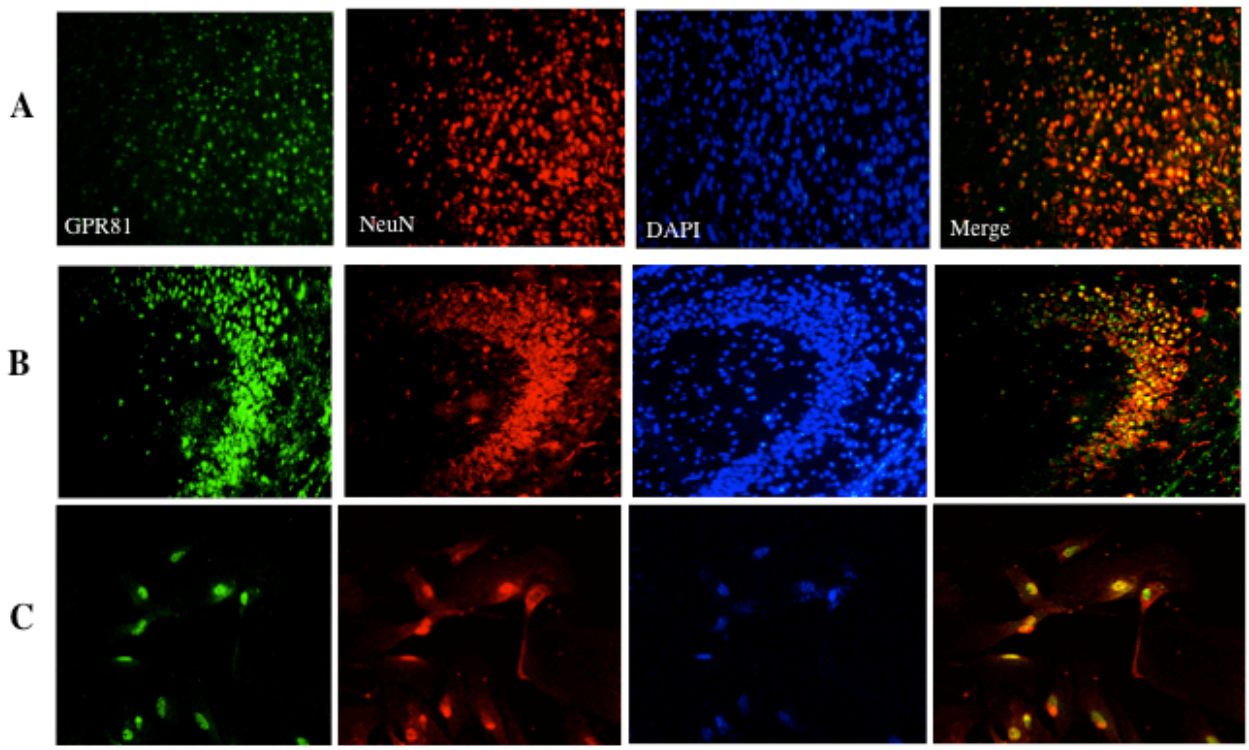

Figure 4.4 GPR81 localization in neurons

A, GPR81 colocalizes with NeuN (i) in the mice cerebral cortex. Rabbit anti-GPR81 was used to label GPR81, and mouse anti-NeuN a neuronal marker—was used to mark neurons. 4,6-diamidino-2-phenylindole (DAPI) was used to stain nuclei (scale bar, 25 μm). B. GPR81

colocalizes with NeuN (ii) in the mice hippocampus. C. GPR81 (Green) colocalizes with NeuN (i) (Red) pyramidal hippocampal primary cell culture. Images are quanitified as collective of 3 experiements.

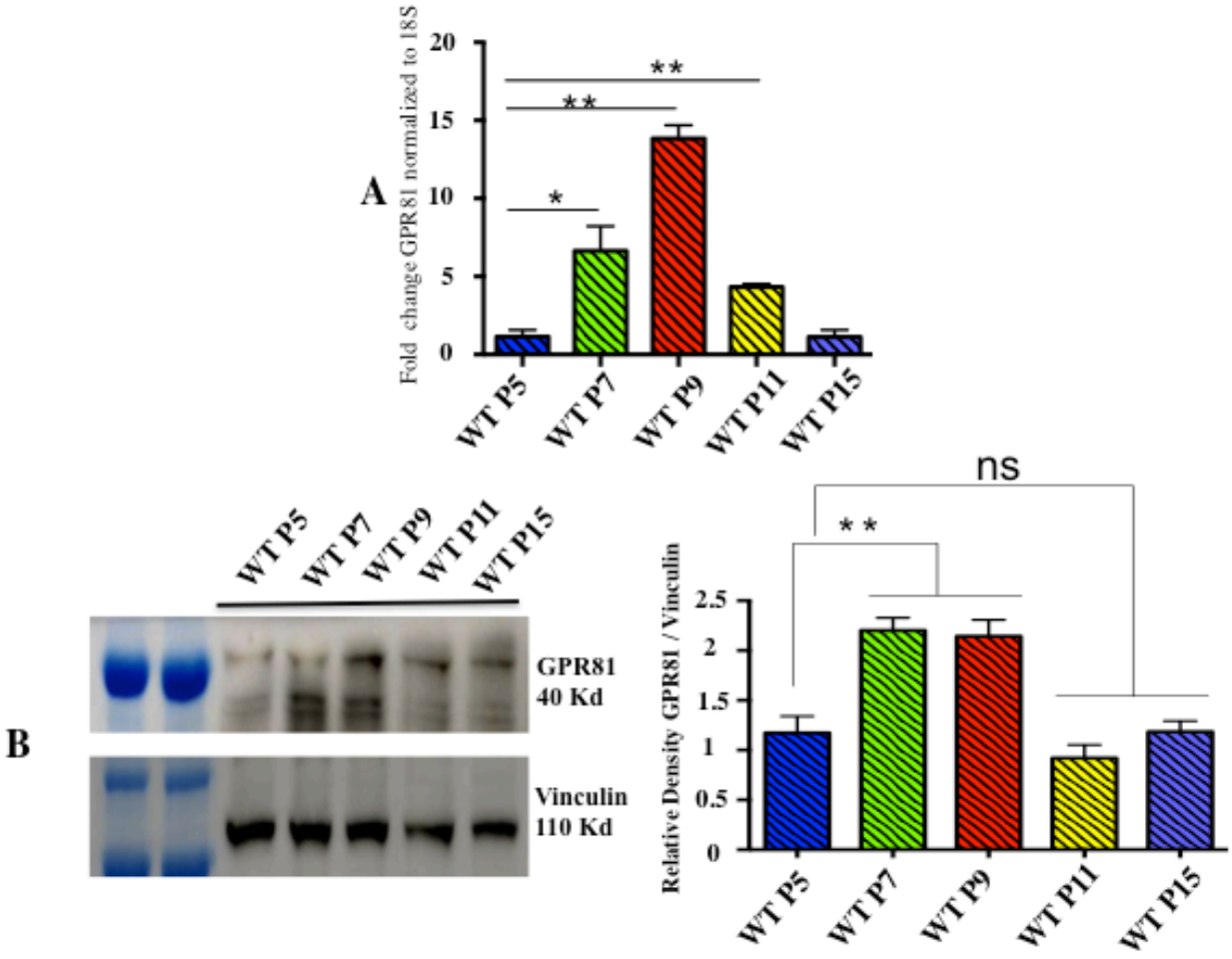

Figure 4.5 Post-natal GPR81 expression at different time points in the WT mice brains.

(A) mRNA GPR81 expression and B) protein expression from P5 to P19. *, $p<0.05$; **, $p<0.01$; with Tukey's multiple comparison test compared to P5 WT, as indicated. Values are presented, as mean ± S.E.M. Data are representative of 5 animals per group.

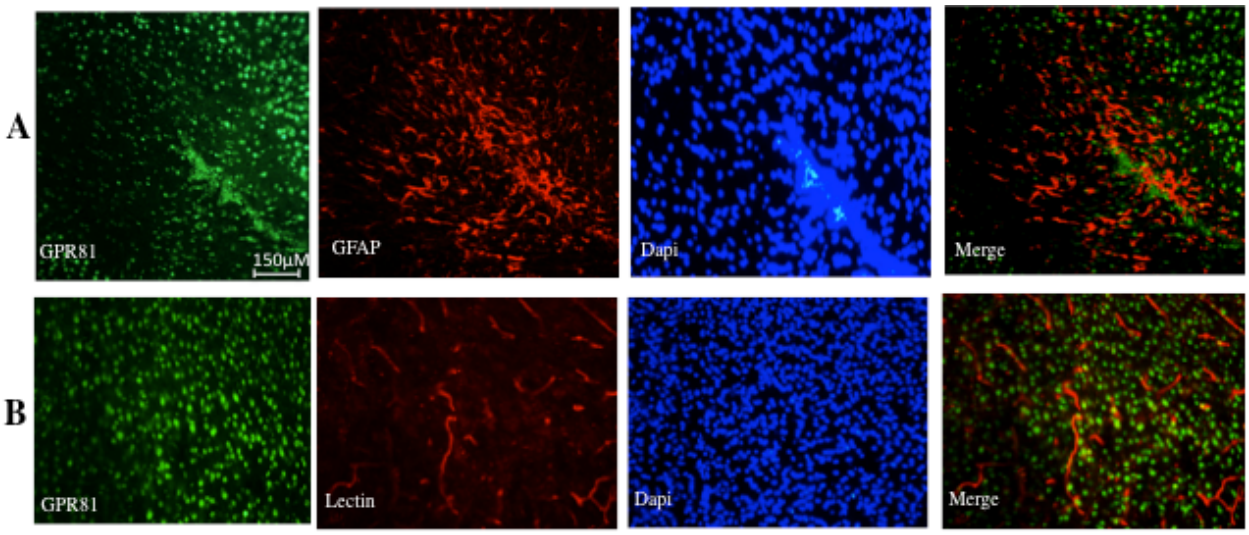

Figure 4.6 GPR81 co-localization in astrocyte and endothelial cells.

A, GPR81 (green) does not colocalize with GFAP (red) in astrocytes. B, GPR81 (green) does not colocalize with lectin (red) in endothelial cells. Images are collective of 4 experiments.

4.5 The role of GPR81 in developmental brain angiogenesis

In order to determine the post-natal effect of GPR81 on brain vasculature, lectin staining was performed at various postnatal time points ranging from P5 to P19 in aged matched WT and GPR81 KO mice. Coronal brain cryosections of 12um of WT and KO GPR81 mice were treated with *Griffonia simplicifolia* (1:100, Sigma) to stain endothelial cells, which subsequently can be used to calculate blood vessel area. A significant decrease in vessel density (20 % delay) is observed in GPR81-/- mice as compared to the aged matched WT mice during the early post-natal phases (P7, P9 and P11) of brain development **(Figure 4.8)**. However, with an increase in age, a gradual amelioration in brain vasculature is observed in KO GPR81 mice especially from P15 to P19. Here we noticed that the vessel area in the brain sections from KO GPR81 is similar to the WT mice. In the further experiments we sought to understand the factors that GPR81 could contribute to the time specific vessel area changes in GPR81 KO mice and also elucidate the potential underlying mechanism for the same.

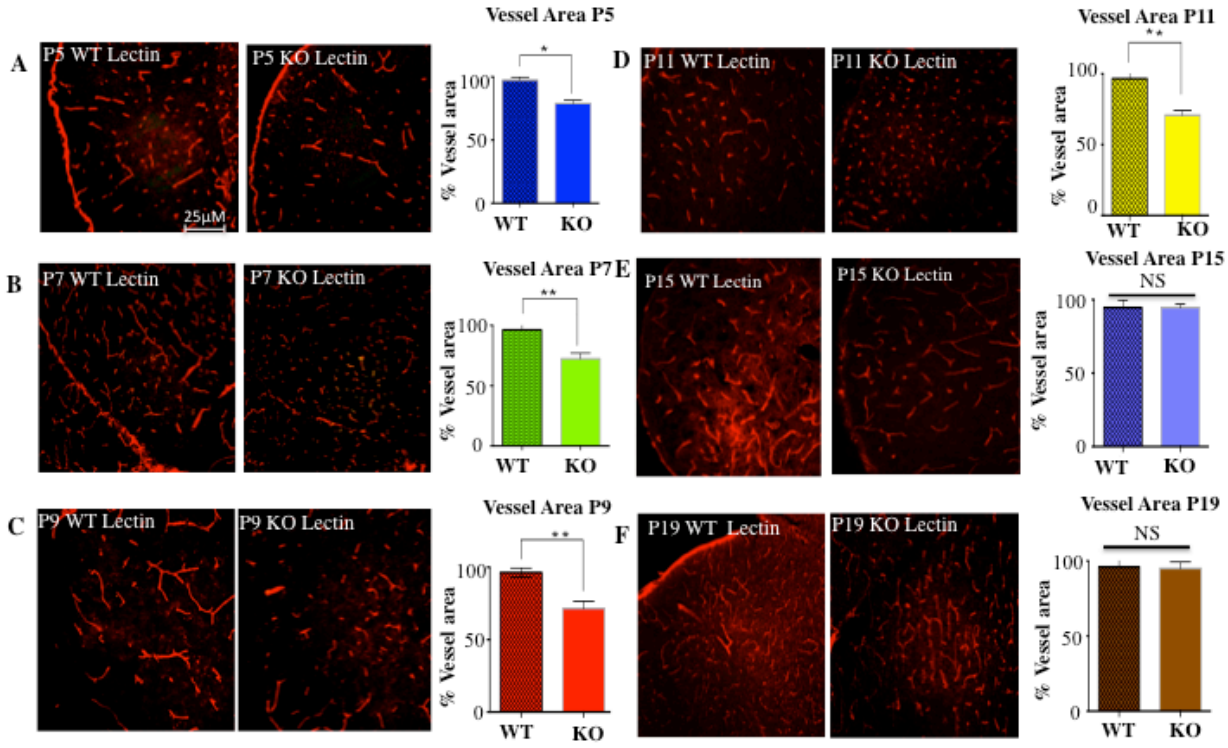

Figure 4.7 GPR81 role in developmental brain angiogenesis

GPR81 role in developmental brain angiogenesis: A to D) A decrease of 20 to 25 % in brain vasculature is seen in GPR81 KO mice in the initial post-natal stages from P5 to P11 followed by a prominent improvement in microvasculature in the later stages from P15 to P19 (Figure E and F). Values are presented, as mean ± S.E.M. Data are representative of 5 animals per group. *, $p<0.05$; **, $p<0.01$; with Tukey's multiple comparison test compared to KO or WT, as indicated.

4.6 GPR81 controls angiogenesis and inflammatory factors

To determine the potential causes for the decrease in brain vessel density in the GPR81-/- mice, we hypothesized that loss of GPR81 receptor might regulate certain mitogens and cytokines that regulate brain angiogenesis. In order to test this hypothesis, we performed a time course real time quantitative polymerase chain reaction (RT-PCR) on whole brain samples spanning from postnatal ages P5 to P11. As seen in **Figure 4.9**, during initial postnatal stages from P7 to P11 there is a prominent increase in anti-angiogenesis factor thrombospondin-1 (TSP-

1) and a corresponding decrease in angiogenic factor VEGFA. However, during the latter stages, more specifically at P19, there is a corresponding increase in angiogenesis factors vascular endothelial growth factor (VEGF) and decrease in TSP-1 expression. The increase in inflammatory factors in the GPR81-/- mice was also evident, specifically in monocyte chemokine attractant 2 (CCL-2) and cyclooxygenase 2 (COX-2) in GPR81-/- mice at P9 and P11. These results indicate that the GPR81 plays an important role in developmental brain angiogenesis through regulating the expression of pro-angiogenic factors, and also in controlling inflammatory mediators. In addition we also observed a subsequent increased expression of TSP-1 and the decreased VEGF protein levels at P9 and P11 in the GPR81 KO mice as depicted in **Figure 4.5**. Since expression of GPR81 was restricted to neurons we also confirmed increased expression of TSP-1 in GPR81 KO primary neurons compared to its wild type neuronal counterpart evident in **Figure 4.8 and Figure 4.9**. Furthermore to confirm the pro-angiogenic effect was mediated via GPR81 and lactate interaction, we performed invitro tube formation assay and exvivo aortic explants assay from WT and KO neurons and showed increased pro-angiogenic activity in the conditioned media. Collectively, we observed that loss of GPR81 causes a significant time dependent vasculature decrease, and GPR81/lactate interaction plays a vital role in modulating angiogenesis, which could be attributed to increase in TSP-1 and suppression in VEGF expression.

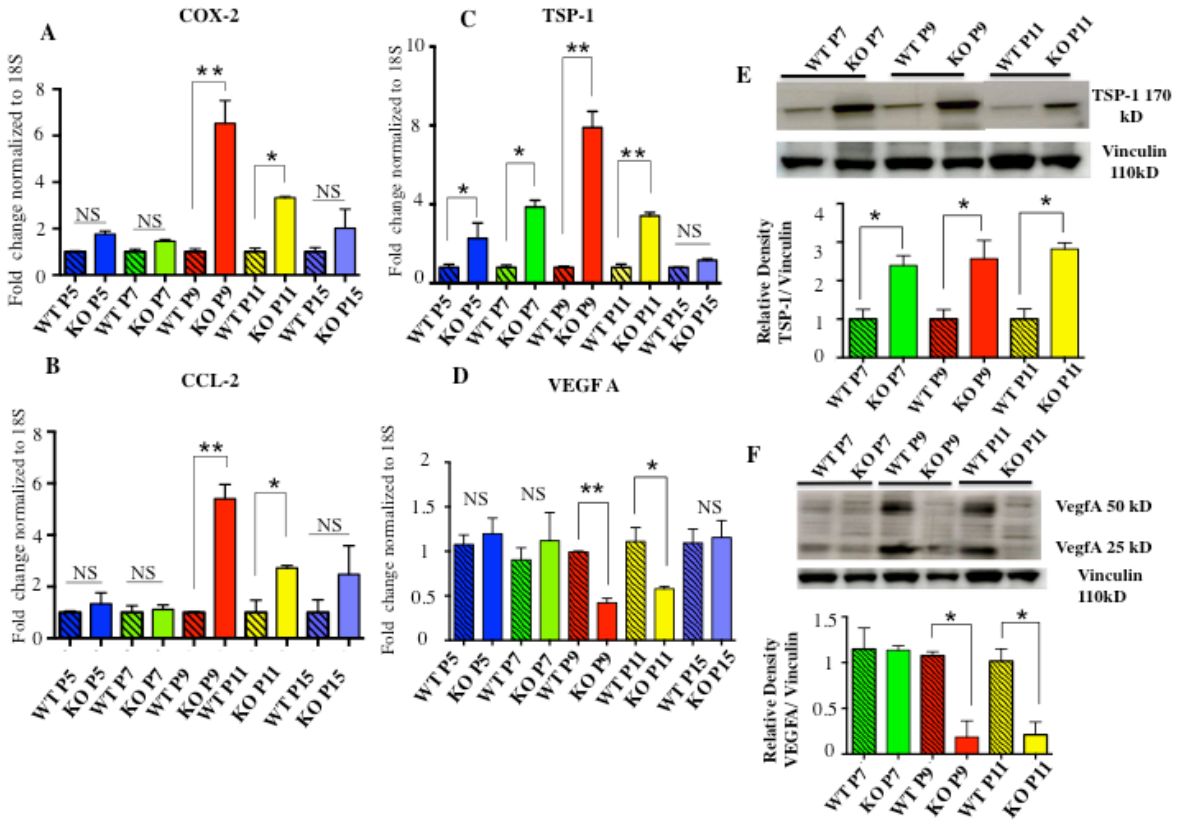

Figure 4.8 GPR81 regulated inflammatory and angiogenic factors to regulate developmental brain angiogenesis.

GPR81 and brain angiogenesis: mRNA expression of (A) COX-2, B) CCL-2, C) TSP-1 and D) VEGFA. (E) Western blot analysis and the quantification of protein expression of angiostatic factor TSP-1 and a pro-angiogenic factor (F) VEGFA is evident during the initial postnatal stage of P9 and P11 in the GPR81 KO mice. *, $p<0.05$; **, $p<0.01$; with Tukey's multiple comparison test compared to KO or WT, as indicated

4.7 Potential mechanism of GPR81 in regulating brain developmental angiogenesis

Since, during the postnatal development, loss of GPR81 resulted in an increase of inflammatory cytokines namely, CCL-2 and COX-2 and a corresponding change in angiogenic factors associated with an increase in TSP-1 and decrease VEGFA, we sought to determine the potential cause of mechanism that can relate to the aforementioned changes in pro-inflammatory and angiogenic cytokines. **Figure 4.10**, demonstrates a significant increase in TSP-1 levels in the neurons of GPR81 KO mice compared to its WT counterpart at P7 and P9 postnatal development phase determined by confocal microscopy. During these postnatal phases at P7 and P9, the mRNA expression of GPR81 and protein levels are also increased in the WT mice **Figure 4.6**. As depicted in **Figure 4.10** the increase in TSP-1 levels corresponded to a subsequent decrease in ERK phosphorylation and HIF1a levels in the GPR81 KO mice. Furthermore, since HIF1a also regulates the production of angiogenic factor VEGFA. We also determine the VEGF mRNA and protein levels at P9 and P11 in GPR81 KO mice and found that there was direct proportional decrease in VEGF A levels in the GPR81 KO mice as shown in **Figure 4.9**.

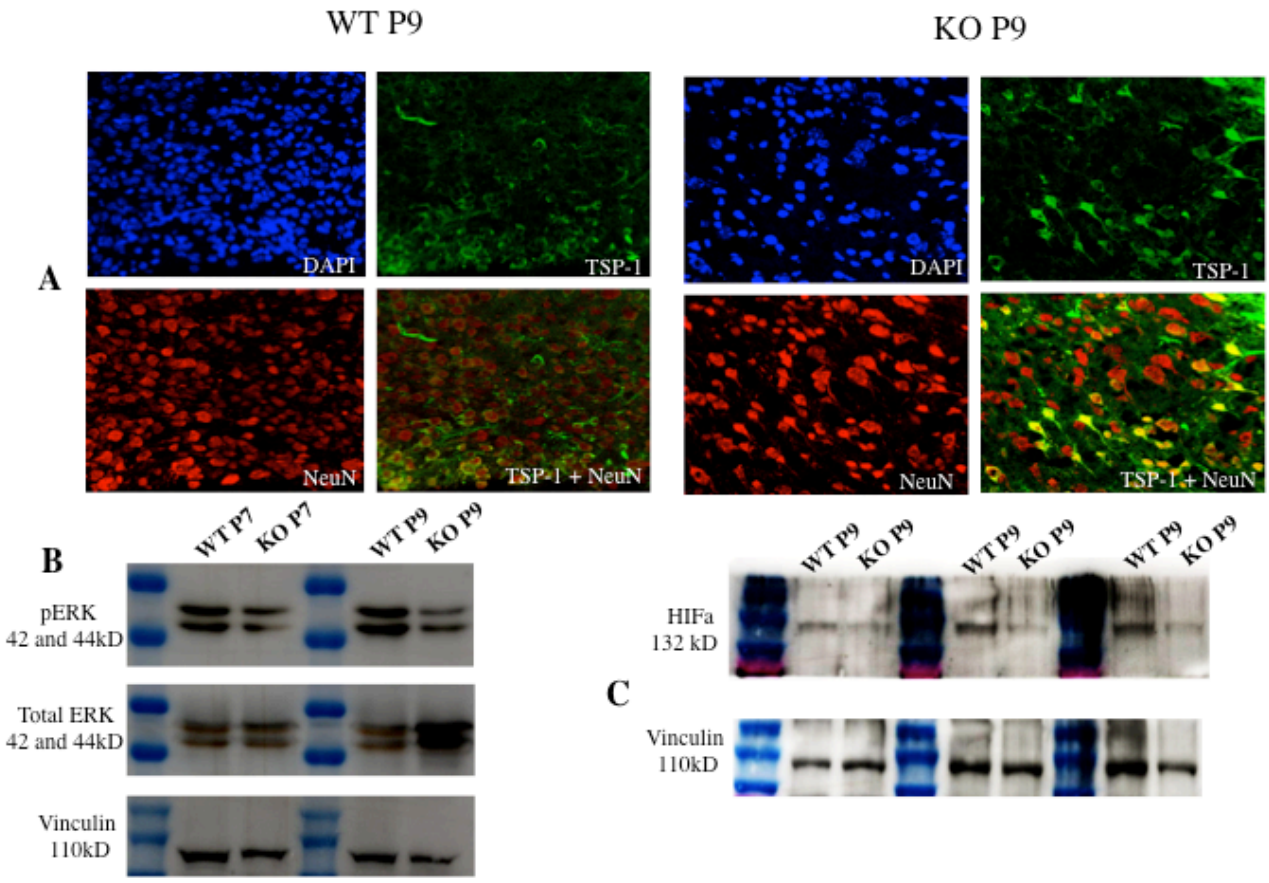

Figure 4.9 Potential mechanisn of GPR81 in regulating brain developmental angiogenesis.

Increased TSP-1 expression was evident in postnatal P9 GPR81 KO mice as compared to the WT mice. b) ERK activation showing increased phosphorylated ERK in WT mice compared to KO mice. c) Increased HIF1a levels in WT mice compared to KO mice. Images are quanitified as collective of 3 mice experiments per group.

4.8 GPR81 in neurons stimulates production of TSP-1 and VEGFA

To confirm the role of GPR81, which is highly expressed in neurons, stimulates the production of pro-angiogenic cytokines such as TSP-1 and VEGFA, we performed an *ex-vivo* experiment on aortic explants. The principle was based on the fact that lactate/GPR81 interaction

would stimulate the production of pro-angiogenic cytokines which inturn would induce angiogenic sprouting in the aorta or tube formation in endothelial cells embedded in matrigel. We treated the WT and KO primary neurons with PBS and lactate for a period of 24h. The conditioned media was collected, concentrated and used for the invitro matrigel and aortic explants experiments, whereas the cells were used for protein analysis of VEGFA and TSP-1 by western blot. **Figure 4.11 and Figure 4.12** shows that treatment with WT lactate containing conditioned media caused prominent angiogenesis sprouting in the aortic rings and extensive tube formation in the endothelial cells, compared to lactate treatment or PBS containing conditioned media obtained from KO neurons. This result portraits, that GPR81 modulates the secretion of pro-angiogenic factors into conditioned media upon its stimulation with lactate. Moreover, western blots of lactate stimulated WT primary neurons after 24h showed a decrease in TSP-1 and increase in VEGF-A expression, while neurons cultured from GPR81-/- did not respond to lactate stimulation **(Figure 4.13)**. Interestingly, confocal imaging of primary neurons from GPR81-/- also showed a prominent increase in TSP-1 as compared to WT counterpart as evident in **Figure 4.14**.

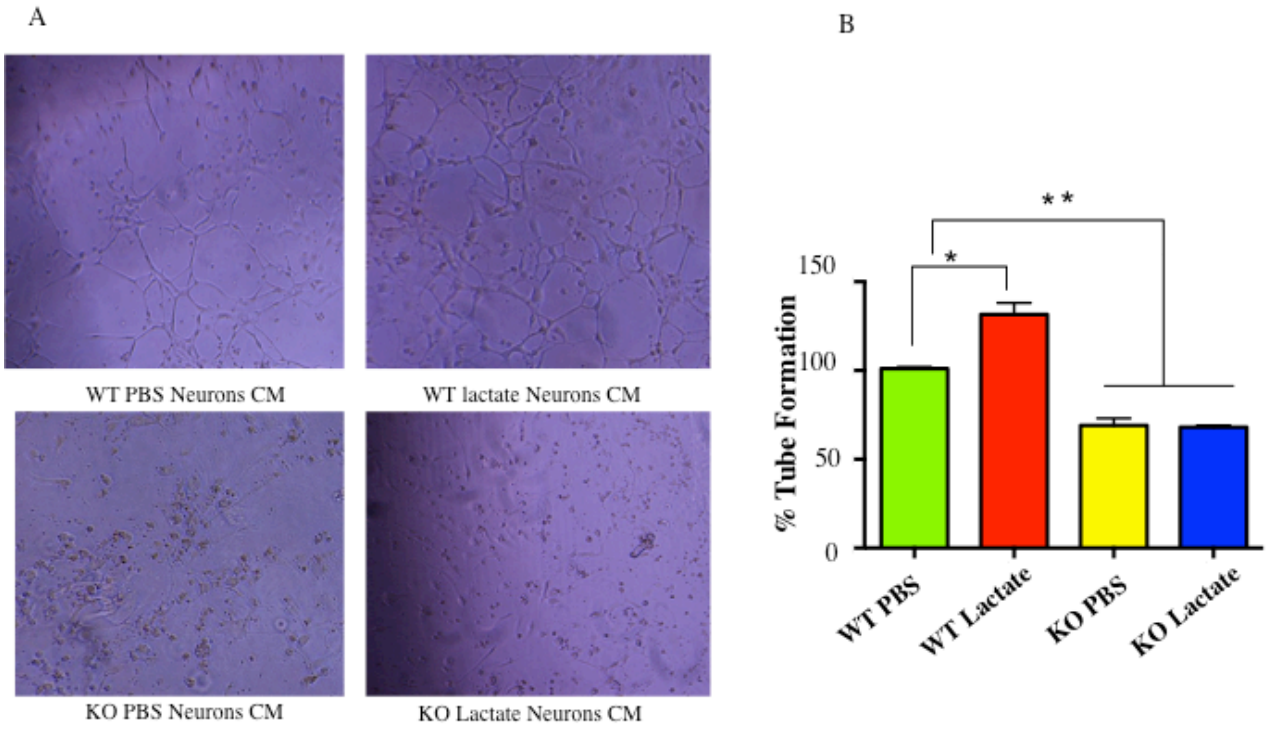

Figure 4.10 Invitro angiogenic effect of lactate/GPR81 interaction on endothelial cells.

A. In vitro matrigel gel assay indicating increased tube formation is seen on treatment with lactate conditioned media from WT primary neurons compared to the control PBS vehicle and conditioned media obtained from KO neurons. B. Quantification of tube formation in percentage. Values are presented, as mean ± S.E.M. Data are representative of 3 experiments per group. *, $p<0.05$; **, $p<0.01$; with ANOVA multiple comparison test compared to KO or WT, as indicated.

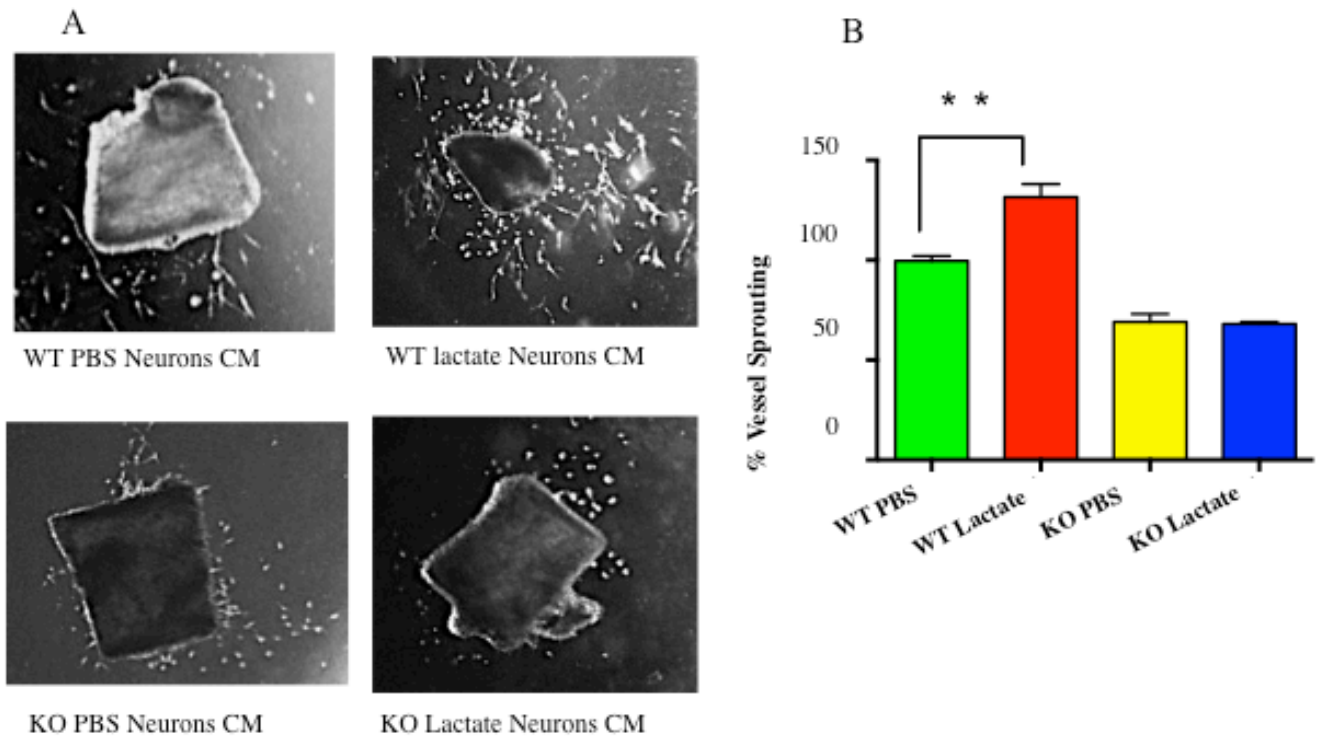

Figure 4.11 *Exvivo* angiogenic effect of lactate/GPR81 interaction on aortic explants

A. Aortic Explants indicating increased angiogenesis sprouting on treatment with lactate conditioned media from primary neurons. Increased angiogenesis sprouting is seen in aortic rings treated with Lactate containing conditioned media compared to KO counterpart. B. Quantification of aortic sprouting of blood vessels in percentage. Values are presented, as mean ± S.E.M. Data are representative of 4 animals per group. *, $p<0.05$; **, $p<0.01$; with ANOVA multiple comparison test compared to KO or WT, as indicated.

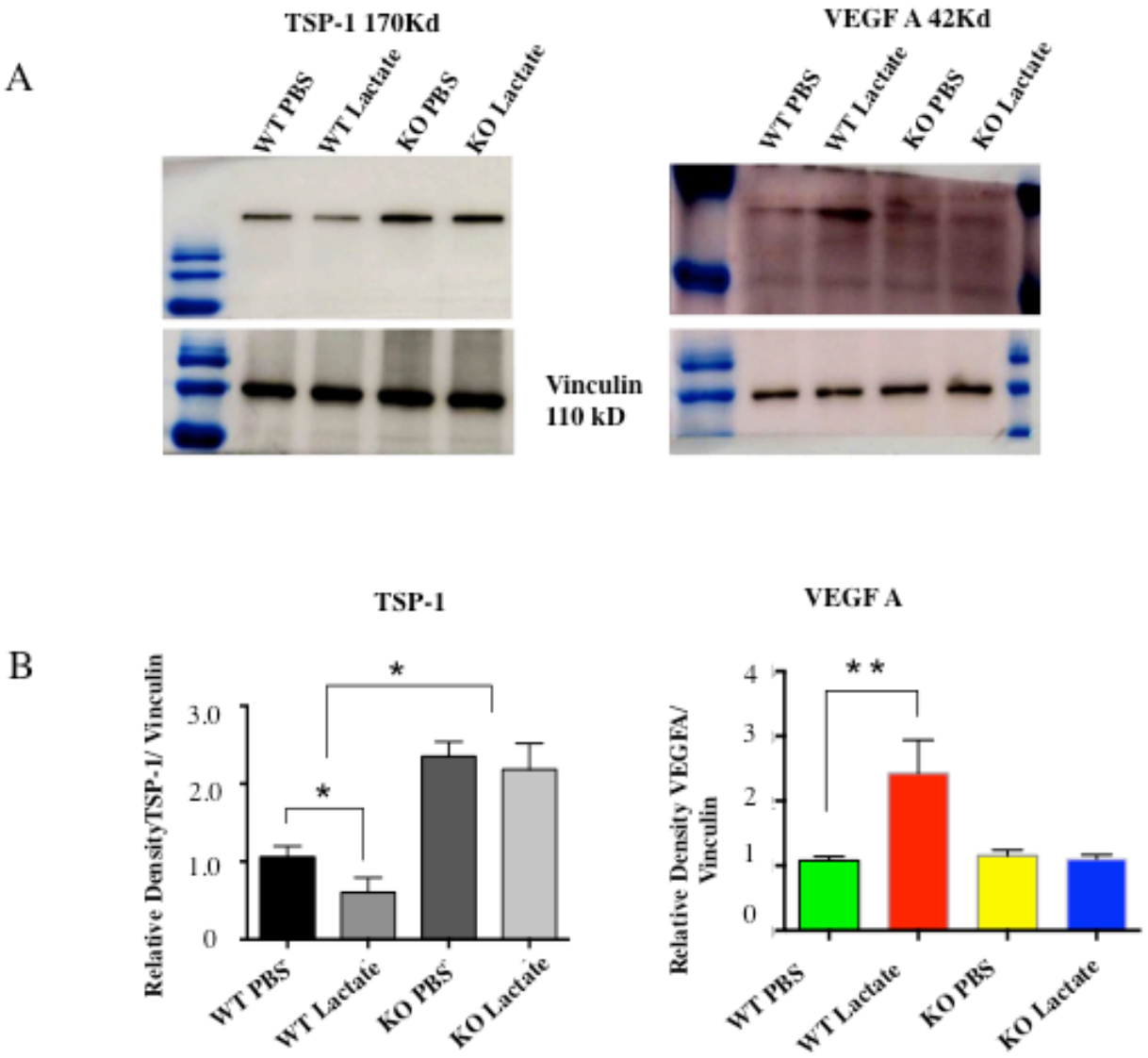

Figure 4.12 Angiogenic effect of GPR81 in neurons involving TSP-1 and VEGF.

A. Decrease in TSP-1 and a corresponding increase in VEGFA expression in WT primary neurons after lactate treatment. B. Quantification of TSP-1 and VEGFA protein expression with respect to vinculin. Values are presented, as mean ± S.E.M. Data are representative of 4 animals per group. *, $p<0.05$; **, $p<0.01$; ***, $p<0.001$ with ANOVA multiple comparison test compared to KO or WT, as indicated.

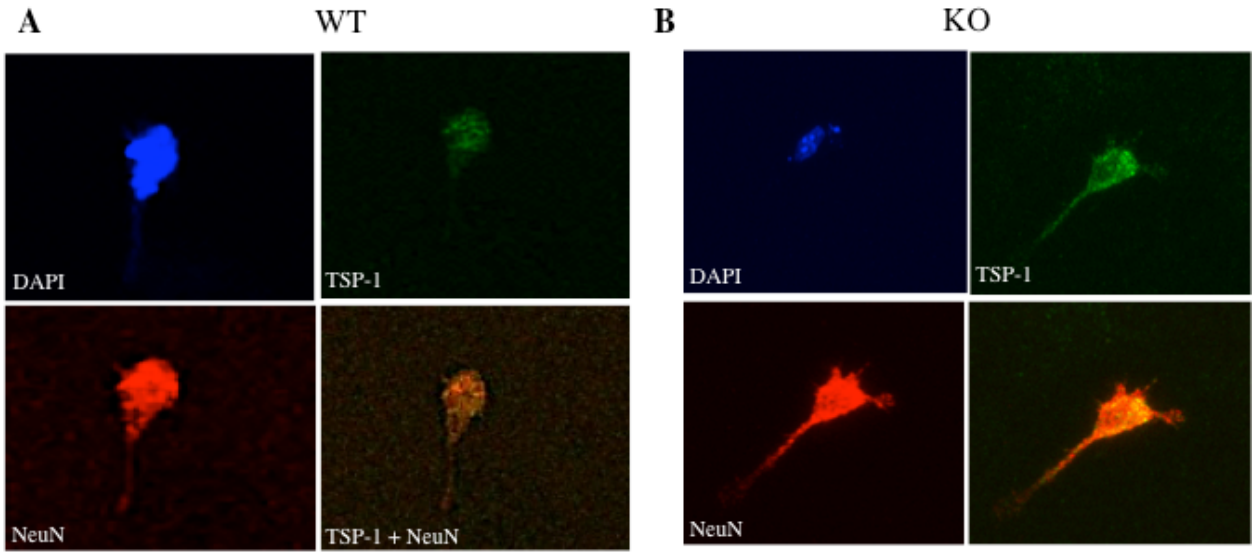

Figure 4.13 TSP-1 expression in WT and GPR81 KO neurons by confocal microscopy.

TSP-1 co-localization: (green) TSP-1 colocalize with NeuN (red) in immature neurons in A) WT and B) KO primary neurons showing a higher expression in KO primary neurons. Images are taken as collective of 3 mice experiments.

4.9 Lactate via GPR81 promotes angiogenesis *Invivo*

To confirm lactate/GPR81 interaction is involved in angiogenesis *inivo,* intracerebroventricular injections were performed in WT and GPR81 KO at P4. The endothelial cell staining by lectin was determined after 6 days on P10 while the expression of inflammatory and angiogenic factors were determined by qPCR after 24 hrs, a day after injections. **Figure 4.15,** showed a 20% increase vascular area in the WT mice after injections compared to the GPR81 KO mice. Furthermore to elucidate which factors partake in this process of angiogenic regulation the whole brain tissue samples after 24hrs of injections were subjected to qPCR analysis. Since it was quite evident that GPR81 controls TSP-1 and VEGFA and pro-inflammatory cytokines COX-2 and CCL-2 during the developmental stages. We determined if lactate treatment could either increase of decrease these aforementioned factors. Indeed, we

found that there was a significant increase in angiogenic and a corresponding decrease in pro-inflammatory factors upon lactate treatment in the WT mice that was not evident in GPR81 KO mice.

4.10 GPR81 reduces infarct size in HIE mice model and brain angiogenesis in HI

To investigate the protective angiogenic role of lactate/GPR81 interaction in a hypoxic ischemic insult, WT and GPR81-/- mice were initially, subjected to Hypoxic ischemic insult (HI) via permanent middle carotid artery ligation followed by hypoxia (8% O2) for 1.5 hours. HI insult resulted in decrease vessel density and increase infarct area in the GPR81-/- mice as compared to the WT mice post 96 hours after HI as evident in **Figure 4.16**. To further elucidate the role of GPR81 in brain angiogenesis, intracerebroventricular lactate injections were performed on WT and GPR81-/- mice at P4 followed by HI insult at P7, and subsequently the vessel density was measured post 48 and 96 hours after HI insult. **Figure 4.17** shows a prominent increase in vessel density in the lactate treated WT mice, whereas the vessel density in the lactated GPR81-/- mice remained unaltered. Moreover, the infarct region in the wild type was substantially reduced as compared to the GPR81-/- mice, suggesting that lactate via its receptor GPR81 promotes angiogenesis and has a neurorestorative effect after an HI insult. In addition a 25% increase in vascular density was observed in the WT mice treated with lactate compared to PBS treated after HI and a corresponding 40 % increase compared to KO mice treated with PBS or lactate. To determine which angiogenic factors GPR81 regulates that reduces infarct size in HI, we performed RT-PCR on brain samples extracted 24 hours post HI after intracerebroventricular lactate injections. **Figure 4.18** depicts, increase in angiogenic factors, predominantly, VEGF, PDGF-BB, angiopoietin 1 (ANG-1), angiopoietin 2 (ANG-2) and importantly a corresponding decrease in TSP-1 expression.

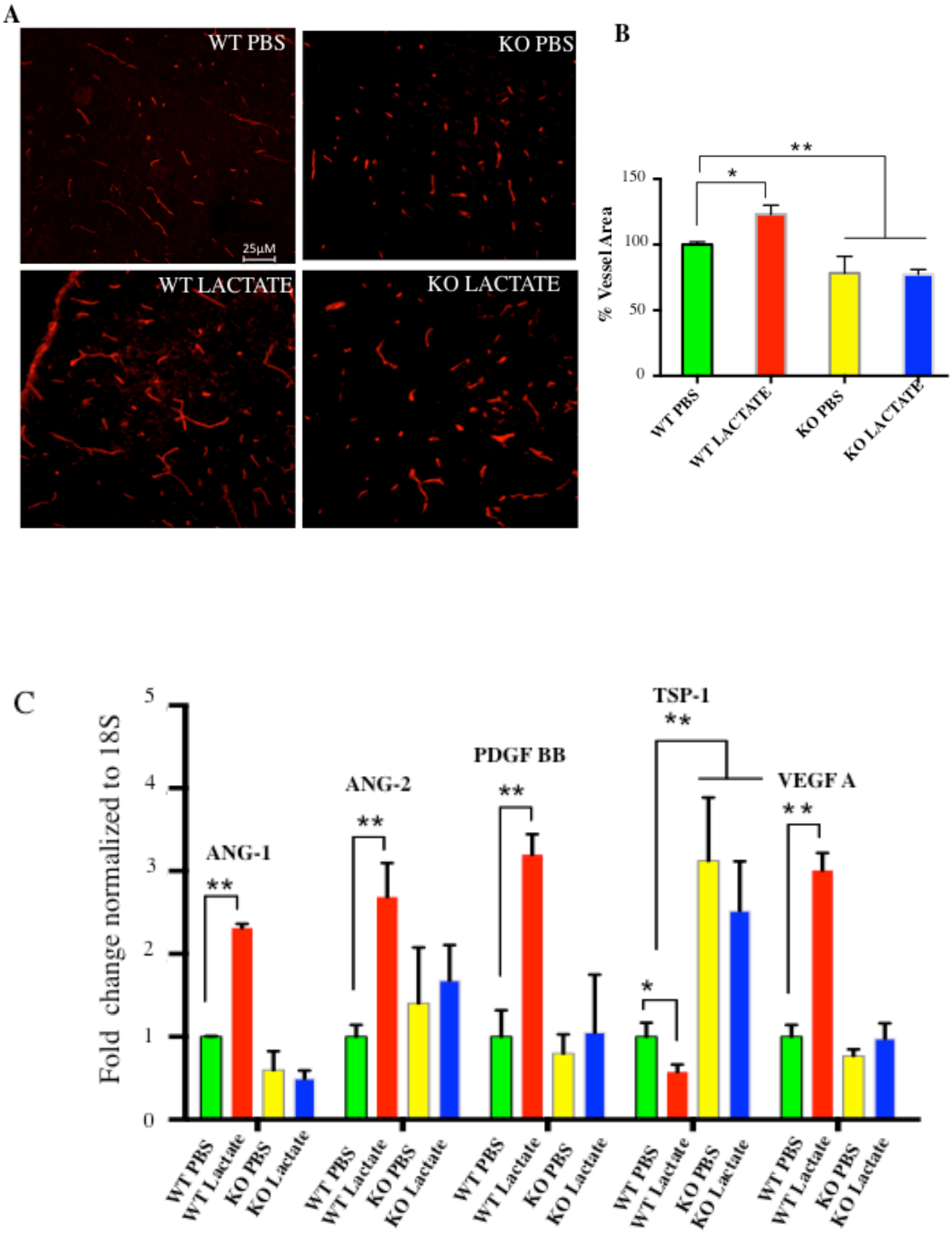
A
WT PBS
KO PBS
25μM
WT LACTATE
KO LACTATE
B
% Vessel Area
150
100
50
0
*
**
WT PBS
WT LACTATE
KO PBS
KO LACTATE
C
Fold change normalized to 18S
5
4
3
2
1
0
ANG-1
ANG-2
PDGF BB
TSP-1
VEGF A
**
*
WT PBS
WT Lactate
KO PBS
KO Lactate

Figure 4.14 Lactate promotes angiogenesis via GPR81 and regulates secretion of angiogenic factors

A. Lactate injections at P4 stimulate a 25 % increase in in vessel Area in WT mice as compared to KO mice. B. Quantification of % vessel area after lactate injections at P9. C. Invivo pro-angiogenic factors regulated by lactate via GPR81. Values are presented, as mean ± S.E.M. Data are representative of 7 animals per group. *, p<0.05; **, p<0.01;with ANOVA multiple comparison test compared to KO or WT, as indicated.

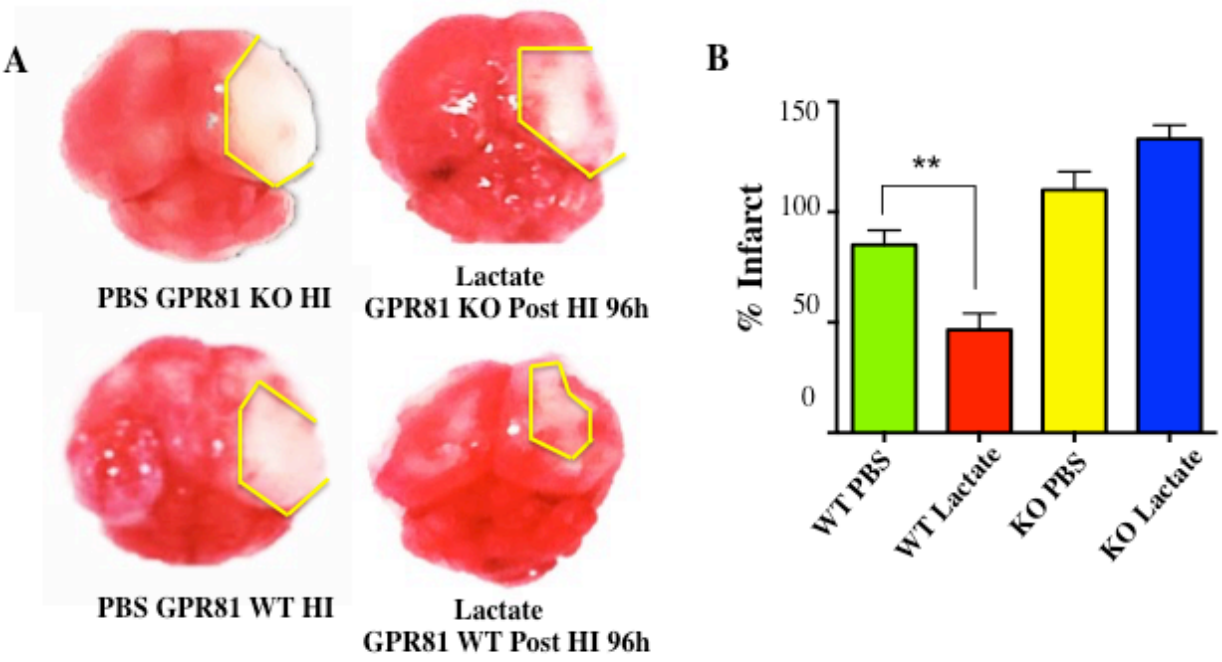

Figure 4.15 GPR81 protective effect in cerebral hypoxia

TTC staining showing decrease infarct size in the GPR81 WT mice compared to WT mice after lactate injections. A. TTC staining showing infarct size in WT and KO mice treated with and without PBS and lactate. B. Quantification of infarct size in percentage. Values are presented, as mean ± S.E.M. Data are representative of 4 animals per group. *, p<0.05; **, p<0.01; with ANOVA multiple comparison test compared to KO or WT, as indicated.

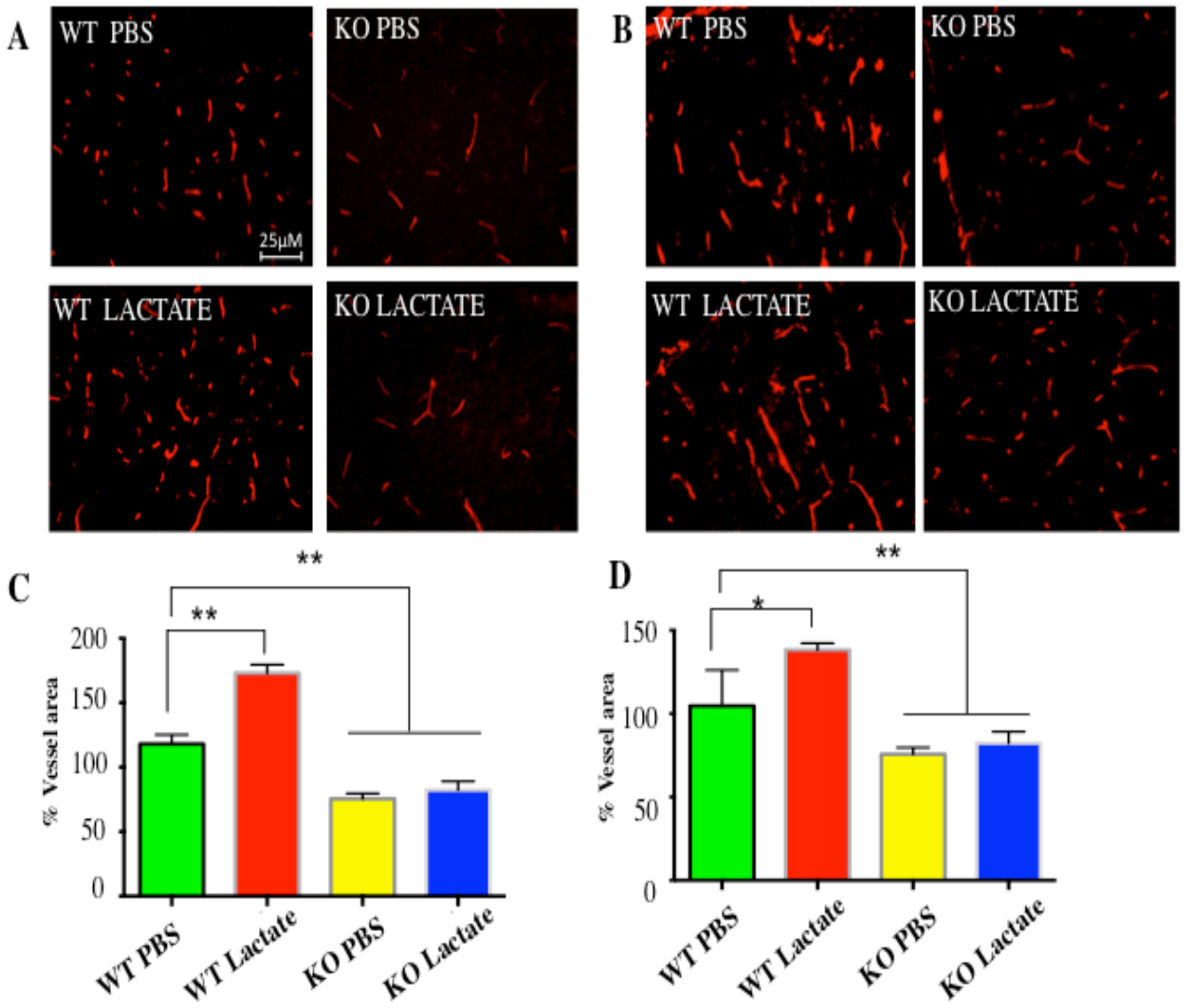

Figure 4.16 GPR81 protective effect in cerebral hypoxia via angiogenesis

Lactate injections at P4 stimulate a 25 % increase in in vessel Area in WT mice as compared to KO mice post (A) 48h and (B) 96h after HI Values are presented, as mean ± S.E.M. C and D. Quantification of % vessel area after 48h and 96h of HI insult. Data are representative of 5 animals per group. *, $p<0.05$; **, $p<0.01$; ***, $p<0.001$ with ANOVA multiple comparison test compared to KO or WT, as indicated.

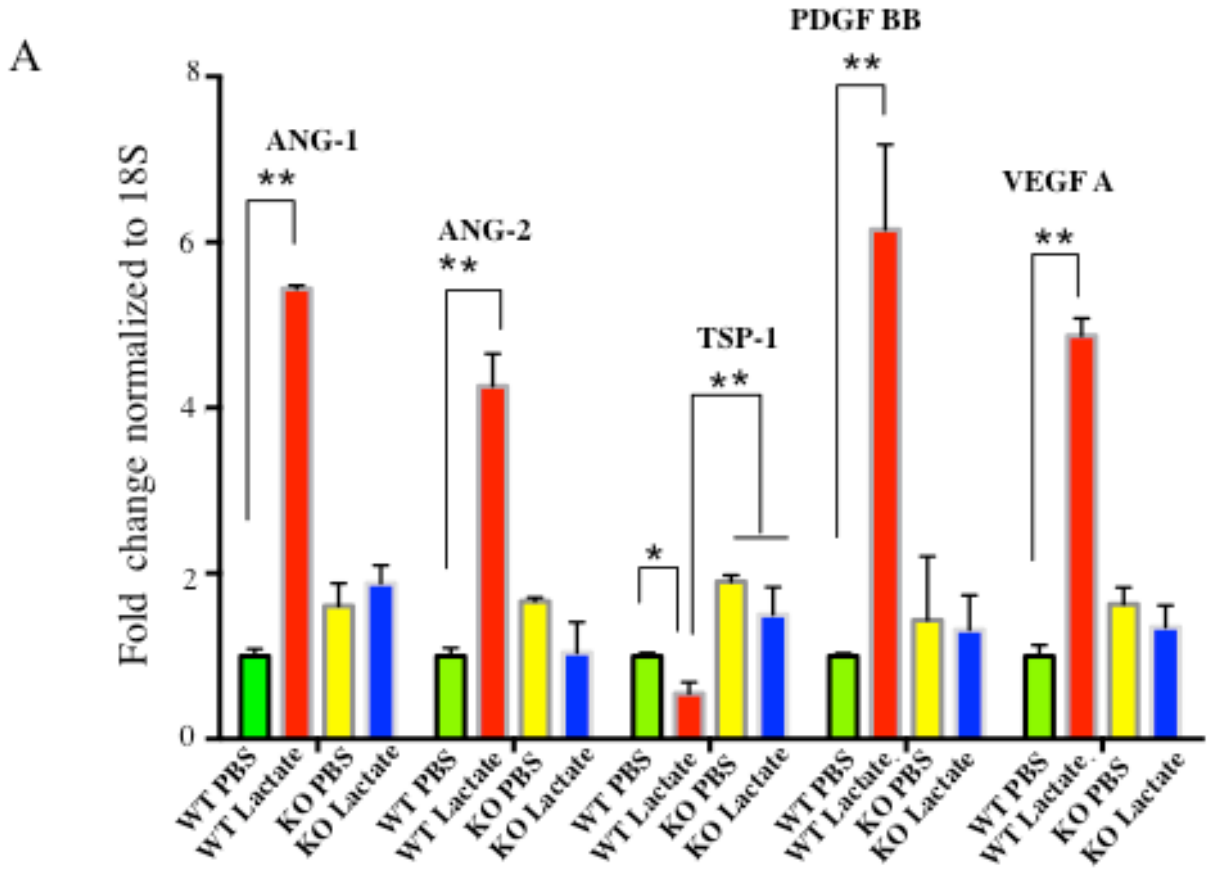

Figure 4.17 GPR81 protective effect in cerebral hypoxia via regulation of angiogenesis factors

A. Lactate injections at P4 stimulates increase in pro-angiogenic factors and a corresponding decrease of TSP-1 in WT mice as compared to KO mice post 24h after HI. Values are presented, as mean ± S.E.M. Data are representative of 4 animals per group. *, $p<0.05$; **, $p<0.01$; with ANOVA multiple comparison test compared to KO or WT, as indicated.

4.11 GPR81 plays an anti-inflammatory role in double hit neuroinflammation mice model

The loss of GPR81 resulted in increase pro-inflammatory cytokines namely, CCL-2 and COX-2 during the postnatal developmental ages at P9 and P11. We ought to determine if GPR81 plays a major and a similar role in a pathological preterm neuroinflammation model. As depicted in **Figure 4.19**, immunohistochemistry analysis for microglia via IBA-1 staining, post HI insult after 4 days or 96h showed an increased activation and infiltration of microglia in the GPR81 KO mice as compared to their WT counterparts. Furthermore to determine the subsequent inflammatory factors that can be modulated by GPR81, quantitative polymerase chain reaction (qPCR) was performed on ipsilateral part of the brain from the WT and GPR81 KO mice. The results indicated there was substantial increase in pro-inflammatory cytokines (IL-1B, TNFa and CCL-2) in GPR81 KO mice upon LPS injection.

A

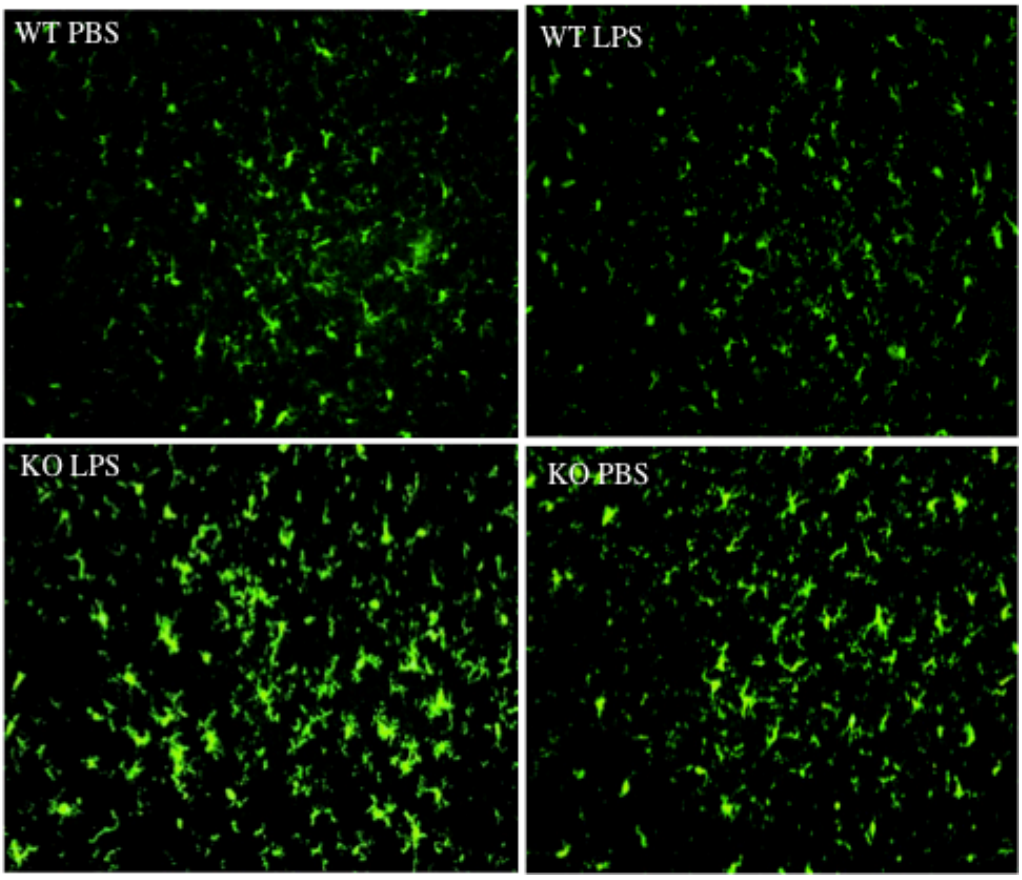

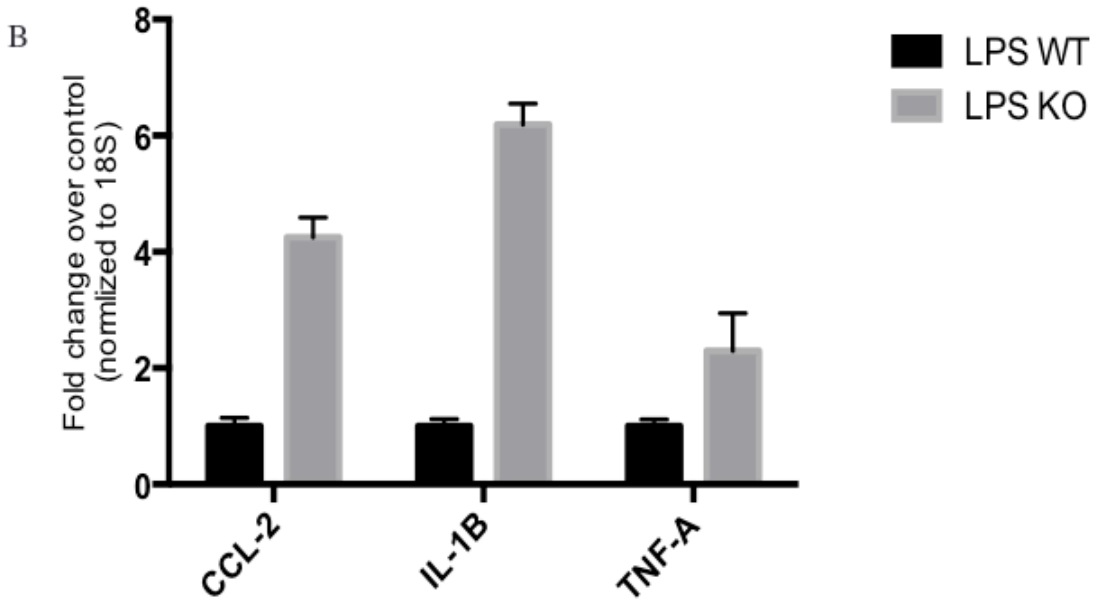

Figure 4.18 GPR81 controls inflammatory factors in preterm double hit neuroinflammation mice model

A. Immunohistochemical analysis after LPS injections in WT and KO mice shows increases microglia (IBA-1) staining in KO mice. B. Lactate injections at P4 stimulates increase in pro-angiogenic factors and a corresponding increase CCL-2, IL1B. and TNFa in KO mice as compared to WT mice post 24h after HI. Values are presented, as mean ± S.E.M. Data are representative of 4 animals per group. *, $p<0.05$; **, $p<0.01$; with ANOVA multiple comparison test compared to KO or WT, as indicated.

4.12 Linking Statement

We previously have described a phenotype in brain wherein loss of GPR81 contributes to decrease in vessel area at specific post-natal time points from P7 to P11. Similarly, we were able to find regression in inner retinal vasculature in the retina at from P8 to P12. This transient phenotype in the retina was regulated by GPR81 via modulating Wnt and Norrin expression [91]. The main aim of this project was to determine GPR81 protein levels in normoxia and oxygen induced retinopathy (OIR) along with identifying the signalling pathways that could mediate Norrin and Wnt signalling via GPR81.

4.13 Post-natal GPR81 protein expression in retina

The initial goal was to determine if there was change in post-natal GPR81 expression in mRNA and protein levels in retina. Indeed, we found that there was a significant increase in GPR81 protein levels at P10 and P12 in the retina as depicted in **Figure 4.20**. This result corresponds to a similar increase in GPR81 protein levels seen in **Figure 4.5** in the brain at post-natal ages from P9 to P11. The brain and retinal post-natal developmental vasculature continues till P21 in mice, in addition coupling with the fact that retina and the brain are high metabolic organs; they have relative high basal levels of lactate. Changes in GPR81 proteins expression from P9 to P12 could attribute to its specific role in developmental angiogenesis in brain and retina along with the prominent role of VEGFA, ANG-1, NOTCH-1, tie-2, Wnt, B-catenin signalling pathways. GPR81 could either regulate some of these factors as evident in the brain via VEGFA or by Wnt/Norrin signalling in the retina.

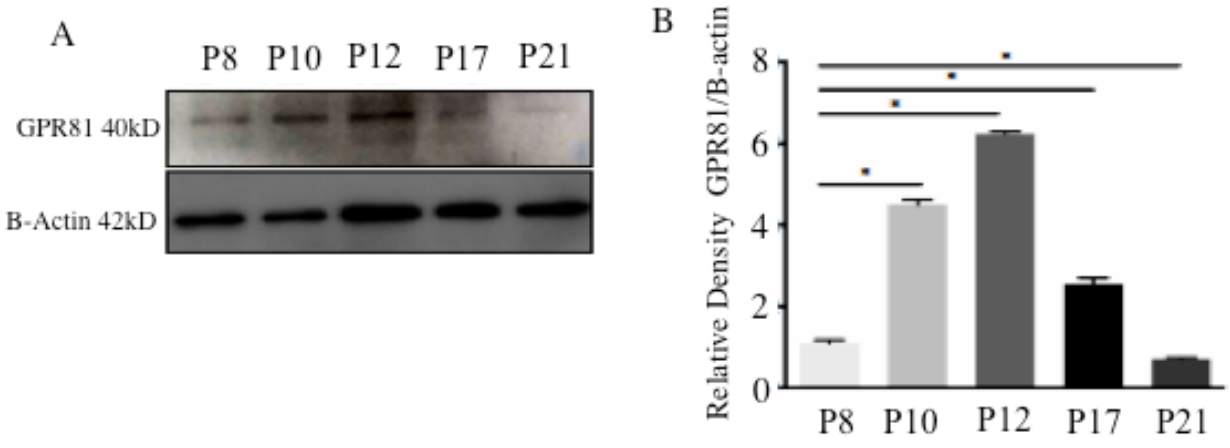

Figure 4.19 Post-natal GPR81 expression at different time points in WT mice retina

A. GPR81 protein expression from P8 to P21. B. Western blot quantification of GPR81 relative to B actin. *, $p<0.05$; **, $p<0.01$; with Tukey's multiple comparison test compared to P5 WT, as indicated. Values are presented, as mean ± S.E.M. Data are representative of 4 animals per group.

4.14 Post-natal GPR81 protein expression in oxygen induced retinopathy in retina

To establish the link between GPR81 and norrin in pathological condition, we used the oxygen-induced retinopathy (OIR) mice model. Wherein we uncovered that the decreased GPR81 expression at vaso-obliteration (VO) and a corresponding increased in GPR81 at neovascularization (NV) phase was directly proportional to norrin expression. Due to technical difficulties of unavailability of Norrin antibodies, norrin protein levels could not be determined by western blotting. However, GPR81 protein levels categorically showed a similar trend with a decrease at VO and increase at NV compared to the mRNA expression. Similarly there was significant decrease in Wnt and norrin expression in KO mice at P9 during post-natal retinal developmental, which was also evident in OIR. Collectively, these results along with GPR81

expression analysis in normoxia and OIR buttress the role of GPR81 in physiological and pathophysiological aspects.

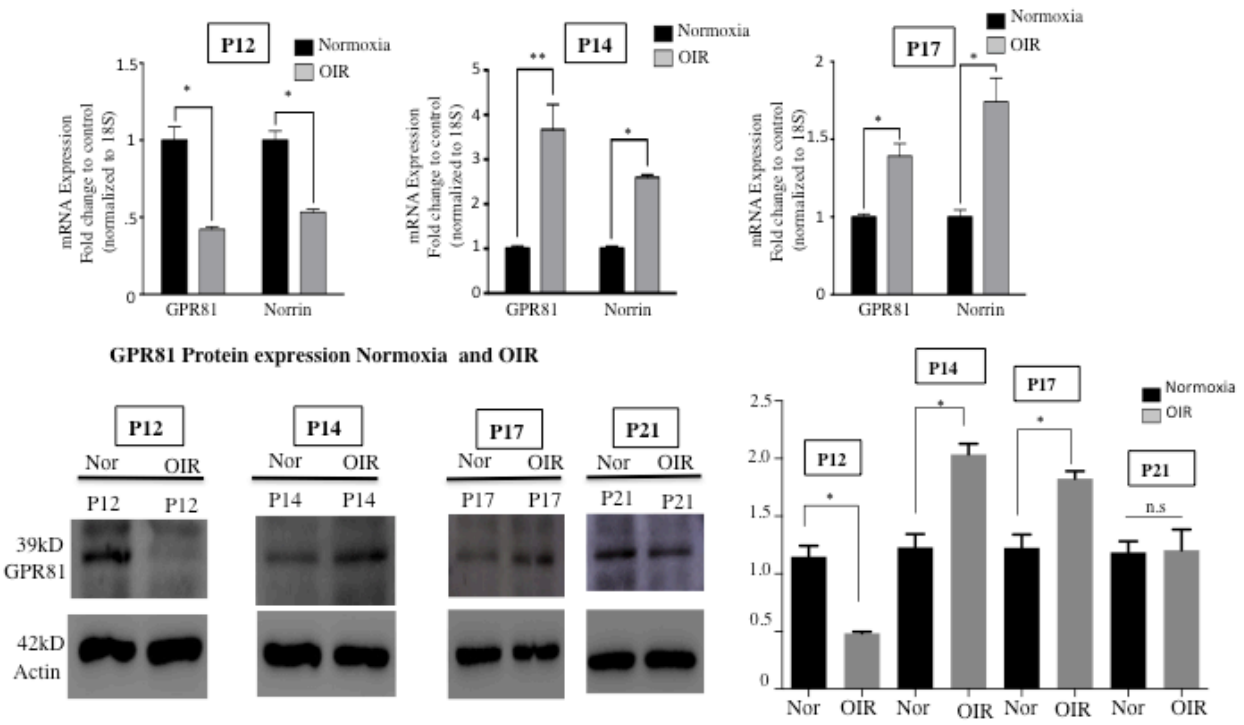

Figure 4.20 Post-natal GPR81 expression at different time points in the WT mice retina in OIR

GPR81 and Norrin mRNA expression determined by qPCR at vaso-obliteration P12 and neovascularization P17 phase in OIR. GPR81 protein expression during vaso-obliteration phase P12 and neovascularization phase P17 and P21 in WT mice model of OIR. *, $p<0.05$; **, $p<0.01$; with Tukey's multiple comparison test compared to P5 WT, as indicated. Values are presented, as mean ± S.E.M. Data are representative of 6 retinas per group.

4.15 GPR81 controls PLVAP and Claudin-5 mRNA expression and protein levels

The expression of claudins have been also been shown to be regulated by Wnt ligands and norrin wherein, via activation of their receptors frizzled-4 (FDZ-4) and coreceptors LRP-5/6 stimulates

translocalization of B catenin to the nucleus. B catenin translocalization in turn promotes the activation of transcription factor TCF that modulates the expression of claudins. Since loss of GPR81 diminishes expression of Norrin and Wnt we souught to determine if there is change in expression of claudin-5

As depicted in **Figure 4.21**, GPR81 regulates the expression of Norrin in normoxia and OIR. Since Norrin along with Wnt signalling ligands are prime regulators of inner retinal vasculature in developmental retina whose expression are also regulated by GPR81 as established in the recent article by Madaan et al. We sought to determine if loss of GPR81 could also modulate the inner or outer blood retinal barrier (iBRB or oBRB). It has been widely reported that Claudin-5 contributes in maintaining tight junctions of the endothelial cells in iBRB and oBRB. Hence we proposed that since loss of GPR81 results in decrease Norrin expression, GPR81 could indirectly regulate iBRB via modulating claudin-5 function. The transient phenotype resulting in decreased angiogenesis in brain owing to reduced VEGFA and increased TSP-1 expression and inner retinal vasculature attributed to decreased norrin and wnt ligands was more prominent from P8 to P12. We determined if the resulting suppression of pro-angiogenic modulators could regulate iBRB via claudin-5. To determine if decrease expression of claudin-5 could reduce tight junction of the endothelial cells and thereby promote increase traversing of plasma lemma vesicle assisted protein (PLVAP), we performed mRNA expression and protein analysis of Claudin-5 and PLVAP as depicted in Figure 4.22. As seen in **Figure 4.22** there is substantial and significant decrease in claudin-5 mRNA and protein levels in GPR81 KO mice at P9. Indeed we were able to detect a corresponding increase in PLVAP mRNA in GPR81 KO mice. Unfortunately due to unavailability of good commercial antibodies for PLVAP, protein levels could not be determined.

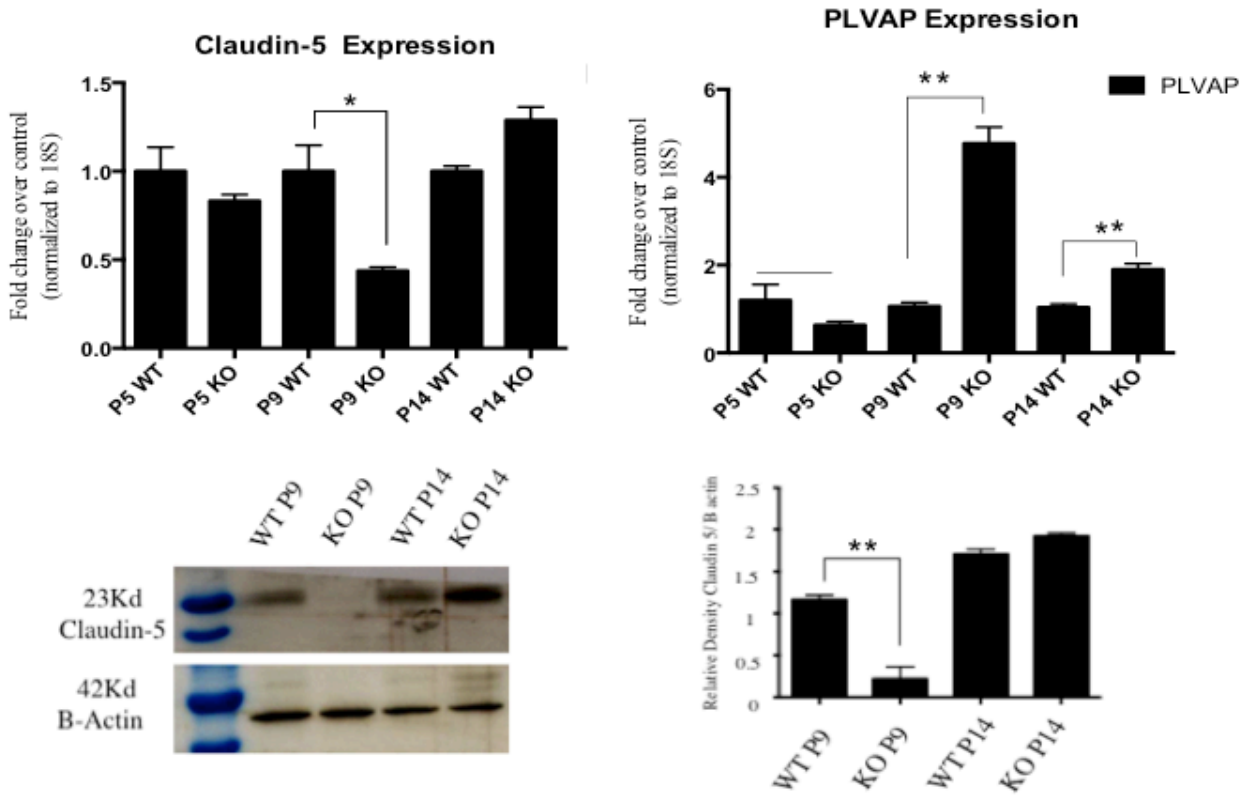

Figure 4.21 Claudin-5 and PLVAP mRNA expression and claudin-5 protein levels in aged matched retina in WT and KO mice at P5, P9 and P14 post-natal stages

A decrease in Claudin-5 mRNA expression and protein levels are evident at P9 and a corresponding increase in plasma lemma vesicular associated protein (PLVAP) mRNA expression at P9 and P14 in GPR81 KO mice. Presented as*, $p<0.05$; **, $p<0.01$; with Tukey's multiple comparison test compared to WT, as indicated. Values are presented, as mean ± S.E.M. Data are representative of 6 retinas per group from 6 mice.

4.16 GPR81 controls Norrin expression via ERK1/2 pathway

The expression of GPR81 in the retina is diverse and varied in different cells ranging from retinal pigmental cells (RPE), retinal ganglion cells (RGC) to Muller cells (MC). In our GPR81KO we

were able to link the decrease in norrin expression to its subsequent diminished inner retinal vasculature and increases iBRB permeability via claudin-5. Since expression of GPR81 is higher in Muller cells and MCs are found to be the main producers of norrin we sought to elucidate the upstream signalling mechanism that could contribute to norrin secretion via GPR81. For this purpose we culture primary muller cells from WT and GPR81 KO mice and treated them with PBS and lactate for 5 min to determine the ERK1/2 protein levels. In addition, pMC were pre-incubated with U0126 (an ERK inhibitor) for a hour followed by lactate or PBS treatment for 6h. The cells were subjected to qPCR analysis to determine norrin expression. As depicted in **Figure 4.23** there was a significant decrease of lactate induced norrin expression by U0126. This effect was not visible in the pMCs from GPR81KO mice, indicating the expression of norrin was specifically mediated by GPR81/lactate interaction. Similarly, there was an increase level of phospho-ERK levels on lactate treatment from the WT mice pMC compared to either PBS treatment or pMC derived from GPR81KO mice. Unfortunately, the protein levels of norrin in the pMC could not be assessed due to unavailability of good antibodies.

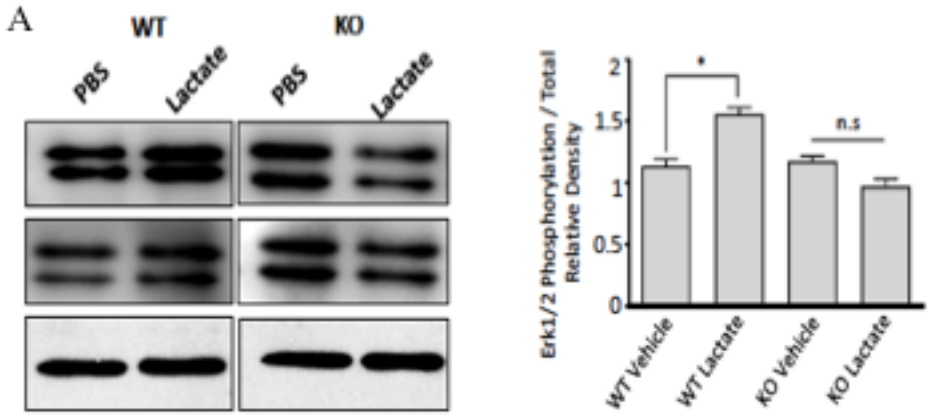
A
WT
KO
PBS
Lactate
PBS
Lactate
Erk1/2 Phosphorylation / Total
Relative Density
2
1.5
1
0.5
0
*
n.s
WT Vehicle
WT Lactate
KO Vehicle
KO Lactate

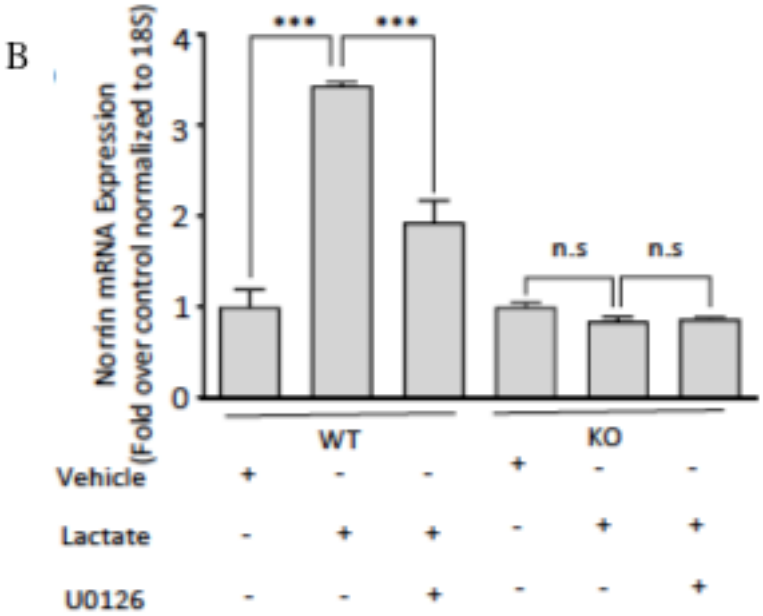
B
Norrin mRNA Expression
(Fold over control normalized to 18S)
4
3
2
1
0
***
***
n.s
n.s
WT
KO
Vehicle + - - + - -
Lactate - + + - + +
U0126 - - + - - +

Figure 4.22 Norrin (upregulation) restores intra-retinal vasculature in GPR81 KO mice.

To investigate the mechanism of action of GPR81 via Norrin, A. Western blot analysis of extracellular signal-regulated kinase (Erk) 1/2 and phosphorylated Erk1/2 (p-Erk1/2) was studied in wild-type (WT) and KO primary Müller cells. Representative images show an increase in Erk1/2 phosphorylation after lactate stimulation in Müller cells from WT mice and not in KO Muller cells. B. mRNA expression of Norrin in WT and KO primary Müller cells treated with or without lactate in the presence of Erk1/2-specific inhibitor (U0126). Values are presented as fold increases over control (vehicle stimulated). Data were analyzed by one-way analysis of variance with Dunnett's postanalysis. . Values are presented, as mean ± S.E.M. Data are representative of 4-5 retina per group.

CHAPTER 5:

DISCUSSION

5.1 Discussion

Hypoxic ischemic insult in premature neonates contributes to brain damage leading to decreased vasculature and neuronal degeneration[1,49]. Premature neonates are susceptible to stroke, and the incidence is as high as 4 in 1000 births, moreover, 95% of infants who do survive a HI insult predisposes them to cognitive disabilities, epilepsy, and motor dysfunction in adulthood. Hence it is important to determine the underlying physiological mechanism for preventing HIE related injuries and developing novel strategies for medical interventions[32,216]. To determine the underlying physiological mechanism of HIE in humans is difficult, hence a Rice-Vannucci rodent model of HIE was used to elucidate the effect of HI insult on neonatal brain injury [2, 28,17,217]. The recovery of the brain after a HI insult is remarkably attributed to an intricate and organized process of angiogenesis[35,218]. Indeed, HIE at the metabolic level is characterized, by increased accumulation of carbohydrate metabolites (succinate and lactate) due to an arrest in aerobic oxidative phosphorylation[34,219]. Recently, the role of GPR91 in HIE was elucidated as a molecular sensing receptor capable of sensing stress-induced in HIE and also protecting cellular damage via orchestrating angiogenesis. GPR91/succinate interaction promotes brain revascularization by prostaglandin-mediated secretion of pro-angiogenic factors such as VEGF, ANG-1, ANG-2 and IL-6[3,22].

Due to unavailability of stable and pure neuronal cell line initial experiments for GPR81 were performed on *invitro* retinal ganglion cell (RGC-5) line. RGC-5 is an immortalized cell line of the retinal ganglion cells of the retina, which resembles similar to the primary neurons of the central nervous system (CNS). Differentiation of RGC-5 by staurosporin by 316nM for 24 hours or 1mM for 6 hours resulted in increased neurite formation and morphology similar to primary pyramidal neurons of the cortex and hippocampus of the brain. Immunocytochemistry (ICC) of GPR81 in differentiated RGCs along with neuronal N (NeuN), a marker for neuron, showed a strong co-localization, indicating GPR81 expression in sRGC-5 (stimulated RGCs). Moreover, to determine that lactate possesses pro-angiogenic activity, which could be mediated via GPR81,

sRGC-5 were treated with 10mM lactate for 6 hours and 24 hours respectively. Expressions of pro-angiogenic genes along with certain neurotrophins were elevated upon lactate treatment whereas expression of interleukin 1B (IL1B) was reduced. Since, lactate increased VEGF, angiopoietins, neurotrophins (BDNF) that belong to the cytokines and/or myokines family. We collected the conditioned media after 24 hours of lactate treatment as these molecules are secreted outside the cells and carries out diverse functions ranging from regulating angiogenesis to neuroprotection via receptor mediated activation. Furthermore, the conditioned media (CM) so collected was used to performed *invitro* matrigel and *exvivo* aortic explant experiments to uncover the role of secreted cytokines or myokines upon lactate stimulation. It has been well demonstrated that lactate accumulation in intracerebral hemorrhage (ICH) promotes angiogenesis and neurogenesis via activation and translocalization of NF-KB into the nucleus. This effect was attributed to increased infiltration of microglia\macrophages in the ipsilateral region of ICH. Since M1 to M2 subtype phenotype change of macrophages is stimulated by lactate which in turn promotes cell proliferation via VEGF secretion coupling with the fact that NF-kB is predominantly activated in microglia, it would be safe to suppose that lactate mediated microglial activation can lead to angiogenesis in ICH. Moreover, in neurons and endothelial cells there is a substantial and significant decrease in basic fibroblast growth factor (bFGF) and VEGF expression respectively, when either NF-kB inhibitor (BAY) or lactate dehydrogenase inhibitor oxamate (OXA) were injected intracerebroventricularly, after ICH. Altogether these results are indicative that lactate neuroprotective role is attributed to increased angiogenesis leading to subsequent neurogenesis resulting from nurturing neurons in the penumbral region via improving oxygen and glucose supply.

Further to elucidate the mechanism of lactate mediated angiogenesis in sRGC-5 and determine the upstream mediators of signal transduction pathways, effect of lactate on ERK and P38 phosphorylation was determined using specific inhibitors and activators of aforementioned pathways.

In this study, we also demonstrate that metabolic receptor GPR81 is predominantly expressed in the neurons of the brain and plays a crucial role in the initial stages of post-natal developmental brain angiogenesis. A significant decrease of 20 to 25% in the vascular area was observed in the GPR81-/- mice from P7 to P11. This decrease in vasculature in KO mice corresponds to the substantial decrease in VEGF and increase in TSP-1 mRNA expression and protein levels determined by RT-PCR and western blot respectively. Indeed, there is an increased expression of GPR81 at P9 and P11 that is normalized at P15. However, at later postnatal ages from at P15 and P19 there is the amelioration of brain vasculature in the GPR81-/- mice. Hence, to determine a plausible cause for improved vasculature in GPR81-/- we looked into the expression of various angiogenic factors during the later postnatal stages. Indeed, an increase in pro-angiogenic factor VEGF and a corresponding decrease in angiostatic factor thrombospondin (TSP-1) in GPR81-/- mice were observed specifically in latter stages at P19. Moreover, confocal imaging and western blot results showed a significant increase in the production of TSP-1 in primary neuron culture from KO mice, compared to WT neuronal culture. The molecular mechanism of TSP-1 and VEGFA interaction has been well elucidated in regulating angiogenesis. TSP-1 direct effect is attributed to interaction with CD-36 and CD-47 receptors on endothelial cells, resulting in decreased endothelial cell proliferation via Akt and PI3K dependent signaling pathway. Indeed, TSP-1 interaction with CD-36 results in decreased phosphorylation of VEGFR-2 receptor thereby; reducing VEGFA mediated angiogenic response[37,220]. In mice models of stroke, it has been proposed that increase TSP-1 production reduces tissue perfusion by limiting the angiogenic response to nitric oxide (NO) [40, 41,221,222]. Furthermore, increase TSP-1 is also associated with increased excitatory synapse formation via its interaction with CACNA2D1 or alpha2/delta1 (α2δ-1) receptor. This increased excitatory synapse formation leads to convulsions and seizures, which are the basis of other neurological disorders such as epilepsy. Recently, the mechanism of gabapentin, an anticonvulsant drug was

elucidated, which inhibited the interaction of TSP-1 with its α2δ-1 receptor and thereby promoting its anticonvulsant activity[38, 39,223,224].

In addition, we observed a corresponding increase in inflammatory factors CCL-2 and COX-2 in the brain of GPR81-/- mice. Neuronal CCL-2 secretion is known to promote an increased infiltration of monocytes in the brain, in a mice model of viral encephalopathy[42,225]. The role of neuronal COX-2 in conferring neurotoxicity via EP-1 receptor in acute, traumatic, excitotoxic brain injury, Alzheimer's disease, cerebral hypoxia and depression is well elucidated[43,44,45,226,227]. CCL-2 and COX-2 expression in preterm labour were significantly increased in the GPR81-/- mice upon induction of lipopolysaccharide, collectively, supporting the role of GRP81 as an angiogenic and anti-inflammatory receptor[46].

Moreover, to confirm that GPR81 promotes angiogenesis, intracerebroventricular lactate injections were performed which resulted in a 15% increase in vessel density in the WT mice compared to KO mice, suggesting angiogenic response is via GPR81. Since GPR81 is specifically expressed in the neurons, we performed western blots on primary neuron cultures treated with vehicle or lactate to determine the angiogenic response is mediated via lactate/GPR81 interaction. After 24 h of stimulation, there was a significant increase in VEGF protein expression and a corresponding decrease in TSP-1 protein expression in the WT neurons with lactate treatment as compared to the GPR81-/- counterpart. This counterbalancing effect of TSP-1 and VEGF A has been well elucidated in the tumor microenvironment. TSP-1 regulates VEGF A expression by direct interaction with VEGF A resulting in an increased clearance of VEGF A from the extracellular matrix, or indirectly by inhibiting matrixmetalloproteinases MMP activity leading to decrease secretion of VEGF A[47, 48,228,229].

Further, the fact that lactate accumulates and promotes angiogenesis in developing retina and retinopathy of prematurity, we explored if GPR81 plays a similar role in HIE. Indeed, after HI insult we observed an increase in lactate levels with a corresponding increase in mRNA expression of GPR81 after 24hrs of an ischemic insult. Intracerebroventricular lactate injections

at P4 followed by HI insult resulted in 20 % increase in vessel density in the WT mice, indicating that GPR81 is a regulator of angiogenesis. Furthermore, pre-administration of lactate before a HI insult resulted in a substantial decrease in the infarct size of the WT mice, which was not evident in the GPR81-/- mice. These results were also supported by a corresponding increase in pro-angiogenic factors VEGF, ANG-1, ANG-2 and PDGFB and decrease in TSP-1 expression that was evident in the lactate treated WT HI mice. Although the increase of the above-mentioned factors could be attributed to the effects of other cell types (astrocytes and leptomeningeal cells) on the endothelial cells in which GPR81 expression has been previously documented[21,46,230,231], here we specifically demonstrate the neuronal cells expressing GPR81 also play a significant role in regulating angiogenesis in the brain during development and in the pathophysiological condition of cerebral hypoxia.

In summary, we have explored a novel receptor GPR81 having a role in developmental and post-HI brain vasculature. Current treatments for HI stroke are based on supportive therapy, involving the rescue of neuronal insult via hypothermia, increasing ventilation, promoting perfusion and surgery to dissolve clots[31,33,232]. Other methods include reducing HI injury by the use of inhibitors of inflammation mediators along with the use of cytoprotective growth factors[34,219]. The current therapies have potential restrictions as they have a substantial low therapeutic window for cellular rescue and repair after HI insult[33,34,219,232]. Hence pharmacological modulation and elucidation of the underlying molecular mechanism of signaling pathways in post-HI cerebral hypoxia provide an improved and effective tool in treating HI insult. In this study, we show that GPR81 plays a vital role in reversing brain injury after HI stroke via neuronal regulation of VEGF A and TSP-1, which also regulates postnatal brain angiogenesis. Considering that lactate accumulates only transiently after HI insult, longer-acting agonists of GPR81 may exert more favorable effects.

Clinically, intracerebroventricular injections in the neonates are not feasible and are considered to be highly invasive. However, scientists were able to use diffusion-weighted

magnetic resonance imaging to show that intra-peritoneal administration of lactate of 40µmol was able to reach the brain and reduce brain lesions after a cerebral hypoxic insult in pre-clinical experimental mice model. Thereby, suggesting a novel mechanism wherein lactate could be used as a neuroprotective curative molecule. In our experiments we used intracerebroventricular (ICV) injections for two main purposes. Firstly, ICV injections of lactate bypasses the blood brain barrier (BBB) and enables us to elucidate local metabolic effects of lactate on angiogenesis in close vicinity of injections performed. Secondly, an ICV injection allows increase in lactate concentration to 6 to 8mM, which is sufficient enough to activate GPR81. In addition when injected intravenously or intraperitonealy, lactate is oxidized in plasma or is transported to highly active organs like the heart, liver and kidneys where it can be used as an alternative source of energy. Collectively, reducing the minimum effective concentration of lactate in the brain required to activate GPR81.

Lactate, in a clinical setting has been used as a biomarker to determine the extent of severity of cerebral hypoxic injury in neonates. Serum concentration measurement of lactate is considered to be a hallmark standard, to co-relate severity of HI insult. Measurement of cerebral lactate and a subsequent co-relation to serum lactate concentration with respect to time, and severity of injury would be more significant to unveil the role of lactate in cerebral hypoxia. This is important due the fact the cerebral hypoxic brain injury in the neonates' follows two different patterns. First, is the central pattern associated with injury to gray matter (thalamus, basal ganglia) and second is a peripheral pattern related to injury to white matter. Currently, it is unknown if the cerebral lactate concentration mimics the severity of pattern during and/or after therapeutic hypothermia. Moreover, lactate can be easily transported from the brain into systemic circulation via MCTs and from systemic circulation to CNS, thereby compounding the problem

to establish a strong co-relation between serum and cerebral lactate measurement. In a recent publication the scientists were able to determine the cerebral lactate levels in 49 neonates by magnetic resonance spectroscopy, whereby they reported that there was a significant increase in cerebral lactate levels in neonates suffering from moderate to severe HI insult during therapeutic hypothermia and after during the rewarming phase[275]. In addition, there was an increase in serum lactate levels that remained elevated after reperfusion and proper oxygenation to the infants were restored. This effect can be explained at the molecular levels in the following terms. Firstly, during HI insult impaired oxidative phosphorylation in the neurons and astrocytes results in shift to aerobic glycolysis. However, if the insult is severe, neuronal death is exacerbated via necrotic pathway, as result neurons are unable to use lactate as alternative source of metabolic energy provided to them by astrocytes, this in turn leads to extracellular accumulation of lactate, which can be transported into the systemic circulation leading to increased serum lactate levels. Another reason for increased serum lactate levels could be attributed to stress induced secretion epinephrine, which induces aerobic glycolysis in skeletal muscles. In all, suggesting that during therapeutic hypothermia and rewarming lactate may also play a vital role in salvaging neurons during primary and secondary HI insult. However, not denying the fact that higher concentration of lactate in the range of 15mM to 20mM is detrimental to neonates and is an important biomarker to predict the severity of HI insult in newborns, further research needs to be conducted to establish a strong link between lactate production, consumption by other organs, transport across BBB and systemic circulation when co-relating it with severity of HI injuries[275,276]. In addition, cerebral and serum lactate concentration in the neonates at birth are relatively higher irrespective to HIE. This is attributed to the inability of the brain to utilize glucose due to

significant reduced expression of glucose transporters. The brain is therefore, is highly dependent on lactate and ketone bodies as source of energy[17,275].

GPR81 or Hydroxyl carboxylic acid (HCA-1) was primarily discovered as a receptor activated physiologically by carbohydrate metabolic ligand called lactate[77,79,233,234,235,236]. Initial research on GPR81 was focused on adipocytes owing to its higher expression in adipocytes compared to other cells. In adipocytes, postprandially, along with insulin, GPR81 synergistically reduced cyclic AMP levels resulting in decreased lipolysis[33,237,238]. However, recently GPR81 expression in brain, retina, cancer cell lines, myometrium, colon and liver was elucidated, wherein it performed tissue and cell specific functions[32,93,230,239–241,80,84,242]. In brain, for example, GPR81 is strongly expressed in the neurons, regulating spiking firing frequency of inhibitory neurons in hippocampus[93]. In retina, the expression is more diversified in Muller cells, retinal-pigmented epithelial cells (RPE) and retinal ganglion cells (RGCs), wherein it takes part in therapeutic angiogenesis associated in mice model of retinopathy of prematurity[92,243]. Unlike most of the GPCRs, which have a minimum effective concentration EC50 in nanomolar range, GPR81 has EC50 between 1mM to 10mM[92,235,241]. The higher EC50 can be explained in both physiological and pathophysiological terms. Physiologically, the minimum circulating serum lactate concentration is approximately around 1mM[244,245,31]. In retina and brain, which are highly metabolic organs, the basal lactate concentration varies between 1mM to 4 mM. In pathophysiological conditions such as cerebral hypoxia ischemia (HI), retinopathy of prematurity (ROP), cancer and diseases associated with inflammation (preterm labour, colitis) lactate levels surges to 10mM[241,243,246,247]. In aforementioned pathological conditions of HI and ROP, the underlying cause is attributed to arrest in oxidative phosphorylation resulting in anaerobic accumulation of carbohydrate metabolites such as lactate, succinate and alpha-ketoglutarate, which serve as ligands for GPR81, GPR91 and GPR99 respectively[15,22,248,13]. Neonatal hypoxic-ischemia encephalopathy (HIE) at molecular level is characterized by reduced blood flow to the brain resulting in decreased oxygen and glucose supply, resulting in increased lactate production via anaerobic glycolysis[172,249]. Collectively, we

hypothesized that lactate via GPR81 can promote therapeutic angiogenesis that would significantly reduce infarction, vaso-obliteration and neovascular tufts formation in metabolic disorders such as HIE and ROP respectively. Since we injected lactate prophylactically, the protective effect via angiogenesis is sought to be a pre-conditioning effect of lactate via GPR81. Wherein GPR81 acts as a metabolic signalling receptor. Hence, to explore the therapeutic potential of GPR81, agonists of GPR81 (3,5 dihydroxybenzoic acid, 3-chloro-5-hydroxybenzoic acid) have to be essayed before and after a cerebral hypoxic insult.

Our results have shown that GPR81 plays an important role in developmental brain angiogenesis and reduces infarction after an HI insult in a neonatal mice model of Rice-Vannucci by augmenting pro-angiogenic response. Since GPR81 is predominantly expressed in the neurons and leptomeningeal cells as previously documented, it would be of great interest to speculate the neuroprotective role of GPR81 in neurological disorders related to epilepsy, cerebral malaria, Alzheimer's and Parkinson's[32,231,250].

Epilepsy is associated with uncontrolled seizures, whose underlying pathophysiological aetiology is attributed to excessive neuronal firing in the hippocampus[251,252]. One of the major underlying causes of Temporal lobe epilepsy (TLE) is impaired cerebral energy metabolism. Indeed, about 40 % of adults suffering with TLE are irresponsive to the pharmacotherapeutic agents. At cellular level, TLE is characterized by mitochondrial dysfunctioning related to decreased ATP production due to hypometabolism[250]. Furthermore, TLE are also associated with elevated levels of lactate with decreased expression of monocarboxylate transporters-1 and 2 (MCT-1 and MCT-2) in the microvessels, and corresponding increase in astrocytes in the hippocampal neuropil. These cell specific expression changes could be an adaptive mechanism wherein; reduced expression of MCTs would maintain high lactate levels. Lactate in turn via GPR81 can reduce cAMP production resulting in suppression of seizures[250,239,253].

In our study, we have observed an increased expression of thrombospondin (TSP-1) from the GPR81-/- neurons. TSP-1 interaction with α2δ-1 receptor on neurons is known for excitatory

synapse formation contributing to enhance neuronal firing that results in uncontrolled seizures. Recently it was shown that an antiepileptic drug called gabapentin inhibits this TSP-1/ α2δ-1 receptor interaction. In addition, activation of GPR81 by lactate in hippocampal neurons resulted in reduced neuronal firing via Gi mediated reduction of cAMP. Collectively, providing strong evidence, that agonists of GPR81 could be potentially useful in modulating neuronal activity in treatment of epileptic seizures[233,253].

The main cause of Alzheimer disease (AD) for the last 3 decades was believed to be increased accumulation of B amyloid protein in the neurons resulting in neuronal degeneration and subsequent dementia in these patients[123,233,254–257]. However, recently it has been proposed that the underlying cause of inflammation related neuronal degeneration in AD can be attributed to the microflora in the gut. This is based upon the hypothesis that increase in age is associated with leakage of intestinal epithelial barrier (IEB) leading to translocation of microbes via the circulation to the blood brain barrier (BBB)[258,259]. Increased permeabilization of BBB is facilitated by secretion of pro-inflammatory cytokines (IL-1β, IL-6, TNFα) which ultimately results in neuronal inflammation and subsequent necrosis[260]. Moreover, it has been documented that brain and specifically neurons can have a unique ability of using lactate as a source of energy generated by aerobic glycolysis (AG) in physiological and pathological conditions such as AD[261–263]. The metabolic stress and depleted rate of oxidative phosphorylation with ageing in AD can alter GPR81/lactate signalling mechanism which can cause premature senescence of astrocytes and neurons[264,265]. Since senescent cells primarily use oxidative phosphorylation as a source of ATP, cells can revert to AG for ATP production which would either result in apoptosis of the senescent cells or may reprogram their normal functioning[262,266,267]. Recently the expression of GPR81 in colonic dendritic cells and macrophages in the intestine has been associated with anti-inflammatory action via reducing the aforementioned pro-inflammatory cytokines along with corresponding increase in Treg cells and increase in anti-inflammatory cytokines such as IL-10[241]. Indeed, at molecular level, GPR81 mediates its anti-inflammatory action by inhibiting NRLP3

inflammasome activation in macrophages resulting in decrease caspase-1 activity and subsequent decrease in IL-1B expression[240]. Hence it would be interesting to see whether agonist of GPR81 can ameliorate neuroinflammation and reverse senescence in AD

Cerebral malaria (CB) is another pathophysiological condition, which is characterized by impaired metabolic functioning resulting in increased levels of lactate, disruption of BBB and predisposing children to TLE. Erythrocytes infected with *Plasmodium falcifarium* use aerobic glycolysis (AG) to utilize high level of glucose for ATP production leading to accumulation of lactate near the BBB. Increased lactate levels, in turn can activate GPR81 in the endothelial cells and reduce cAMP production causing vasoconstriction and leakage in BBB[268]. However, since the expression of GPR81 in endothelial cells is localized to abluminal and luminal ends, this effect could be cell specific and restricted to endothelium[230]. Moreover, the role of GPR81 has been documented in macrophages, smooth muscle cells, neurons and leptomeningeal cells where it promotes an anti-inflammatory and angiogenic response via activation of B-arrestin, ERK1/2 and AKT signalling transduction pathways[269]. Hence it would be interesting to determine if an agonist or antagonist of GPR81 would either ameliorate/worsen CB pathogenesis.

Retinopathy of Prematurity (ROP) is a biphasic retinal disorder characterized by vaso-obliteration (VO) followed by formation of nonvascular tufts (NV). Recently, *Madaan et al* proposed a novel mechanism of GPR81 in the model of ROP, wherein there is significant decrease in VO and NV tufts formation via GPR81 inner vascular regulation of Wnt/Norrin pathway[243]. Interestingly this effect was mediated via ERK1/2 signalling in the Muller cells. Moreover, GPR81 co-localization with DAPI in the Muller cells and NeuN in the neurons predicts that GPR81 might be a nuclear or perinuclear receptor. The presence of nuclear GPCRs is not novel per se, the presence of nuclear GPCRs such as prostaglandin receptors (EP3), platelet activating receptor (PAFR) on the nuclear membrane have been confirmed by confocal and electron microscopy. Furthermore, these receptors are functionally active and mediate their actions via activation of nuclear factor kappa B (NFkB), mitogen activated protein kinases (Erk1,

Erk2 and Erk3) and PI3K/Akt system[270]. Indeed, they significantly differ in their mode of action; for example, activation of nuclear prostaglandin receptor promotes increased expression of nitric oxidase synthase (sNOS) in the endothelial cells, leading to vasodilation via secretion of substance P[270–272]. On the contrary the plasma membrane localized prostaglandin receptor controls muscle and neuron contractile responses. Concerning, GPR81 localization in the cell nuclear membrane and potentially on the plasma membrane it would be interesting to dissect if their difference in cell organelle localization can modulate different pathways in cell signalling.

CHAPTER 6:

CONCLUSION AND FUTURE DIRECTIONS

6.1 Conclusion (original findings in the thesis):

To our knowledge this is the first documented evidence where we have elucidated a novel role of GPR81 in developmental brain angiogenesis and its neuroprotective pro-angiogenic effect in neonatal hypoxic ischemia (HI). Herein we demonstrate that: (a) GPR81-/- showed a transient post-natal phenotype associated with decrease in vessel area specifically between P7 to P11, and modulated by inflammatory, angiogenic and angiostatic factors. (b) GPR81 is primarily expressed on neurons and specifically controls secretion of angiogenic (VEGF) and anti-angiogenic (TSP-1) factors respectively. (c) Intracerebroventricular injection of lactate increased vessel area only in WT mice, suggesting the specific interaction of GPR81 and lactate promotes angiogenesis. (d) In the Rice-Vannucci model of neonatal cerebral hypoxia intracerebroventricular injection of lactate significantly reduced infarct size in WT compared to GPR81-/- mice by regulating of pro-angiogenic and angiostatic factors specifically VEGF and TSP-1. (e) Finally, we determined that ERK1/2 signalling pathway is responsible for norrin mediated regulation of inner retinal vasculature.

The regulation of angiogenesis by neuronal GPR81 provides new insights in uncovering mechanism of cross talk in the neovascular unit of the brain. This is an important finding since neurodegenerative disorders as mentioned above are complex at molecular level involving multicellular mechanisms. For example, in Alzheimer's Diseases (AD) neurodegeneration can be attributed to combination of increase pro-inflammatory cytokine secretion by macrophages, leukocytes and also to accumulation of B amyloid protein by the neurons. Since loss of GPR81 increases CCL-2 and COX-2 expression, we therein confirmed the role of GPR81 as an anti-inflammatory receptor. Targeting GPR81 via an agonist could prove to be beneficial in other neurodegenerative diseases such as Parkinson's and epilepsy.

Although, we uncover a novel role of GPR81 in brain angiogenesis and cerebral hypoxia, the following questions needs to be addressed.

1. Lactate and 3,5 DHBA injections should be performed after and just before the cerebral hypoxic insult to determine therapeutic potential of agonist activity of GPR81.
2. We need to use lactate dehydrogenase inhibitors (Oxamate) or MCT-1 inhibitors (4-hydroxycinnamate), to differentiate if the protective effect is attributed to the metabolic effect of lactate which could be either GPR81 dependent or independent.
3. Since, we did observe increase in COX-2 and CCL-2 expression in GPR81-/- mice. It would be intriguing to delineate the role of GPR81 in macrophages and microglia neurovascular unit of cerebral hypoxia. GPR81 expression in microglia and its effects on inflammation, oxidative stress and apoptosis would help us to better understand the diverse function of GPR81 in modulating the neurovascular unit.

CHAPTER 7:

REFERENCES

1. Yang SN, Lai MC. Perinatal hypoxic-ischemic encephalopathy. *J Biomed Biotechnol*. 2011;2011. doi:10.1155/2011/609813
2. Ferriero DM. Neonatal Brain Injury. *N Engl J Med*. 2004. doi:10.1056/nejmra041996
3. Shankaran S. Neonatal encephalopathy: Treatment with hypothermia. *J Neurotrauma*. 2009. doi:10.1089/neu.2008.0678
4. Nair J, Kumar V. Current and Emerging Therapies in the Management of Hypoxic Ischemic Encephalopathy in Neonates. *Children*. 2018;5(7):99. doi:10.3390/children5070099
5. Eltzschig HK, Collard CD. Vascular ischaemia and reperfusion injury. *Br Med Bull*. 2004;70:71-86. doi:10.1093/bmb/ldh025
6. Perlman JM. Intervention strategies for neonatal hypoxic-ischemic cerebral injury. *Clin Ther*. 2006;28(9):1353-1365. doi:10.1016/j.clinthera.2006.09.005
7. Sun Y, Jin K, Xie L, et al. VEGF-induced neuroprotection, neurogenesis, and angiogenesis after focal cerebral ischemia. *J Clin Invest*. 2003. doi:10.1172/JCI200317977
8. Li L, Welser-Alves J, van der Flier A, Boroujerdi A, Hynes RO, Milner R. An angiogenic role for the α5β1 integrin in promoting endothelial cell proliferation during cerebral hypoxia. *Exp Neurol*. 2012. doi:10.1016/j.expneurol.2012.06.005
9. Milner R, Hung S, Erokwu B, Dore-Duffy P, LaManna JC, del Zoppo GJ. Increased expression of fibronectin and the α5β1 integrin in angiogenic cerebral blood vessels of mice subject to hypobaric hypoxia. *Mol Cell Neurosci*. 2008. doi:10.1016/j.mcn.2008.01.013
10. Kim S, Bell K, Mousa SA, Varner JA. Regulation of angiogenesis in vivo by ligation of integrin α5β1 with the central cell-binding domain of fibronectin. *Am J Pathol*. 2000. doi:10.1016/S0002-9440(10)65005-5
11. Krupinski J, Kaluza J, Kumar P, Kumar S, Wang JM. Role of angiogenesis in patients with cerebral ischemic stroke. *Stroke*. 1994. doi:10.1161/01.STR.25.9.1794

12. Gilissen J, Jouret F, Pirotte B, Hanson J. Insight into SUCNR1 (GPR91) structure and function. *Pharmacol Ther*. 2016. doi:10.1016/j.pharmthera.2016.01.008
13. Wittenberger T, Hellebrand S, Munck A, Kreienkamp J, Schaller HC, Hampe W. GPR99, a new G protein-coupled receptor with homology to a new subgroup of nucleotide receptors. *BMC Genomics*. 2002. doi:10.1186/1471-2164-3-17
14. Kuei C, Yu J, Zhu J, et al. Study of GPR81, the lactate receptor, from distant species identifies residues and motifs critical for GPR81 functions. *Mol Pharmacol*. 2011;80(5):848-858. doi:10.1124/mol.111.074500
15. Sapieha P, Sirinyan M, Hamel D, et al. The succinate receptor GPR91 in neurons has a major role in retinal angiogenesis. *Nat Med*. 2008. doi:10.1038/nm.1873
16. Fatemi A, Wilson MA, Johnston M V. Hypoxic-Ischemic Encephalopathy in the Term Infant. *Clin Perinatol*. 2009. doi:10.1016/j.clp.2009.07.011
17. Vannucci SJ, Hagberg H. Hypoxia-ischemia in the immature brain. *J Exp Biol*. 2004. doi:10.1242/jeb.01064
18. Baburamani AA, Ek CJ, Walker DW, Castillo-Melendez M. Vulnerability of the developing brain to hypoxic-ischemic damage: Contribution of the cerebral vasculature to injury and repair? *Front Physiol*. 2012. doi:10.3389/fphys.2012.00424
19. Hamel D, Sanchez M, Duhamel F, et al. G-protein-coupled receptor 91 and succinate are key contributors in neonatal postcerebral hypoxia-ischemia recovery. *Arterioscler Thromb Vasc Biol*. 2014;34(2):285-293. doi:10.1161/ATVBAHA.113.302131
20. Sirinyan M, Sennlaub F, Dorfman A, et al. Hyperoxic exposure leads to nitrative stress and ensuing microvascular degeneration and diminished brain mass and function in the immature subject. *Stroke*. 2006. doi:10.1161/01.STR.0000245082.19294.ff
21. Rana BK, Shiina T, Insel PA. Genetic variations and polymorphisms of G protein-coupled receptors: and Therapeutic Implications. *Annu Rev Pharmacol Toxicol*. 2001.
22. Hamel D, Sanchez M, Duhamel F, et al. G-protein-coupled receptor 91 and succinate are

key contributors in neonatal postcerebral hypoxia-ischemia recovery. *Arterioscler Thromb Vasc Biol*. 2014. doi:10.1161/ATVBAHA.113.302131

23. Honoré JC, Kooli A, Hamel D, et al. Fatty acid receptor GPR40 mediates neuromicrovascular degeneration induced by transarachidonic acids in rodents. *Arterioscler Thromb Vasc Biol*. 2013. doi:10.1161/ATVBAHA.112.300943
24. Thwaites JW, Reebye V, Mintz P, Levicar N, Habib N. Cellular replacement and regenerative medicine therapies in ischemic stroke. *Regen Med*. 2012. doi:10.2217/rme.12.2
25. Beck H, Plate KH. Angiogenesis after cerebral ischemia. *Acta Neuropathol*. 2009. doi:10.1007/s00401-009-0483-6
26. Bélanger M, Allaman I, Magistretti PJ. Brain energy metabolism: Focus on Astrocyte-neuron metabolic cooperation. *Cell Metab*. 2011. doi:10.1016/j.cmet.2011.08.016
27. Nauta TD, van Hinsbergh VWM, Koolwijk P. Hypoxic signaling during tissue repair and regenerative medicine. *Int J Mol Sci*. 2014. doi:10.3390/ijms151119791
28. Ziyad S, Iruela-Arispe ML. Molecular Mechanisms of Tumor Angiogenesis. *Genes and Cancer*. 2011. doi:10.1177/1947601911432334
29. Hayashi T, Noshita N, Sugawara T, Chan PH. Temporal profile of angiogenesis and expression of related genes in the brain after ischemia. *J Cereb Blood Flow Metab*. 2003;23(2):166-180. doi:10.1097/01.WCB.0000041283.53351.CB
30. Horn T, Klein J. Neuroprotective effects of lactate in brain ischemia: Dependence on anesthetic drugs. *Neurochem Int*. 2013. doi:10.1016/j.neuint.2012.12.017
31. Berthet C, Lei H, Thevenet J, Gruetter R, Magistretti PJ, Hirt L. Neuroprotective role of lactate after cerebral ischemia. *J Cereb Blood Flow Metab*. 2009. doi:10.1038/jcbfm.2009.97
32. Morland C, Lauritzen KH, Puchades M, et al. The lactate receptor, G-protein-coupled receptor 81/hydroxycarboxylic acid receptor 1: Expression and action in brain. *J Neurosci*

Res. 2015. doi:10.1002/jnr.23593

33. Liu C, Wu J, Zhu J, et al. Lactate inhibits lipolysis in fat cells through activation of an orphan G-protein-coupled receptor, GPR81. *J Biol Chem*. 2009;284(5):2811-2822. doi:10.1074/jbc.M806409200
34. DiNuzzo M. Astrocyte-neuron interactions during learning may occur by lactate signaling rather than metabolism. *Front Integr Neurosci*. 2016. doi:10.3389/fnint.2016.00002
35. Cao Y. Adipose tissue angiogenesis as a therapeutic target for obesity and metabolic diseases. *Nat Rev Drug Discov*. 2010. doi:10.1038/nrd3055
36. Stevens RC, Cherezov V, Katritch V, et al. The GPCR Network: A large-scale collaboration to determine human GPCR structure and function. *Nat Rev Drug Discov*. 2013. doi:10.1038/nrd3859
37. Wess J. Molecular basis of receptor/G-protein-coupling selectivity. *Pharmacol Ther*. 1998. doi:10.1016/S0163-7258(98)00030-8
38. Schöneberg T, Schulz A, Gudermann T. The structural basis of G-protein-coupled receptor function and dysfunction in human diseases. *Rev Physiol Biochem Pharmacol*. 2002. doi:10.1007/bfb0116587
39. LABURTHE M, COUVINEAU A, GAUDIN P, MAORET J-J, ROUYER-FESSARD C, NICOLE P. Receptors for VIP, PACAP, Secretin, GRF, Glucagon, GLP-1, and Other Members of Their New Family of G Protein-Linked Receptors: Structure-Function Relationship with Special Reference to the Human VIP-1 Receptora. *Ann N Y Acad Sci*. 2006. doi:10.1111/j.1749-6632.1996.tb17476.x
40. Polak M. Hyperfunctioning thyroid adenoma and activating mutations in the TSH receptor gene. *Arch Med Res*. 1999. doi:10.1016/S0188-4409(99)00067-3
41. Sadee W, Hoeg JLE, Wang D. Genetic variations in human G protein-coupled receptors: implications for drug therapy. *AAPS J*. 2001.
42. Green SA, Turki J, Liggett SB, Innis M. Corrections: Amino-Terminal Polymorphisms of

the Human β2-Adrenergic Receptor Impart Distinct Agonist-Promoted Regulatory Properties (Biochemistry (1994) 33(32) (9414–9419) (10.1021/bi00198a006)). *Biochemistry*. 1994. doi:10.1021/bi00251a600

43. Okazaki R, Chikatsu N, Nakatsu M, et al. A novel activating mutation in calcium-sensing receptor gene associated with a family of autosomal dominant hypocalcemia. *J Clin Endocrinol Metab*. 1999. doi:10.1210/jc.84.1.363

44. George ST, Ruoho AE, Malbon CC. N-Glycosylation in expression and function of□??-adrenergic receptors. *J Biol Chem*. 1986.

45. Wess J, Nanavati S, Vogel Z, Maggio R. Functional role of proline and tryptophan residues highly conserved among G protein-coupled receptors studied by mutational analysis of the m3 muscarinic receptor. *EMBO J*. 1993. doi:10.1002/j.1460-2075.1993.tb05661.x

46. Tanaka H, Moroi K, Iwai J, et al. Novel mutations of the endothelin B receptor gene in patients with Hirschsprung's disease and their characterization. *J Biol Chem*. 1998. doi:10.1074/jbc.273.18.11378

47. Liu ISC, Seeman P, Sanyal S, et al. Dopamine D4 Receptor Variant in Africans, D4Valine194Glycine, Is Insensitive to Dopamine and Clozapine: Report of a Homozygous Individual. *Am J Med Genet - Semin Med Genet*. 1996. doi:10.1002/(SICI)1096-8628(19960122)61:3<277::AID-AJMG14>3.0.CO;2-Q

48. Kotlar TJ, Young RH, Albanese C, Crowley WF, Scully RE, Jameson JL. A mutation in the follicle-stimulating hormone receptor occurs frequently in human ovarian sex cord tumors. *J Clin Endocrinol Metab*. 1997. doi:10.1210/jc.82.4.1020

49. Pearce SHS, Trump D, Wooding C, et al. Calcium-sensing receptor mutations in familial benign hypercalcemia and neonatal hyperparathyroidism. *J Clin Invest*. 1995. doi:10.1172/JCI118335

50. Yu H, Chen JK, Feng S, Dalgarno DC, Brauer AW, Schrelber SL. Structural basis for the

binding of proline-rich peptides to SH3 domains. *Cell*. 1994. doi:10.1016/0092-8674(94)90367-0

51. Van Tol HHM, Bunzow JR, Guan HC, et al. Cloning of the gene for a human dopamine D4 receptor with high affinity for the antipsychotic clozapine. *Nature*. 1991. doi:10.1038/350610a0

52. Rasmussen SøGF, Jensen AD, Liapakis G, Ghanouni P, Javitch JA, Gether U. Mutation of a highly conserved aspartic acid in the β2 adrenergic receptor: Constitutive activation, structural instability, and conformational rearrangement of transmembrane segment 6. *Mol Pharmacol*. 1999. doi:10.1124/mol.56.1.175

53. Savarese TM, Wang CD, Fraser CM. Site-directed mutagenesis of the rat m1 muscarinic acetylcholine receptor. Role of conserved cysteines in receptor function. *J Biol Chem*. 1992.

54. Bouvier M, Hausdorff WP, De Blasi A, et al. Removal of phosphorylation sites from the β2-adrenergic receptor delays onset of agonist-promoted desensitization. *Nature*. 1988. doi:10.1038/333370a0

55. Bockaert J. Molecular tinkering of G protein-coupled receptors: an evolutionary success. *EMBO J*. 1999. doi:10.1093/emboj/18.7.1723

56. Farrens DL, Altenbach C, Yang K, Hubbell WL, Khorana HG. Requirement of rigid-body motion of transmembrane helices for light activation of rhodopsin. *Science (80-)*. 1996. doi:10.1126/science.274.5288.768

57. Oldham WM, Hamm HE. Heterotrimeric G protein activation by G-protein-coupled receptors. *Nat Rev Mol Cell Biol*. 2008. doi:10.1038/nrm2299

58. Traut TW. Physiological concentrations of purines and pyrimidines. *Mol Cell Biochem*. 1994. doi:10.1007/BF00928361

59. Baylor DA, Lamb TD, Yau KW. The membrane current of single rod outer segments. *J Physiol*. 1979. doi:10.1113/jphysiol.1979.sp012715

60. Carman C V., Benovic JL. G-protein-coupled receptors: Turn-ons and turn-offs. *Curr Opin Neurobiol*. 1998. doi:10.1016/S0959-4388(98)80058-5

61. Wettschureck N, Offermanns S. Mammalian G proteins and their cell type specific functions. *Physiol Rev*. 2005. doi:10.1152/physrev.00003.2005

62. Métrich M, Berthouze M, Morel E, Crozatier B, Gomez AM, Lezoualc'h F. Role of the cAMP-binding protein Epac in cardiovascular physiology and pathophysiology. *Pflugers Arch Eur J Physiol*. 2010. doi:10.1007/s00424-009-0747-y

63. R.-Borlado L, Redondo C, Alvarez B, et al. Increased phosphoinositide 3-kinase activity induces a lymphoproliferative disorder and contributes to tumor generation in vivo. *FASEB J*. 2000. doi:10.1096/fasebj.14.7.895

64. Docherty JR. Subtypes of functional α1-adrenoceptor. *Cell Mol Life Sci*. 2010. doi:10.1007/s00018-009-0174-4

65. Koch WJ, Hawes BE, Inglese J, Luttrell LM, Lefkowitz RJ. Cellular expression of the carboxyl terminus of a G protein-coupled receptor kinase attenuates G(βγ)-mediated signaling. *J Biol Chem*. 1994.

66. Kühn H. Light-dependent phosphorylation of rhodopsin in living frogs. *Nature*. 1974. doi:10.1038/250588a0

67. Inglese J, Luttrell LM, Iniguez-Lluhi JA, Touhara K, Koch WJ, Lefkowitz RJ. Functionally active targeting domain of the β-adrenergic receptor kinase: An inhibitor of G(βγ)-mediated stimulation of type II adenylyl cyclase. *Proc Natl Acad Sci U S A*. 1994. doi:10.1073/pnas.91.9.3637

68. Gurevich V V., Dion SB, Onorato JJ, et al. Arrestin interactions with G protein-coupled receptors. Direct binding studies of wild type and mutant arrestins with rhodopsin, β2-adrenergic, and m2 muscarinic cholinergic receptors. *J Biol Chem*. 1995. doi:10.1074/jbc.270.2.720

69. Wilden U, Hall SW, Kuhn H. Phosphodiesterase activation by photoexcited rhodopsin is

quenched when rhodopsin is phosphorylated and binds the intrinsic 48-kDa protein of rod outer segments. *Proc Natl Acad Sci U S A*. 1986. doi:10.1073/pnas.83.5.1174

70. Benovic JL, Kühn H, Weyand I, Codina J, Caron MG, Lefkowitz RJ. Functional desensitization of the isolated beta-adrenergic receptor by the beta-adrenergic receptor kinase: potential role of an analog of the retinal protein arrestin (48-kDa protein). *Proc Natl Acad Sci U S A*. 1987. doi:10.1073/pnas.84.24.8879
71. Wilden U. Duration and Amplitude of the Light-Induced cGMP Hydrolysis in Vertebrate Photoreceptors Are Regulated by Multiple Phosphorylation of Rhodopsin and by Arrestin Binding. *Biochemistry*. 1995. doi:10.1021/bi00004a040
72. Gurevich V V., Gurevich E V. The new face of active receptor bound arrestin attracts new partners. *Structure*. 2003. doi:10.1016/S0969-2126(03)00184-9
73. Eichel K, Jullié D, Von Zastrow M. β-Arrestin drives MAP kinase signalling from clathrin-coated structures after GPCR dissociation. *Nat Cell Biol*. 2016. doi:10.1038/ncb3307
74. Attramadal H, Arriza JL, Aoki C, et al. β-Arrestin2, a novel member of the arrestin/β-arrestin gene family. *J Biol Chem*. 1992.
75. Ahn S, Shenoy SK, Wei H, Lefkowitz RJ. Differential kinetic and spatial patterns of β-arrestin and G protein-mediated ERK activation by the angiotensin II receptor. *J Biol Chem*. 2004. doi:10.1074/jbc.M405878200
76. Benned-Jensen T, Rosenkilde M. The Role of Transmembrane Segment II in 7TM Receptor Activation. *Curr Mol Pharmacol*. 2010. doi:10.2174/1874467210902020140
77. Ahmed K. Biological roles and therapeutic potential of hydroxy-carboxylic acid receptors. *Front Endocrinol (Lausanne)*. 2011;2(OCT):1-12. doi:10.3389/fendo.2011.00051
78. Ahmed K, Tunaru S, Tang C, et al. An Autocrine Lactate Loop Mediates Insulin-Dependent Inhibition of Lipolysis through GPR81. *Cell Metab*. 2010;11(4):311-319. doi:10.1016/j.cmet.2010.02.012

79. Blad CC, Ahmed K, IJzerman AP, Offermanns S. *Biological and Pharmacological Roles of HCA Receptors*. Vol 62. 1st ed. Elsevier Inc.; 2011. doi:10.1016/B978-0-12-385952-5.00005-1

80. Roland CL, Arumugam T, Deng D, et al. Cell surface lactate receptor GPR81 is crucial for cancer cell survival. *Cancer Res*. 2014;74(18):5301-5310. doi:10.1158/0008-5472.CAN-14-0319

81. Wagner W, Kania KD, Blauz A, Ciszewski WM. The lactate receptor (HCAR1/GPR81) contributes to doxorubicin chemoresistance via abcb1 transporter up-regulation in human cervical cancer hela cells. *J Physiol Pharmacol*. 2017;68(4):555-564.

82. Wagner W, Kania KD, Ciszewski WM. Stimulation of lactate receptor (HCAR1) affects cellular DNA repair capacity. *DNA Repair (Amst)*. 2017. doi:10.1016/j.dnarep.2017.02.007

83. Stäubert C, Broom OJ, Nordström A. Hydroxycarboxylic acid receptors are essential for breast cancer cells to control their lipid/fatty acid metabolism. *Oncotarget*. 2015. doi:10.18632/oncotarget.3565

84. Garcia-Flores AE, Sollome JJ, Thavathiru E, Bower JL, Vaillancourt RR. HER2/HER3 regulates lactate secretion and expression of lactate receptor mRNA through the MAP3K4 associated protein GIT1. *Sci Rep*. 2019. doi:10.1038/s41598-019-46954-7

85. Lee YJ, Shin KJ, Park SA, et al. G-protein-coupled receptor 81 promotes a malignant phenotype in breast cancer through angiogenic factor secretion. *Oncotarget*. 2016;7(43):70898-70911. doi:10.18632/oncotarget.12286

86. Feng J, Yang H, Zhang Y, et al. Tumor cell-derived lactate induces TAZ-dependent upregulation of PD-L1 through GPR81 in human lung cancer cells. *Oncogene*. 2017;36(42):5829-5839. doi:10.1038/onc.2017.188

87. R. H, A. F, A. G, F. G, W.Z. M. Lactate reduces liver and pancreatic injury in toll-like receptor- and inflammasome-mediated inflammation via gpr81-mediated suppression of

innate immunity. *Gastroenterology*. 2014. doi:10.1053/j.gastro.2014.03.014 LK - http://sfx.unimi.it:9003/unimi?sid=EMBASE&issn=15280012&id=doi:10.1053%2Fj.gastro.2014.03.014&atitle=Lactate+reduces+liver+and+pancreatic+injury+in+toll-like+receptor-+and+inflammasome-mediated+inflammation+via+gpr81-mediated+suppression+of+innate+immunity&stitle=Gastroenterology&title=Gastroenterology&volume=146&issue=7&spage=1763&epage=1774&aulast=Hoque&aufirst=Rafaz&auinit=R.&aufull=Hoque+R.&coden=GASTA&isbn=&pages=1763-1774&date=2014&auinit1=R&auinitm=

88. Errea A, Cayet D, Marchetti P, et al. Lactate Inhibits the Pro-Inflammatory Response and Metabolic Reprogramming in Murine Macrophages in a GPR81-Independent Manner. *PLoS One*. 2016;11(11):e0163694. doi:10.1371/journal.pone.0163694

89. Feingold KR, Moser A, Shigenaga JK, Grunfeld C. Inflammation inhibits GPR81 expression in adipose tissue. *Inflamm Res*. 2011. doi:10.1007/s00011-011-0361-2

90. Ranganathan P, Shanmugam A, Swafford D, et al. GPR81, a Cell-Surface Receptor for Lactate, Regulates Intestinal Homeostasis and Protects Mice from Experimental Colitis. *J Immunol*. 2018. doi:10.4049/jimmunol.1700604

91. Madaan A, Chaudhari P, Nadeau-Vallée M, et al. Müller Cell-Localized GPR81 (HCA1) Regulates Inner Retinal Vasculature via Norrin/Wnt Pathways. *Am J Pathol*. 2019. doi:10.1016/j.ajpath.2019.05.016

92. Vohra R, Aldana BI, Waagepetersen H, Bergersen LH, Kolko M. Dual properties of lactate in müller cells: The effect of GPR81 activation. *Investig Ophthalmol Vis Sci*. 2019. doi:10.1167/iovs.18-25458

93. Abrantes H de C, Briquet M, Schmuziger C, et al. The Lactate Receptor HCAR1 Modulates Neuronal Network Activity through the Activation of Gα and Gβγ Subunits. *J Neurosci*. 2019;39(23):4422-4433. doi:10.1523/JNEUROSCI.2092-18.2019

94. Bozzo L, Puyal J, Chatton JY. Lactate Modulates the Activity of Primary Cortical Neurons

through a Receptor-Mediated Pathway. *PLoS One*. 2013. doi:10.1371/journal.pone.0071721

95. Boitsova EB, Morgun A V., Osipova ED, et al. The inhibitory effect of LPS on the expression of GPR81 lactate receptor in blood-brain barrier model in vitro. *J Neuroinflammation*. 2018. doi:10.1186/s12974-018-1233-2
96. Philp A, Macdonald AL, Watt PW. Lactate - A signal coordinating cell and systemic function. *J Exp Biol*. 2005. doi:10.1242/jeb.01961
97. Sun S, Li H, Chen J, Qian Q. Lactic acid: No longer an inert and end-product of glycolysis. *Physiology*. 2017;32(6):453-463. doi:10.1152/physiol.00016.2017
98. Peretó J. Embden-Meyerhof-Parnas Pathway. In: *Encyclopedia of Astrobiology*. ; 2011. doi:10.1007/978-3-642-11274-4_503
99. Kresge N, Simoni RD, Hill RL. Otto Fritz Meyerhof and the elucidation of the glycolytic pathway. *J Biol Chem*. 2005.
100. Deuticke B. Monocarboxylate transport in erythrocytes. *J Membr Biol*. 1982. doi:10.1007/BF01870219
101. Gladden LB. Lactate metabolism: A new paradigm for the third millennium. *J Physiol*. 2004. doi:10.1113/jphysiol.2003.058701
102. Shen D, Gregory CD, Dawson MJ. Observation and quantitation of lactate in oxidative and glycolytic fibers of skeletal muscles. *Magn Reson Med*. 1996. doi:10.1002/mrm.1910360107
103. Brooks GA. The lactate shuttle during exercise and recovery. *Med Sci Sports Exerc*. 1986. doi:10.1249/00005768-198606000-00019
104. Kinoshita PF, Leite JA, Orellana AMM, et al. The influence of Na+, K+-ATPase on glutamate signaling in neurodegenerative diseases and senescence. *Front Physiol*. 2016. doi:10.3389/fphys.2016.00195
105. Semenza GL. Hydroxylation of HIF-1: Oxygen sensing at the molecular level. *Physiology*.

2004. doi:10.1152/physiol.00001.2004

106. Husain Z, Huang Y, Seth P, Sukhatme VP. Tumor-Derived Lactate Modifies Antitumor Immune Response: Effect on Myeloid-Derived Suppressor Cells and NK Cells. *J Immunol*. 2013. doi:10.4049/jimmunol.1202702

107. Margineanu MB, Mahmood H, Fiumelli H, Magistretti PJ. L-Lactate Regulates the Expression of Synaptic Plasticity and Neuroprotection Genes in Cortical Neurons: A Transcriptome Analysis. *Front Mol Neurosci*. 2018. doi:10.3389/fnmol.2018.00375

108. Wang Q, Hu Y, Wan J, Dong B, Sun J. Lactate: A Novel Signaling Molecule in Synaptic Plasticity and Drug Addiction. *BioEssays*. 2019;41(8). doi:10.1002/bies.201900008

109. Hunt TK, Aslam R, Hussain Z, Beckert S. Lactate, with oxygen, incites angiogenesis. *Adv Exp Med Biol*. 2008;614:73-80. doi:10.1007/978-0-387-74911-2_9

110. Ruan GX, Kazlauskas A. Lactate engages receptor tyrosine kinases Axl, Tie2, and vascular endothelial growth factor receptor 2 to activate phosphoinositide 3-kinase/AKT and promote angiogenesis. *J Biol Chem*. 2013;288(29):21161-21172. doi:10.1074/jbc.M113.474619

111. de Alteriis E, Cartenì F, Parascandola P, Serpa J, Mazzoleni S. Revisiting the Crabtree/Warburg effect in a dynamic perspective: a fitness advantage against sugar-induced cell death. *Cell Cycle*. 2018. doi:10.1080/15384101.2018.1442622

112. Epstein T, Gatenby RA, Brown JS. The Warburg effect as an adaptation of cancer cells to rapid fluctuations in energy demand. *PLoS One*. 2017. doi:10.1371/journal.pone.0185085

113. Burns JS, Manda G. Metabolic pathways of thewarburg effect in health and disease: Perspectives of choice, chain or chance. *Int J Mol Sci*. 2017. doi:10.3390/ijms18122755

114. Blacker TS, Duchen MR. Investigating mitochondrial redox state using NADH and NADPH autofluorescence. *Free Radic Biol Med*. 2016. doi:10.1016/j.freeradbiomed.2016.08.010

115. Mullarky E, Cantley LC. Diverting Glycolysis to Combat Oxidative Stress. In: *Innovative*

Medicine. ; 2015. doi:10.1007/978-4-431-55651-0_1

116. Liberti M V., Locasale JW. The Warburg Effect: How Does it Benefit Cancer Cells? *Trends Biochem Sci*. 2016;41(3):211-218. doi:10.1016/j.tibs.2015.12.001

117. Stuss DT, Gow CA, Hetherington CR. "No Longer Gage": Frontal Lobe Dysfunction and Emotional Changes. *J Consult Clin Psychol*. 1992. doi:10.1037/0022-006X.60.3.349

118. Durani SK, Ford R, Sajjad SHA. Capgras syndrome associated with a frontal lobe tumour. *Ir J Psychol Med*. 1991. doi:10.1017/S0790966700015093

119. Khan AZ, Pisella L, Vighetto A, et al. Optic ataxia errors depend on remapped, not viewed, target location. *Nat Neurosci*. 2005. doi:10.1038/nn1425

120. Vossel S, Weiss PH, Eschenbeck P, Fink GR. Anosognosia, neglect, extinction and lesion site predict impairment of daily living after right-hemispheric stroke. *Cortex*. 2013. doi:10.1016/j.cortex.2012.12.011

121. Squire LR, Stark CEL, Clark RE. THE MEDIAL TEMPORAL LOBE. *Annu Rev Neurosci*. 2004. doi:10.1146/annurev.neuro.27.070203.144130

122. DiCarlo JJ, Zoccolan D, Rust NC. How does the brain solve visual object recognition? *Neuron*. 2012. doi:10.1016/j.neuron.2012.01.010

123. Anand K, Dhikav V. Hippocampus in health and disease: An overview. *Ann Indian Acad Neurol*. 2012. doi:10.4103/0972-2327.104323

124. Pertzov Y, Miller TD, Gorgoraptis N, et al. Binding deficits in memory following medial temporal lobe damage in patients with voltage-gated potassium channel complex antibody-associated limbic encephalitis. *Brain*. 2013. doi:10.1093/brain/awt129

125. Kravitz DJ, Saleem KS, Baker CI, Ungerleider LG, Mishkin M. The ventral visual pathway: An expanded neural framework for the processing of object quality. *Trends Cogn Sci*. 2013. doi:10.1016/j.tics.2012.10.011

126. Adcock JE, Panayiotopoulos CP. Occipital lobe seizures and epilepsies. *J Clin Neurophysiol*. 2012. doi:10.1097/WNP.0b013e31826c98fe

127. Miall RC. Cerebellum. In: *Encyclopedia of the Neurological Sciences*. ; 2014. doi:10.1016/B978-0-12-385157-4.01131-3

128. Butts T, Chaplin N, Wingate RJT. Can clues from evolution unlock the molecular development of the cerebellum? *Mol Neurobiol*. 2011. doi:10.1007/s12035-010-8160-2

129. Fredericks CM. Disorders of the Cerebellum and Its Connections. *Pathophysiol Mot Syst Princ Clin Present*. 1996.

130. Haines DE, Mihailoff GA. *Fundamental Neuroscience for Basic and Clinical Applications: Fifth Edition*.; 2017. doi:10.1016/c2014-0-03718-5

131. Gerhard D. Neuroscience. 5th Edition. *Yale J Biol Med*. 2013.

132. Sciacca S, Lynch J, Davagnanam I, Barker R. Midbrain, pons, and medulla: Anatomy and syndromes. *Radiographics*. 2019. doi:10.1148/rg.2019180126

133. Benjamin EJ, Virani SS, Callaway CW, et al. Heart disease and stroke statistics - 2018 update: A report from the American Heart Association. *Circulation*. 2018. doi:10.1161/CIR.0000000000000558

134. Bamford J, Sandercock P, Dennis M, Warlow C, Burn J. Classification and natural history of clinically identifiable subtypes of cerebral infarction. *Lancet*. 1991. doi:10.1016/0140-6736(91)93206-O

135. Dirnagl U. Cerebral ischemia: The microcirculation as trigger and target. *Prog Brain Res*. 1993. doi:10.1016/S0079-6123(08)63258-6

136. Bramlett HM, Dietrich WD. Pathophysiology of cerebral ischemia and brain trauma: Similarities and differences. *J Cereb Blood Flow Metab*. 2004;24(2):133-150. doi:10.1097/01.WCB.0000111614.19196.04

137. Fluri F, Schuhmann MK, Kleinschnitz C. Animal models of ischemic stroke and their application in clinical research. *Drug Des Devel Ther*. 2015. doi:10.2147/DDDT.S56071

138. Casals JB, Pieri NCG, Feitosa MLT, et al. The use of animal models for stroke research: A review. *Comp Med*. 2011.

139. T. Neumann J, H. Cohan C, R. Dave K, B. Wright C, A. Perez-Pinzon M. Global Cerebral Ischemia: Synaptic and Cognitive Dysfunction. *Curr Drug Targets*. 2013. doi:10.2174/138945013804806514

140. MEYER FB, SUNDT TM, YANAGIHARA T, ANDERSON RE. Focal Cerebral Ischemia: Pathophysiologic Mechanisms and Rationale for Future Avenues of Treatment. *Mayo Clin Proc*. 1987. doi:10.1016/S0025-6196(12)61523-7

141. Chen W, He Y, Su Y. Multifocal cerebral infarction as the first manifestation of occult malignancy: Case series of trousseau's syndrome and literature review. *Brain Circ*. 2018. doi:10.4103/bc.bc_1_18

142. Braeuninger S, Kleinschnitz C. Rodent models of focal cerebral ischemia: procedural pitfalls and translational problems. *Exp Transl Stroke Med*. 2009. doi:10.1186/2040-7378-1-8

143. Belayev L, Alonso OF, Busto R, Zhao W, Ginsberg MD. Middle cerebral artery occlusion in the rat by intraluminal suture: Neurological and pathological evaluation of an improved model. *Stroke*. 1996. doi:10.1161/01.STR.27.9.1616

144. Longa EZ, Weinstein PR, Carlson S, Cummins R. Reversible middle cerebral artery occlusion without craniectomy in rats. *Stroke*. 1989. doi:10.1161/01.STR.20.1.84

145. Kabat H, Dennis C, Baker AB. RECOVERY OF FUNCTION FOLLOWING ARREST OF THE BRAIN CIRCULATION. *Am J Physiol Content*. 1941. doi:10.1152/ajplegacy.1941.132.3.737

146. Woodruff TM, Thundyil J, Tang SC, Sobey CG, Taylor SM, Arumugam T V. Pathophysiology, treatment, and animal and cellular models of human ischemic stroke. *Mol Neurodegener*. 2011. doi:10.1186/1750-1326-6-11

147. Pulsinelli WA, Brierley JB. A new model of bilateral hemispheric ischemia in the unanesthetized rat. *Stroke*. 1979. doi:10.1161/01.STR.10.3.267

148. Traystman RJ. Animal models of focal and global cerebral ischemia. *ILAR J*.

2003;44(2):85-95. doi:10.1093/ilar.44.2.85

149. Vannucci RC, Vannucci SJ. A model of perinatal hypoxic-ischemic brain damage. In: *Annals of the New York Academy of Sciences*. ; 1997. doi:10.1111/j.1749-6632.1997.tb48634.x

150. Vannucci RC, Vannucci SJ. Perinatal hypoxic-ischemic brain damage: Evolution of an animal model. *Dev Neurosci*. 2005. doi:10.1159/000085978

151. Rumajogee P, Bregman T, Miller SP, Yager JY, Fehlings MG. Rodent hypoxia-ischemia models for cerebral palsy research: A systematic review. *Front Neurol*. 2016;7(APR). doi:10.3389/fneur.2016.00057

152. Martinello K, Hart AR, Yap S, Mitra S, Robertson NJ. Management and investigation of neonatal encephalopathy: 2017 update. *Arch Dis Child Fetal Neonatal Ed*. 2017;102(4):F346-F358. doi:10.1136/archdischild-2015-309639

153. Millar LJ, Shi L, Hoerder-Suabedissen A, Molnár Z. Neonatal hypoxia ischaemia: Mechanisms, models, and therapeutic challenges. *Front Cell Neurosci*. 2017;11(May):1-36. doi:10.3389/fncel.2017.00078

154. Carmen M, la Veg C de C. Neuroprotection in Perinatal Hypoxic-Ischemic Encephalopathy — Pharmacologic Combination Therapy. In: *Cerebral Palsy - Challenges for the Future*. ; 2014. doi:10.5772/57459

155. Pfister RH, Soll RF. Hypothermia for the treatment of infants with hypoxic-ischemic encephalopathy. In: *Journal of Perinatology*. ; 2010. doi:10.1038/jp.2010.91

156. Lemyre B, Chau V. Hypothermia for newborns with hypoxic-ischemic encephalopathy. *Paediatr Child Heal*. 2018. doi:10.1093/pch/pxy028

157. Mccall EM, Alderdice F, Halliday HL, Vohra S, Johnston L. Interventions to prevent hypothermia at birth in preterm and/or low birth weight infants. *Cochrane Database Syst Rev*. 2018. doi:10.1002/14651858.CD004210.pub5

158. P.A. L. Erythropoietin molecules to treat acute ischemic stroke: A translational dilemma!

Expert Opin Investig Drugs. 2010. doi:10.1517/13543784.2010.517954 LK - http://WT3CF4ET2L.search.serialssolutions.com?sid=EMBASE&issn=13543784&id=doi:10.1517%2F13543784.2010.517954&atitle=Erythropoietin+molecules+to+treat+acute+ischemic+stroke%3A+A+translational+dilemma%21&stitle=Expert+Opin.+Invest.+Drugs&title=Expert+Opinion+on+Investigational+Drugs&volume=19&issue=10&spage=1179&epage=1186&aulast=Lapchak&aufirst=Paul+A&auinit=P.A.&aufull=Lapchak+P.A.&coden=EOIDE&isbn=&pages=1179-1186&date=2010&auinit1=P&auinitm=A

159. Rogers EE, Bonifacio SL, Glass HC, et al. Erythropoietin and hypothermia for hypoxic-ischemic encephalopathy. *Pediatr Neurol*. 2014. doi:10.1016/j.pediatrneurol.2014.08.010

160. Juul SE, Pet GC. Erythropoietin and Neonatal Neuroprotection. *Clin Perinatol*. 2015. doi:10.1016/j.clp.2015.04.004

161. Jantzie LL, Scafidi J, Robinson S. Stem cells and cell-based therapies for cerebral palsy: A call for rigor. *Pediatr Res*. 2018. doi:10.1038/pr.2017.233

162. Herberts CA, Kwa MSG, Hermsen HPH. Risk factors in the development of stem cell therapy. *J Transl Med*. 2011. doi:10.1186/1479-5876-9-29

163. Barker-Haliski M, Steve White H. Glutamatergic mechanisms associated with seizures and epilepsy. *Cold Spring Harb Perspect Med*. 2015. doi:10.1101/cshperspect.a022863

164. Schubert S, Brandl U, Brodhun M, et al. Neuroprotective effects of topiramate after hypoxia-ischemia in newborn piglets. *Brain Res*. 2005. doi:10.1016/j.brainres.2005.07.061

165. Dingley J, Tooley J, Porter H, Thoresen M. Xenon provides short-term neuroprotection in neonatal rats when administered after hypoxia-ischemia. *Stroke*. 2006. doi:10.1161/01.STR.0000198867.31134.ac

166. Hobbs C, Thoresen M, Tucker A, Aquilina K, Chakkarapani E, Dingley J. Xenon and hypothermia combine additively, offering long-term functional and histopathologic neuroprotection after neonatal hypoxia/ischemia. *Stroke*. 2008. doi:10.1161/STROKEAHA.107.499822

167. Dinse A, Föhr KJ, Georgieff M, Beyer C, Bulling A, Weigt HU. Xenon reduces glutamate-, AMPA-, and kainate-induced membrane currents in cortical neurones. *Br J Anaesth*. 2005. doi:10.1093/bja/aei080

168. Suganuma H, Arai Y, Kitamura Y, Hayashi M, Okumura A, Shimizu T. Maternal docosahexaenoic acid-enriched diet prevents neonatal brain injury. *Neuropathology*. 2010. doi:10.1111/j.1440-1789.2010.01114.x

169. Berman DR, Mozurkewich E, Liu YQ, Barks J. Docosahexaenoic acid pretreatment confers neuroprotection in a rat model of perinatal cerebral hypoxia-ischemia. *Am J Obstet Gynecol*. 2009. doi:10.1016/j.ajog.2009.01.020

170. Fernández-López D, Pazos MR, Tolón RM, et al. The cannabinoid agonist WIN55212 reduces brain damage in an in vivo model of hypoxic-ischemic encephalopathy in newborn rats. *Pediatr Res*. 2007. doi:10.1203/PDR.0b013e318123fbb8

171. Chaudhari T, McGuire W. Allopurinol for preventing mortality and morbidity in newborn infants with hypoxic-ischaemic encephalopathy. *Cochrane Database Syst Rev*. 2012. doi:10.1002/14651858.cd006817.pub3

172. Allen KA, Brandon DH. Hypoxic Ischemic Encephalopathy: Pathophysiology and Experimental Treatments. *Newborn Infant Nurs Rev*. 2011. doi:10.1053/j.nainr.2011.07.004

173. Thornton C, Rousset CI, Kichev A, et al. Molecular mechanisms of neonatal brain injury. *Neurol Res Int*. 2012;2012. doi:10.1155/2012/506320

174. McLean C, Ferriero D. Mechanisms of hypoxic-ischemic injury in the term infant. *Semin Perinatol*. 2004. doi:10.1053/j.semperi.2004.10.005

175. Back T. Pathophysiology of the ischemic penumbra - Revision of a concept. *Cell Mol Neurobiol*. 1998. doi:10.1023/A:1020265701407

176. Cassidy-Stone A, Chipuk JE, Ingerman E, et al. Chemical Inhibition of the Mitochondrial Division Dynamin Reveals Its Role in Bax/Bak-Dependent Mitochondrial Outer

Membrane Permeabilization. *Dev Cell*. 2008. doi:10.1016/j.devcel.2007.11.019

177. Cheng G, Kong RH, Zhang LM, Zhang JN. Mitochondria in traumatic brain injury and mitochondrial-targeted multipotential therapeutic strategies. *Br J Pharmacol*. 2012. doi:10.1111/j.1476-5381.2012.02025.x

178. Albertsson AM, Bi D, Duan L, et al. The immune response after hypoxia-ischemia in a mouse model of preterm brain injury. *J Neuroinflammation*. 2014;11(1):1-14. doi:10.1186/s12974-014-0153-z

179. Breier G. Angiogenesis in embryonic development - A review. *Placenta*. 2000. doi:10.1053/plac.1999.0525

180. Plate KH. Mechanisms of angiogenesis in the brain. *J Neuropathol Exp Neurol*. 1999;58(4):313-320. doi:10.1097/00005072-199904000-00001

181. Ribatti D, Crivellato E. "Sprouting angiogenesis", a reappraisal. *Dev Biol*. 2012. doi:10.1016/j.ydbio.2012.09.018

182. Risau W. Mechanisms of angiogenesis. *Nature*. 1997. doi:10.1038/386671a0

183. Ribatti D, Crivellato E. Mast cells, angiogenesis, and tumour growth. *Biochim Biophys Acta - Mol Basis Dis*. 2012. doi:10.1016/j.bbadis.2010.11.010

184. Nguyen G, Park SY, Le CT, Park WS, Choi DH, Cho EH. Metformin ameliorates activation of hepatic stellate cells and hepatic fibrosis by succinate and GPR91 inhibition. *Biochem Biophys Res Commun*. 2018;495(4):2649-2656. doi:10.1016/j.bbrc.2017.12.143

185. Phng LK, Gerhardt H. Angiogenesis: A Team Effort Coordinated by Notch. *Dev Cell*. 2009. doi:10.1016/j.devcel.2009.01.015

186. Hofmann JJ, Iruela-Arispe ML. Notch signaling in blood vessels: Who is talking to whom about what? *Circ Res*. 2007. doi:10.1161/01.RES.0000266408.42939.e4

187. Shah PK, Kaul S, Nilsson J, Cercek B. Exploiting the vascular protective effects of high-density lipoprotein and its apolipoproteins: An idea whose time for testing is coming, part I. *Circulation*. 2001. doi:10.1161/hc4401.098467

188. Schiffrin EL. Effects of antihypertensive drugs on vascular remodeling: Do they predict outcome in response to antihypertensive therapy? *Curr Opin Nephrol Hypertens*. 2001. doi:10.1097/00041552-200109000-00011

189. Cipolla MJ, Lessov N, Hammer ES, Curry AB. Threshold duration of ischemia for myogenic tone in middle cerebral arteries: Effect on vascular smooth muscle actin. *Stroke*. 2001. doi:10.1161/01.STR.32.7.1658

190. Cipolla MJ, Curry AB. Middle cerebral artery function after stroke: The threshold duration of reperfusion for myogenic activity. *Stroke*. 2002. doi:10.1161/01.STR.0000020712.84444.8D

191. Matsuo Y, Mihara SI, Ninomiya M, Fujimoto M. Protective effect of endothelin type A receptor antagonist on brain edema and injury after transient middle cerebral artery occlusion in rats. *Stroke*. 2001. doi:10.1161/hs0901.94259

192. Macrae IM, Robinson MJ, Graham DI, Reid JL, McCulloch J. Endothelin-1-induced reductions in cerebral blood flow: Dose dependency, time course, and neuropathological consequences. *J Cereb Blood Flow Metab*. 1993. doi:10.1038/jcbfm.1993.34

193. Kapakos G, Bouallegue A, Bou Daou G, K. Srivastava A. Modulatory Role of Nitric Oxide/cGMP System in Endothelin-1-Induced Signaling Responses in Vascular Smooth Muscle Cells. *Curr Cardiol Rev*. 2010. doi:10.2174/157340310793566055

194. Nelson CW, Wei EP, Povlishock JT, Kontos HA, Moskowitz MA. Oxygen radicals in cerebral ischemia. *Am J Physiol - Hear Circ Physiol*. 1992. doi:10.1152/ajpheart.1992.263.5.h1356

195. Murakami K, Kondo T, Kawase M, et al. Mitochondrial susceptibility to oxidative stress exacerbates cerebral infarction that follows permanent focal cerebral ischemia in mutant mice with manganese superoxide dismutase deficiency. *J Neurosci*. 1998. doi:10.1523/jneurosci.18-01-00205.1998

196. Hayashi T, Noshita N, Sugawara T, Chan PH. Temporal profile of angiogenesis and

expression of related genes in the brain after ischemia. *J Cereb Blood Flow Metab*. 2003. doi:10.1097/01.WCB.0000041283.53351.CB

197. Tilton RG, Berens KL. Functional role for selectins in the pathogenesis of cerebral ischemia. *Drug News Perspect*. 2002. doi:10.1358/dnp.2002.15.6.701654

198. Gong C, Qin Z, Betz AL, Liu XH, Yang GY. Cellular localization of tumor necrosis factor alpha following focal cerebral ischemia in mice. *Brain Res*. 1998. doi:10.1016/S0006-8993(98)00489-2

199. Rosenberg GA, Cunningham LA, Wallace J, et al. Immunohistochemistry of matrix metalloproteinases in reperfusion injury to rat brain: Activation of MMP-9 linked to stromelysin-1 and microglia in cell cultures. *Brain Res*. 2001. doi:10.1016/S0006-8993(00)03294-7

200. Rosenberg GA, Estrada EY, Dencoff JE. Matrix metalloproteinases and TIMPs are associated with blood-brain barrier opening after reperfusion in rat brain. *Stroke*. 1998. doi:10.1161/01.STR.29.10.2189

201. Tsurumi Y, Murohara T, Krasinski K, et al. Reciprocal relation between VEGF and NO in the regulation of endothelial integrity. *Nat Med*. 1997. doi:10.1038/nm0897-879

202. Servos S, Zachary I, Martin JF. VEGF modulates NO production: The basis of a cytoprotective effect. Editorial. *Cardiovasc Res*. 1999. doi:10.1016/S0008-6363(98)00293-4

203. Chen J, Zhu RL, Nakayama M, et al. Expression of the Apoptosis-Effector Gene, Bax, Is Up-Regulated in Vulnerable Hippocampal CA1 Neurons Following Global Ischemia. *J Neurochem*. 2002. doi:10.1046/j.1471-4159.1996.67010064.x

204. Hara A, Iwai T, Niwa M, et al. Immunohistochemical detection of Bax and Bcl-2 proteins in gerbil hippocampus following transient forebrain ischemia. *Brain Res*. 1996. doi:10.1016/0006-8993(95)01436-5

205. Gariano RF, Gardner TW. Retinal angiogenesis in development and disease. *Nature*. 2005.

doi:10.1038/nature04482

206. Stahl A, Connor KM, Sapieha P, et al. The mouse retina as an angiogenesis model. *Investig Ophthalmol Vis Sci*. 2010. doi:10.1167/iovs.10-5176

207. Hasegawa T, McLeod DS, Bhutto IA, et al. The embryonic human choriocapillaris develops by hemo-vasculogenesis. *Dev Dyn*. 2007. doi:10.1002/dvdy.21231

208. Liu CH, Wang Z, Sun Y, Chen J. Animal models of ocular angiogenesis: From development to pathologies. *FASEB J*. 2017. doi:10.1096/fj.201700336R

209. Lad EM, Hernandez-Boussard T, Morton JM, Moshfeghi DM. Incidence of Retinopathy of Prematurity in the United States: 1997 through 2005. *Am J Ophthalmol*. 2009. doi:10.1016/j.ajo.2009.04.018

210. Yau JWY, Rogers SL, Kawasaki R, et al. Global prevalence and major risk factors of diabetic retinopathy. *Diabetes Care*. 2012. doi:10.2337/dc11-1909

211. Bottoni F, Massacesi A, Cigada M, Viola F, Musicco I, Staurenghi G. Treatment of retinal angiomatous proliferation in age-related macular degeneration: A series of 104 cases of retinal angiomatous proliferation. *Arch Ophthalmol*. 2005. doi:10.1001/archopht.123.12.1644

212. Ferrara N. VEGF and intraocular neovascularization: From discovery to therapy. *Transl Vis Sci Technol*. 2016. doi:10.1167/tvst.5.2.10

213. Shih SC, Ju M, Liu N, Smith LEH. Selective stimulation of VEGFR-1 prevents oxygen-induced retinal vascular degeneration in retinopathy of prematurity. *J Clin Invest*. 2003. doi:10.1172/JCI17808

214. Watanabe D, Suzuma K, Matsui S, et al. Erythropoietin as a retinal angiogenic factor in proliferative diabetic retinopathy. *N Engl J Med*. 2005. doi:10.1056/NEJMoa041773

215. Wang Y, Rattner A, Zhou Y, Williams J, Smallwood PM, Nathans J. Norrin/Frizzled4 signaling in retinal vascular development and blood brain barrier plasticity. *Cell*. 2012. doi:10.1016/j.cell.2012.10.042

216. Linares G, Mayer SA. Hypothermia for the treatment of ischemic and hemorrhagic stroke. *Crit Care Med*. 2009. doi:10.1097/CCM.0b013e3181aa5de1

217. Roohey T, Raju TNK, Moustogiannis AN. Animal models for the study of perinatal hypoxic-ischemic encephalopathy: A critical analysis. *Early Hum Dev*. 1997. doi:10.1016/S0378-3782(96)01773-2

218. Li Y, Gonzalez P, Zhang L. Fetal stress and programming of hypoxic/ischemic-sensitive phenotype in the neonatal brain: Mechanisms and possible interventions. *Prog Neurobiol*. 2012. doi:10.1016/j.pneurobio.2012.05.010

219. Jaffer H, Morris VB, Stewart D, Labhasetwar V. Advances in stroke therapy. *Drug Deliv Transl Res*. 2011. doi:10.1007/s13346-011-0046-y

220. Chu LY, Ramakrishnan DP, Silverstein RL. Thrombospondin-1 modulates VEGF signaling via CD36 by recruiting SHP-1 to VEGFR2 complex in microvascular endothelial cells. *Blood*. 2013. doi:10.1182/blood-2013-01-482315

221. Isenberg JS, Annis DS, Pendrak ML, et al. Differential interactions of thrombospondin-1, -2, and -4 with CD47 and effects on cGMP signaling and ischemic injury responses. *J Biol Chem*. 2009;284(2):1116-1125. doi:10.1074/jbc.M804860200

222. Maxhimer JB, Shih HB, Isenberg JS, Miller TW, Roberts DD. Thrombospondin-1/CD47 blockade following ischemia-reperfusion injury is tissue protective. *Plast Reconstr Surg*. 2009. doi:10.1097/PRS.0b013e3181bceec3

223. Patel R, Dickenson AH. Mechanisms of the gabapentinoids and α2δ-1 calcium channel subunit in neuropathic pain. *Pharmacol Res Perspect*. 2016. doi:10.1002/prp2.205

224. Eroglu Ç, Allen NJ, Susman MW, et al. Eroglu et al. - The Gabapentin Receptor α2δ-1 is the Neuronal Thrombospondin Receptor Responsible for Excitatory CNS Synaptogenesis - 2009.pdf. 2010;139(2):380-392. doi:10.1016/j.cell.2009.09.025.The

225. Howe CL, LaFrance-Corey RG, Goddery EN, Johnson RK, Mirchia K. Neuronal CCL2 expression drives inflammatory monocyte infiltration into the brain during acute virus

infection. *J Neuroinflammation*. 2017. doi:10.1186/s12974-017-1015-2

226. Hoozemans JJM, Rozemuller AJM, Janssen I, De Groot CJA, Veerhuis R, Eikelenboom P. Cyclooxygenase expression in microglia and neurons in Alzheimer's disease and control brain. *Acta Neuropathol*. 2001. doi:10.1016/s0197-4580(00)82335-0

227. Iadecola C, Forster C, Nogawa S, Clark HB, Ross ME. Cyclooxygenase-2 immunoreactivity in the human brain following cerebral ischemia. *Acta Neuropathol*. 1999. doi:10.1007/s004010051045

228. Lawler PR, Lawler J. Molecular basis for the regulation of angiogenesis by thrombospondin-1 and -2. *Cold Spring Harb Perspect Med*. 2012;2(5):1-13. doi:10.1101/cshperspect.a006627

229. Gupta K, Gupta P, Wild R, Ramakrishnan S, Hebbel RP. Binding and displacement of vascular endothelial growth factor (VEGF) by thrombospondin: Effect on human microvascular endothelial cell proliferation and angiogenesis. *Angiogenesis*. 1999. doi:10.1023/A:1009018702832

230. Lauritzen KH, Morland C, Puchades M, et al. Lactate receptor sites link neurotransmission, neurovascular coupling, and brain energy metabolism. *Cereb Cortex*. 2014. doi:10.1093/cercor/bht136

231. Morland C, Andersson KA, Haugen ØP, et al. Exercise induces cerebral VEGF and angiogenesis via the lactate receptor HCAR1. *Nat Commun*. 2017;8(7491):1-9. doi:10.1038/ncomms15557

232. Lakhan SE, Kirchgessner A, Hofer M. Inflammatory mechanisms in ischemic stroke: Therapeutic approaches. *J Transl Med*. 2009. doi:10.1186/1479-5876-7-97

233. Jorwal P, Sikdar SK, Greenberg DA, et al. Biological roles and therapeutic potential of G protein-coupled receptors for free fatty acids and metabolic intermediates. *Nature*. 2005;438(7070):954-959. doi:10.1038/nature04481

234. Husted AS, Trauelsen M, Rudenko O, Hjorth SA, Schwartz TW. GPCR-Mediated

Signaling of Metabolites. *Cell Metab*. 2017;25(4):777-796. doi:10.1016/j.cmet.2017.03.008

235. Liu C, Kuei C, Zhu J, et al. 3,5-Dihydroxybenzoic acid, a specific agonist for hydroxycarboxylic acid 1, inhibits lipolysis in adipocytes. *J Pharmacol Exp Ther*. 2012. doi:10.1124/jpet.112.192799
236. Alarcon P, Manosalva C, Carretta MD, et al. Fatty and hydroxycarboxylic acid receptors: The missing link of immune response and metabolism in cattle. *Vet Immunol Immunopathol*. 2018;201(January):77-87. doi:10.1016/j.vetimm.2018.05.009
237. Ahmed K, Tunaru S, Tang C, et al. An Autocrine Lactate Loop Mediates Insulin-Dependent Inhibition of Lipolysis through GPR81. *Cell Metab*. 2010. doi:10.1016/j.cmet.2010.02.012
238. Rooney K, Trayhurn P. Lactate and the GPR81 receptor in metabolic regulation: Implications for adipose tissue function and fatty acid utilisation by muscle during exercise. *Br J Nutr*. 2011;106(9):1310-1316. doi:10.1017/S0007114511004673
239. Bergersen LH. Lactate transport and signaling in the brain: Potential therapeutic targets and roles in body-brain interaction. *J Cereb Blood Flow Metab*. 2015;35(2):176-185. doi:10.1038/jcbfm.2014.206
240. Hoque R, Farooq A, Ghani A, Gorelick F, Mehal WZ. Lactate reduces liver and pancreatic injury in toll-like receptor- and inflammasome-mediated inflammation via gpr81-mediated suppression of innate immunity. *Gastroenterology*. 2014;146(7):1763-1774. doi:10.1053/j.gastro.2014.03.014
241. Ranganathan P, Shanmugam A, Swafford D, et al. GPR81, a Cell-Surface Receptor for Lactate, Regulates Intestinal Homeostasis and Protects Mice from Experimental Colitis. *J Immunol*. 2018;200(5):1781–1789. doi:10.4049/jimmunol.1700604
242. Wagner W, Ciszewski WM, Kania KD. L- and D-lactate enhance DNA repair and modulate the resistance of cervical carcinoma cells to anticancer drugs via histone

deacetylase inhibition and hydroxycarboxylic acid receptor 1 activation. *Cell Commun Signal*. 2015. doi:10.1186/s12964-015-0114-x

243. Madaan A, Chaudhari P, Nadeau-Vallée M, et al. Müller Cell–Localized G-Protein–Coupled Receptor 81 (Hydroxycarboxylic Acid Receptor 1) Regulates Inner Retinal Vasculature via Norrin/Wnt Pathways. *Am J Pathol*. 2019;189(9). doi:10.1016/j.ajpath.2019.05.016

244. Chatham JC. Lactate - The forgotten fuel! *J Physiol*. 2002. doi:10.1113/jphysiol.2002.020974

245. Goodwin ML, Harris JE, Hernández A, Gladden LB. Blood lactate measurements and analysis during exercise: A guide for clinicians. *J Diabetes Sci Technol*. 2007. doi:10.1177/193229680700100414

246. Madaan A, Nadeau-Vallée M, Rivera JC, et al. Lactate produced during labor modulates uterine inflammation via GPR81 (HCA 1). *Am J Obstet Gynecol*. 2017;216(1):60.e1-60.e17. doi:10.1016/j.ajog.2016.09.072

247. Wagner W, Ciszewski WM, Kania KD. L- and D-lactate enhance DNA repair and modulate the resistance of cervical carcinoma cells to anticancer drugs via histone deacetylase inhibition and hydroxycarboxylic acid receptor 1 activation. *Cell Commun Signal*. 2015;13(1):1-16. doi:10.1186/s12964-015-0114-x

248. Offermanns S. Hydroxy-Carboxylic Acid Receptor Actions in Metabolism. *Trends Endocrinol Metab*. 2017;28(3):227-236. doi:10.1016/j.tem.2016.11.007

249. Efstathiou N, Theodoridis G, Sarafidis K. Understanding neonatal hypoxic-ischemic encephalopathy with metabolomics. *Hippokratia*. 2017.

250. Lauritzen F, Eid T, Bergersen LH. Monocarboxylate transporters in temporal lobe epilepsy: Roles of lactate and ketogenic diet. *Brain Struct Funct*. 2015;220(1):1-12. doi:10.1007/s00429-013-0672-x

251. Stafstrom CE, Carmant L. Seizures and epilepsy: An overview for neuroscientists. *Cold*

Spring Harb Perspect Biol. 2015. doi:10.1101/cshperspect.a022426

252. Pack AM. Epilepsy Overview and Revised Classification of Seizures and Epilepsies. *Contin Lifelong Learn Neurol*. 2019. doi:10.1212/CON.0000000000000707

253. Jorwal P, Sikdar S. Epileptiform activity reduced by lactate through HCA1 and GIRK channel activation in rat subicular neurons. *IBRO Reports*. 2019. doi:10.1016/j.ibror.2019.07.1151

254. LaFerla FM, Green KN, Oddo S. Intracellular amyloid-β in Alzheimer's disease. *Nat Rev Neurosci*. 2007. doi:10.1038/nrn2168

255. Murphy MP, Levine H. Alzheimer's disease and the amyloid-β peptide. *J Alzheimer's Dis*. 2010. doi:10.3233/JAD-2010-1221

256. Scheltens P, Blennow K, Breteler MMB, et al. Alzheimer's disease. *Lancet*. 2016. doi:10.1016/S0140-6736(15)01124-1

257. Goedert M, Spillantini MG. A century of Alzheimer's disease. *Science (80-)*. 2006. doi:10.1126/science.1132814

258. Kowalski K, Mulak A. Brain-gut-microbiota axis in Alzheimer's disease. *J Neurogastroenterol Motil*. 2019. doi:10.5056/jnm18087

259. Hu X, Wang T, Jin F. Alzheimer's disease and gut microbiota. *Sci China Life Sci*. 2016. doi:10.1007/s11427-016-5083-9

260. Rochfort KD, Collins LE, Murphy RP, Cummins PM. Downregulation of blood-brain barrier phenotype by proinflammatory cytokines involves NADPH oxidase-dependent ROS generation: Consequences for interendothelial adherens and tight junctions. *PLoS One*. 2014. doi:10.1371/journal.pone.0101815

261. Harris RA, Lone A, Lim H, et al. Aerobic glycolysis is required for spatial memory acquisition but not memory retrieval in mice. *eNeuro*. 2019. doi:10.1523/ENEURO.0389-18.2019

262. Newington JT, Harris RA, Cumming RC. Reevaluating Metabolism in Alzheimer's

Disease from the Perspective of the Astrocyte-Neuron Lactate Shuttle Model. *J Neurodegener Dis*. 2013. doi:10.1155/2013/234572

263. Barros LF. Metabolic signaling by lactate in the brain. *Trends Neurosci*. 2013;36(7):396-404. doi:10.1016/j.tins.2013.04.002

264. Osorio C, Kanukuntla T, Diaz E, Jafri N, Cummings M, Sfera A. The post-amyloid era in Alzheimer's disease: Trust your gut feeling. *Front Aging Neurosci*. 2019. doi:10.3389/fnagi.2019.00143

265. Iadanza MG, Jackson MP, Hewitt EW, Ranson NA, Radford SE. A new era for understanding amyloid structures and disease. *Nat Rev Mol Cell Biol*. 2018. doi:10.1038/s41580-018-0060-8

266. Chi CP, Roberts EL. Energy Substrates for Neurons during Neural Activity: A Critical Review of the Astrocyte-Neuron Lactate Shuttle Hypothesis. *J Cereb Blood Flow Metab*. 2003;23(11):1263-1281. doi:10.1097/01.WCB.0000081369.51727.6F

267. Pellerin L. Lactate as a pivotal element in neuron-glia metabolic cooperation. *Neurochem Int*. 2003;43(4-5):331-338. doi:10.1016/S0197-0186(03)00020-2

268. Mariga ST, Kolko M, Gjedde A, Bergersen LH. Lactate transport and receptor actions in cerebral malaria. *Front Neuroenergetics*. 2014;6(MAY):1-6. doi:10.3389/fnins.2014.00125

269. Ohno Y, Oyama A, Kaneko H, et al. Lactate increases myotube diameter via activation of MEK/ERK pathway in C2C12 cells. *Acta Physiol*. 2018. doi:10.1111/apha.13042

270. Gobeil F, Fortier A, Zhu T, et al. G-protein-coupled receptors signalling at the cell nucleus: An emerging paradigm. *Can J Physiol Pharmacol*. 2006;84(3-4):287-297. doi:10.1139/Y05-127

271. Bhosle VK, Rivera JC, Chemtob S. New insights into mechanisms of nuclear translocation of G-protein coupled receptors. *Small GTPases*. 2019. doi:10.1080/21541248.2017.1282402

272. P. M, M. R, M. W, P. M, R. M, J. B. Perfusion CT guided stroke management. *Schweizer*

Arch fur Neurol und Psychiatr. 2004.

273. Scarpulla R.C. Transcriptional activators and coactivators in the nuclear control of Mitochondrial function in mammalian cells. *Gene*. 2002.

274. Jiang et al. Blood-brain barrier dysfunction and recovery after ischemic stroke. *Progress in Neurobiology*. 2018. 144-171

275. Wu et al. Cerebral Lactate Concentration in Neonatal Hypoxic-Ischemic Encephalopathy: In Relation to Time, Characteristic of Injury, and Serum Lactate Concentration. *Frontiers in Neurosciences*. 2018. 293

276. James JH, Luchette FA, McCarter FD, Fischer JE. Lactate is an unreliable indicator of tissue hypoxia in injury or sepsis. *Lancet* (1999) 354(9177):505–508